Improving Spring Melt Calculations of Surface Runoff in the Upper Þjórsá River Using Measured Snow Accumulation

Reynir Óli Þorsteinsson

Faculty of Civil and Environmental Engineering
University of Iceland
2015

Improving Spring Melt Calculations of Surface Runoff in the Upper Þjórsá River Using Measured Snow Accumulation

Reynir Óli Þorsteinsson

30 ECTS thesis submitted in partial fulfillment of a
Magister Scientiarum degree in Environmental Engineering

Advisors
Dr. Sigurður Magnús Garðarsson
Andri Gunnarsson

Faculty Representative
Dr. Sveinn Óli Pálmarsson

Faculty of Civil and Environmental Engineering
School of Engineering and Natural Sciences
University of Iceland
Reykjavik, October 2015

Improving Spring Melt Calculations of Surface Runoff in the Upper Þjórsá River Using Measured Snow Accumulation
30 ECTS thesis submitted in partial fulfillment of a *Magister Scientiarum* degree in Environmental Engineering

Faculty of Civil and Environmental Engineering
School of Engineering and Natural Sciences
University of Iceland
Hjarðarhaga 6
107, Reykjavik
Iceland

Telephone: 525 4000

Bibliographic information:
Reynir Óli Þorsteinsson, 2015, *Improving Spring Melt Calculations of Surface Runoff in the Upper Þjórsá River Using Measured Snow Accumulation*, Master's thesis, Faculty of Civil and Environmental Engineering, University of Iceland.

Printing: Háskólaprent
Reykjavik, Iceland, October 2015

Abstract

One of the challenges of managing water resources for electricity production in Iceland is the seasonal variation of river discharge. With good discharge predictions it is easier to manage and optimize the hydropower resources. Spring season is of special interest because it brings valuable snowmelt, a resource that is difficult to quantify, predict and simulate. In this project a river catchment in the Upper Þjórsá River was analyzed, in particular the snow accumulation and the resulting spring floods. It involved making hydrological simulations with a HBV rainfall-runoff model. Input meteorological data were obtained from automatic weather stations located in or in the vicinity of the catchment. One of the challenges for these weather stations is to produce reliable precipitation data, especially when the precipitation is in the form of snow. Therefore to adjust the snowpack in the HBV model before spring melt started snow measurements that have been done in the Icelandic highlands were used. The relationship between the snow measurements and the spring melt was analyzed with regression analysis to see if there was a connection between the measured snow water equivalent (SWE) and the resulting spring discharge. The results show that there is a relationship between the measured SWE and spring discharge. The measured SWE provided a valuable point of reference in adjusting the snowpack in the HBV model and thus improving the spring discharge simulations for the catchment.

Útdráttur

Ein af áskorunum við að stýra nýtingu vatnsauðlindar fyrir raforkuframleiðslu á Íslandi eru árstíðarbundnar sveiflur í árrennsli. Með góðum rennslisspám er auðveldara en ella að hámarka nýtingu vatnsafls. Vorið er sérstaklega áhugavert vegna þess að þá kemur dýrmæt snjóbráð, auðlind sem erfitt er að magntaka, spá fyrir um og herma. Í þessu verkefni er vatnasvið í efri hluta Þjórsár kannað, með áherslu á snjósöfnun og snjóbráð sem fylgir. Í því fólst hermun á vatnasviðinu með regn- og afrennslislíkaninu HBV. Veðurgögn voru fengin frá sjálfvirkum veðurstöðum staðsettum á eða nálægt vatnasviðinu. Eitt af þeim vandamálum sem tengjast sjálfvirkum veðurstöðvum er að fá áreiðanlegar mælingar á úrkomu, sérstaklega þegar úrkoma er í formi snævar. Til þess að stilla snjóbunkann (e. snowpack) í HBV líkaninu áður en snjóbráð hefst var notast við snjómælingar sem hafa verið gerðar á hálendi Íslands. Sambandið milli snjómælinga og vorflóða var kannað með aðhvarfsgreiningu til að athuga hvort tengsl væru milli mælds vatnsígildis snævar og vorrennslis sem fylgir. Niðurstöður staðfesta slík tengsl milli mælds vatnsígildis og vorflóða. Mæld vatnsígildi snævar reyndust vera góð viðmiðun til að stilla af snjóbunkann í HBV líkaninu og þar með bæta hermun vorrennslis fyrir vatnasviðið.

Table of Contents

List of Figures

List of Tables

Variable Names

a	Filter parameter in Eckhardt equation
Accdif	Accumulated difference between observed and simulated discharge
b	Computed base flow with Eckhardt equation
BFI_{max}	Maximum base flow index
C_t	Degree-day factor
E	Nash-Sutcliffes efficiency coefficent
E_0	Input monthly mean potential evapotranspiration value
E_a	Actual evapotranspiration
E_{pot}	Potential evaporation
G	Observed value in Root Mean Square Error equation
k	Time step number in Eckhardt equation,
L	Heat from ice fusion
n	Number of nearby stations
N_i	Normal annual precipitation value for the i_{th} station
N_x	Normal annual precipitation value for the x station
P_i	Precipitation at the for i_{th} replacing station
P_x	Missing precipitation value at the interpolation station x
Q	General symbol for water discharge
Q_0	Outflow from the upper reservoir in HBV model
Q_a	Incoming long wave radiation,
QC	Computed discharge,
QC_{log}	Logarithm of computed discharge,
Q_e	Latent heat exchange,
Q_g	Ground surface heat exchange,
Q_h	Sensible heat exchange,
Q_i	Incident solar radiation,
Q_m	Heat content of liquid precipitation,
Q_{melt}	Snowmelt volume
Q_r	Reflected solar radiation
Q_{total}	Total runoff volume
$Q_{baseflow}$	Base flow volume
QR	Recorded discharge
QR_{log}	Logarithm of recorded discharge
$QR_{log,mean}$	Logarithm of mean recorded discharge
QR_{mean}	Recorded mean discharge over the simulation period

Q_s	Outgoing long wave radiation,
Q_{sw}	Short wave radiation
r^2	Coefficient of determination
RMSE	Root Mean Square Error
R_{xi}	Coefficient of correlation
SCA	Snow cover area
SD	Snow depth
SM	Computed soil moisture storage in the HBV model
SWE	Snow water equivalent
T	Observed temperature
T_a	Air temperature
UZ	Amount in upper reservoir in the HBV model
y	Total stream flow in Eckhardt equation
Y	Prediction value in Root Mean Square Error equation
ΔP	Contributed rainfall or snowmelt in the HBV model
ΔQ	Contribution to the response function (effective rainfall)
ρb	Bulk snow density
ρ_i	Ice density

Acknowledgements

I want to thank my advisors Andri Gunnarsson and Sigurður Magnús Garðarsson for their help and guidance throughout the project. Thanks to Landsvirkjun and Icelandic Meteorological Office for providing data and the Swedish Meteorological and Hydrological Institute for providing the HBV model used in the study. I also like to thank Ástráður Eysteinsson for reviewing the text. Special thanks go to my family for support and patience through the process especially Rannveig Jónsdóttir.

1 Introduction

1.1 Background

Almost all electricity produced in Iceland comes from renewable energy. Around 71% is from hydropower, approximately 29% comes from geothermal energy and a small fraction is from wind and fossil fuel (Orkustofnun, n.d.). The first hydropower station in Iceland was built in 1904 in the town Hafnarfjörður which became the first illuminated town in Iceland. Soon others followed and small scale hydropower stations were built in a number of places. In 1965 the power company Landsvirkjun was founded and a few years later the first large scale hydropower station was built, Búrfell powerstation a 210 MW hydropower plant. Today Búrfell power station generates around 270 MW after refurbishment and is one of six hydropower stations in the catchment area of rivers Þjórsá and Tungnaá, with combined energy of 935 MW (Landsvirkjun, n.d.).

The rivers Þjórsá and Tungnaá originates in the highlands of Iceland and are glacially fed rivers with sources in Hofsjökull and Vatnajökull glaciers. The two rivers are joined in the Sultartangalón reservoir above Sultartangi power station and the river is called Þjórsá after that. Þjórsá river is normally divided into upper and lower section. The upper section is where the river flows through the Icelandic highlands. The lower section is after it drops down to the lowlands just downstream of Búrfell station (Landsvirkjun, n.d.). Figure 1.1 shows an overview of the study area.

An extended network of waterways and diversions has been developed in Þjórsá and Tungnaá catchment area to manage and store water resources. Data related to the hydrology of the catchment area has been collected over an extended period to try to improve water resource management and predictions. It is important to manage water resources for hydro power stations in an optimal way to be able to plan the electricity production, reduce uncertainties and finally to increase the assets value (Madsen, Pedersen & Borden, 2009). The task is not simple, especially in a variable and unpredictable climate like that of Iceland.

The hydrology of Þjórsá and Tungnaá catchment area is rather complex. During winter it receives relatively large amounts of snow which becomes a valuable water resource during spring. Being able to quantify the snow volume in the beginning of spring and estimate the snowmelt amount that contributes to spring floods, helps to plan the electricity production. For this study a catchment area above Sultartangi power station was analyzed in terms of snow accumulation and spring discharge. The catchment area studied is a part of Upper Þjórsá River catchment and contributes water to Sultartangi power station and Búrfell power station.

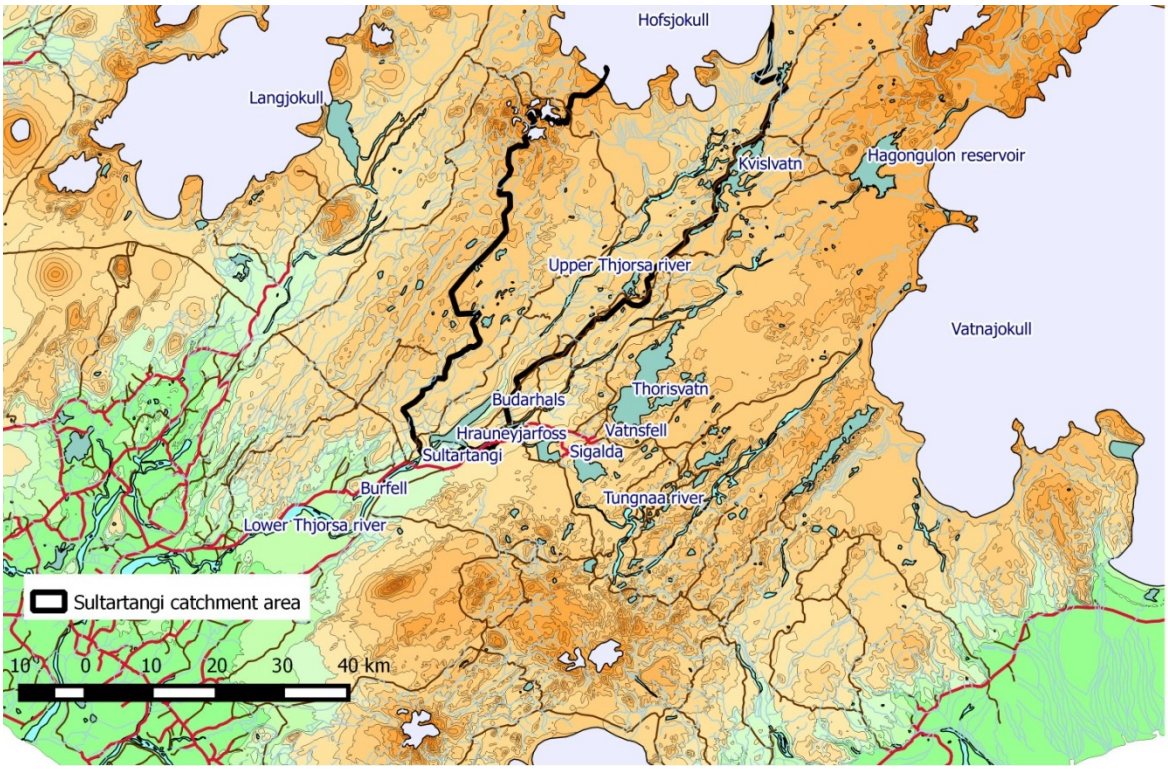

Figure 1.1 Overview of the study area. The location of the hydropower stations (Burfell, Sultartangi, Budarhals, Hrauneyjarfoss, Vatnsfell and Sigalda) in the catchment area of Þjórsá and Tungnaá rivers are represented (based on data from National Land Survey of Iceland).

1.2 Motivation

One of the challenges of managing water resources for electricity production in Iceland is the seasonal variation of river discharge. The electricity system in Iceland is a closed loop system that is not connected to other electricity systems. It needs to provide electricity for homes and companies throughout the year. The water discharge in rivers in Iceland fluctuates over the year and is normally higher in summer than in winter, especially in the glacier fed rivers. Therefore storage reservoirs are needed to have water available during low flow periods and to maximize the water utilization. Most hydropower plants in Iceland need to have some kind of storage in their hydrological system. The water discharge does not only fluctuate over the year but also from year to year, where some years are wetter than other.

To be able to optimize the electricity production it is important to know how much water will be flowing into reservoirs and when. There are many different approaches to predict inflow into reservoirs, such as long term, short term, deterministic and statistical approaches. Inflow forecasting is a valuable tool for real time water management. Forecast information on runoff into the reservoirs can be used to optimize short term benefits by minimizing spills and maximizing the economic value of water for hydropower production (Madsen, Pedersen & Borden, 2009).

The fluctuation of discharge within the seasons is difficult to predict. There are events that cause large deviations from the mean discharge, making long term predictions and

planning difficult. In winter the river discharge in Upper Þjórsá River is normally at its minimum, with the exception of occasional events that can produce small or large winter floods. The melting of snow in the spring normally starts in April/May and the volume of the spring flood dependents upon snowpack accumulation over the winter. It also depends upon meteorological conditions during the spring, as cold springs result in slower discharge response and damping the flood peaks. In May the storage reservoirs in Iceland are normally at minimum. That's the time when the energy companies start to wait for the snow melt to contribute to the runoff. Therefore it is valuable to be able to predict when the snow melt is likely to start and more importantly to be able to predict the amount of snow that is stored in the catchment and is likely to contribute to the runoff.

An important factor in the hydrology of a river catchment is snow. It supplies water to river discharge and aquifers in spring. It also controls the temporal and spatial distribution of soil moisture, evapotranspiration and other hydrological processes. The heterogeneous processes (wind, geology, etc.) that affect snowfall accumulation and snow melt, limit our ability to predict both seasonal runoff and extreme events (Kumar, Marks, Dozier, Reba & Winstra, 2013). With more knowledge on snow accumulation and snow melt within a catchment, winter- and spring floods could be predicted more accurately and thus improve management of the water resource.

The power company Landsvirkjun has been studying the hydrology of Þjórsá River and Tungnaá River catchment and using a few different models to simulate the hydrology. Complex models based on physics have been used, however better results are not always obtained with increased complexity. It would be interesting to see if a simpler conceptual model could give reliable results. The Upper Þjórsá River area is ideal for hydrological studies as various measurements have been conducted there over decades. Snow measurements have been done in the area that has not been studied fully in relations with spring runoff. If there is a connection between the snow measurements and the spring runoff the snow measurements might provide valuable information.

1.3 Objective

The aim of this project is to study and analyze the snow accumulation and the resulting spring floods for a catchment in Upper Þjórsá River. It involves making hydrological simulations with a HBV rainfall runoff model. The snow accumulation and snow melt for the catchment will be modeled with a simple degree-day approach where temperature and precipitation are the main input parameters. Available snowpack measurements will be studied and an attempt will be made to connect available annual snowpack data to simulated snow accumulations. Good estimations on size and distribution of the snowpack before spring melt starts could help to improve spring flood predictions and to estimate the volume of water stored as snow.

1.4 Literature Review

Many different methods have been developed to evaluate the hydrology of a catchment and estimate discharge. Which method to choose depends on the purpose of the study, data available, whether the catchment is gauged or not, and the level of complexity one aims. Regression models have been used for a long time, to estimate peak- and mean discharge for an area (Viessman & Lewis, 2003). Stochastic methods are widely used for modeling

hydrological time series where the most popular early methods involved using ARMA (autoregressive moving average) models (Pisarenko et al., 2005). As a contrast to stochastic models we have deterministic approaches. Water balance models are used to approximate the hydrological cycle and to estimate runoff based on the law of conservation of mass (Zhang, Walker & Dawes, 2002). There are all kinds of complex rainfall-runoff and hydrological models that are based on water balance equations and empirical relations, a variety of different conceptual models and physically based models.

1.4.1 Hydrological modeling

A river catchment is a complex hydrological system with countless features that effect runoff, for example variations in landscape, soil, vegetation, groundwater, meteorology, etc. A simulation model is a simplified enactment of reality based on equations and algorithms (Viessman & Lewis, 2003). Many different hydrological models have been developed to simulate river catchments with different strategies and processes. The models can be distinguished by three basic features: (i) the description of the process, (ii) the way to represent the catchment and (iii) whether a stochastic or deterministic approach is taken (Grayson & Bloschl, 2001; Viessman & Lewis, 2003).

The description of the modeling process can be categorized in three groups: empirical, conceptual and physically based models. Empirical models (black box model) are normally simpler than conceptual and physical models. They are based on input (e.g. rainfall) output (e.g. discharge) relations, encapsulated through statistical or similar techniques without attempting to describe the behavior of the processes (Grayson & Bloschl, 2001; Aghakouchak & Habibi, 2010).

Conceptual models use simple mathematical equations to describe basic processes such as infiltration, evaporation, surface storage, surface and subsurface runoff etc. Instead of solving governing partial equations, simple statements with different model parameters are introduced and they are used to calibrate using input-output relationship. An example of a conceptual model is the HBV rainfall- runoff model (Ortha, Staudingerb, Seneviratnea, Seibertb, & Zappac, 2015). Physically based models solve the governing equations such as conservation of mass and energy to simulate the output variable. With that approach less calibration is needed but more detailed and accurate field measurements and data are necessary (Aghakouchak & Habibi, 2010).

The model can represent the catchment as lumped, semi-distributed or distributed catchment. With lumped models, the whole catchment is treated as a single unit while distributed models divided the catchment into elements or cells so that the spatial landscape and processes can be described in more detailed ways (Grayson & Bloschl, 2001; Ortha, Staudingerb, Seneviratnea, Seibertb, & Zappac, 2015). Most models are deterministic where a single set of input and parameters describes a single set of output values. Stochastic models are often described as a statistical model, where the inputs and parameters have some statistical distribution (Grayson & Bloschl, 2001).

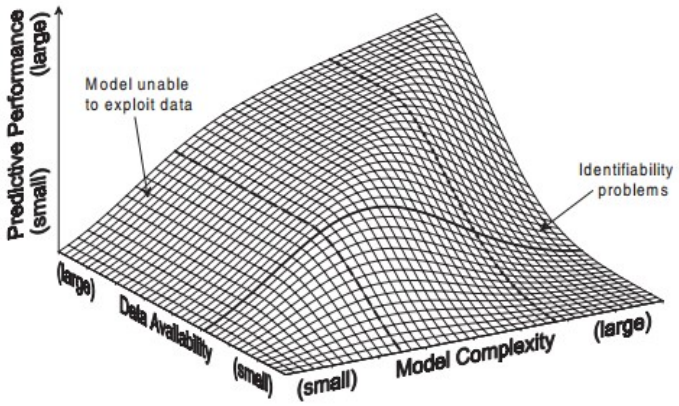

Figure 1.2 Relationship between complexity of model, the availability of data and the predictive performance of the model (Grayson & Bloschl, 2001)

Choosing the right model depends on the objective of the study and the data available. If the data are limited or the quality of the data is low, a complex model will return less accurate results than a simple model would, as is demonstrated in Figure 1.2.

1.4.2 Snow distribution and accumulation

In Iceland, it is crucial to have correct assessments of snow accumulation and snow melt for optimal simulation of runoff in winter and spring (Crochet, 2014). In an unstable climate, as the Icelandic one, it can be difficult to estimate snowmelt, accumulation and distribution.

In river catchments where much of the runoff produced comes from snowmelt the most important parameter for hydrological forecasting is the total volume of water stored in the snowpack (Elder, Rosenthal & Davis, 1998). A large part of the precipitation that falls on Sultartangi catchment falls as snow and is stored in the snow cover until melting starts. Snow is therefore one of the key parameter for the hydrology of the catchment and represents an important water reservoir (Thirela et al., 2012). Snowmelt can increase the discharge from a rain storm event but a deep snowpack can also support flood retention (Schöbera et al., 2013; Schöber, Achleitner, Kirnbauer, Schöberl & Schönlaub, 2012). To be able to make a better assessment on snow dynamics for a catchment it is important to research the total amount stored in a catchment and the evolution of the snowpack in space and time, especially in the melting period (Grunewald, Schirmer, Mott & Lehning, 2010).

The main properties of a snow cover that are of interest in terms of hydrology of catchments are snow depth, snow density, snow water equivalent (SWE) and snow cover area (SCA). The interest lies in identifying and characterizing the spatial and temporal variations of these properties. With more understanding of the relationship between the variability of the snow cover properties and environmental and hydro-meteorological variables, improvements can be made in the snowmelt modeling of a catchment (Trujillo, Ramírez & Elde, 2009).

In-situ snow measurements can be obtained using conventional rain gages, storage precipitation gages, snow boards and snow stakes. These measurements have large limitations as they are dependent on site location and local weather condition (wind, sun

exposure etc). They also cannot represent or estimate the snow distribution over large area (Viessman & Lewis, 2003; Thirela et al., 2012). It has been shown that measurements from conventional precipitation gages underestimate grossly true precipitation, mostly due to wind effects. For example in Hveravellir in the highlands of Iceland it is estimated that the gages underestimate the true value up to around 63% depending on wind. Correction factor formulas to get real precipitation have been developed with large uncertainties involved (Friðriksson & Ólafsson, 2005).

Field measurements on snow depth are much more common than SWE measurements since it is easier to measure the snow depth by using for example snow stakes. However, in most hydrological applications the snow cover is represented in SWE (Schöbera et al., 2013). A good quality spatial distribution data of snow depth and SWE for a catchment is generally rare. In the past few decades remote sensing techniques have become common practice in deriving spatial distribution of snow cover (Thirela et al., 2012; Schöbera et al., 2013). Recent year's areal Lidar (light detection and ranging) measurements have been used to evaluate spatial distribution in snow depth with high definition and relatively good results (Trujillo et al, 2009). Areal measurements are done prior to and after snow accumulation and digital terrain models are obtained. The terrain model before snow accumulation is subtracted from a terrain model obtained after snow accumulation; the results include spatial distribution of snow depth (Schöbera et al., 2013).

To obtain good, reliable information about spatial distribution of snow depth, Lidar measurements from air give best results. It has been shown that there is strong correlation between snow depth and SWE (Jonas, Marty, & Magnusson, 2009). Statistical models are sometimes used to convert Lidar snow depth data into SWE for catchments, in order to find the water reservoir stored as snow cover (Schöbera, et al., 2013; Trujillo et al., 2009). Field measurements on snow density are done to find average snow cover density to calculate the SWE,

$$SWE = SD * \rho b \tag{1}$$

where SD is snow depth and ρb is bulk snow density. The difficulty is to estimate a good spatially and temporal distributed SD parameter. Studies have shown that compared to snow depth, spatial variability of density is relatively small (Grunewald et al, 2010). Small number of topographical and meteorological parameters is assumed to control depth-average snow density. They are total snow depth, elevation, solar radiation, climatic region and vegetation patterns (Grunewald et al., 2010; Jonas et al., 2009).

1.4.3 Snow melt

Two common approaches have been used to model snow melt, energy balance and temperature-index methods (Kumar, Marks, Dozier, Reba, & Winstra, 2013). Energy balance method is linking the energy budget equation to snow melt rate,

$$S = \frac{(Q_{sw}+Q_a-Q_s+Q_h+Q_e+Q_m+Q_g)}{\rho_i * L} \tag{2}$$

where S is the snow melt rate, Q_{sw} is short wave radiation, Q_a is incoming long wave radiation, Q_s is the outgoing long wave radiation, Q_h is the sensible heat exchange, Q_e is the latent heat exchange, Q_m is the heat content of liquid precipitation, Q_g is the ground

surface heat exchange, L is the heat from ice fusion and ρ_i is the ice density (Kuchment & Gelfan, 1996).

The temperature index-method, also referred to as degree-day approach, is widely used. It is simpler and requires fewer parameters to estimate the snow melt. It simply assumes that the air temperature is proportional to snow melt and the relation is linear between melt rate and air temperature above the melting temperature (Kokkonena, Koivusaloa, Jakemanb & Norton, 2006). The equation for snow melt rate,

$$S = C_t * T_a \tag{3}$$

where C_t is the degree-day factor ($mm^oC^{-1}\Delta t^{-1}$) and T_a is the air temperature ($T_a>0°C$) (Kuchment & Gelfan, 1996; Kokkonena et al., 2006).

The HBV model is one of the hydrological models that use degree-day approach (Ortha et al, 2015). The advantage of a degree-day approach lies in its simplicity and less input of parameters. However, the energy balance method describes the system in a more accurate way and if the input data for the catchment is accurate, some research shows that the energy balance method needs less calibration and gives better results (Kumar et al., 2013).

1.5 Organization of the thesis

The thesis is divided into five chapters:

Chapter 1: A general introduction to the subject, presentation of basic ideas and a literature review of the subject.

Chapter 2: An overview of the methodology used in the study.

Chapter 3: Explanation and evaluation of the data used in this study.

Chapter 4: Results are presented and discussed.

Chapter 5: The results are summarized in conclusion.

2 Methods

2.1 Introduction to study area

The catchment analyzed in this study is located in the highlands of Iceland and drains water into Upper Þjórsá River. Figure 2.1 shows the location of the catchment. Coordinates for Sultartangi catchment were obtained from Landsvirkjun. A discharge gauging station is located within Sultartangi catchment, a few km upstream of Sultartangi reservoir, close to the waterfall Dynkur. The measured discharge at Dynkur was used to calibrate the rainfall runoff model and therefore a new catchment was defined with Dynkur gauging station as the outflow point for the catchment. This new catchment will be called Dynkur catchment. Various measurements have been collected in the catchment area over decades including snow measurements, as it is an important area for electricity production. It was therefore an ideal place to conduct a hydrological study on and the results could possibly help to improve runoff predictions and water management.

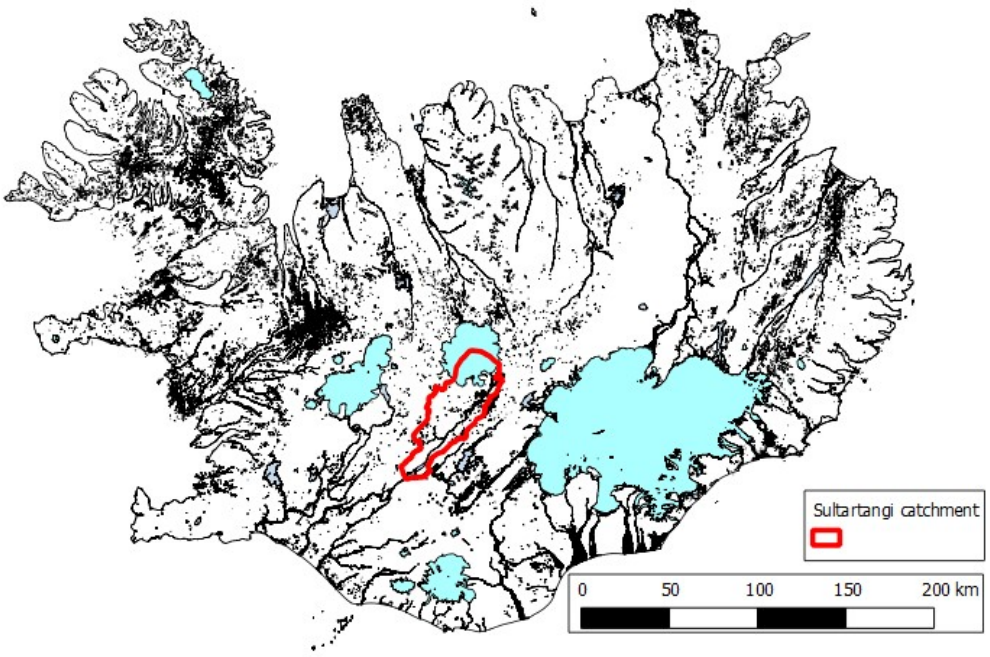

Figure 2.1 Location of Sultartangi catchment, contributing area from Upper Þjórsá River (based on data from National Land Survey of Iceland and coordinates from Landsvirkjun).

Figure 2.2 shows an overview of the catchment areas. A large portion of Dynkur catchment is covered by Hofsjökull glacier. The catchment is scarcely vegetated, since a large part of the area is covered by lava and gravel. There are a few relatively small lakes within the catchment. The highest elevation in the catchment is around 1800 MASL and the lowest is

390 MASL. Dynkur catchment covers around 84% of Sultartangi catchment, with the glacier within its zone. Therefore the discharge gauging station at Dynkur gives a close approximation for the total runoff coming from Sultartangi catchment into Sultartangi reservoir.

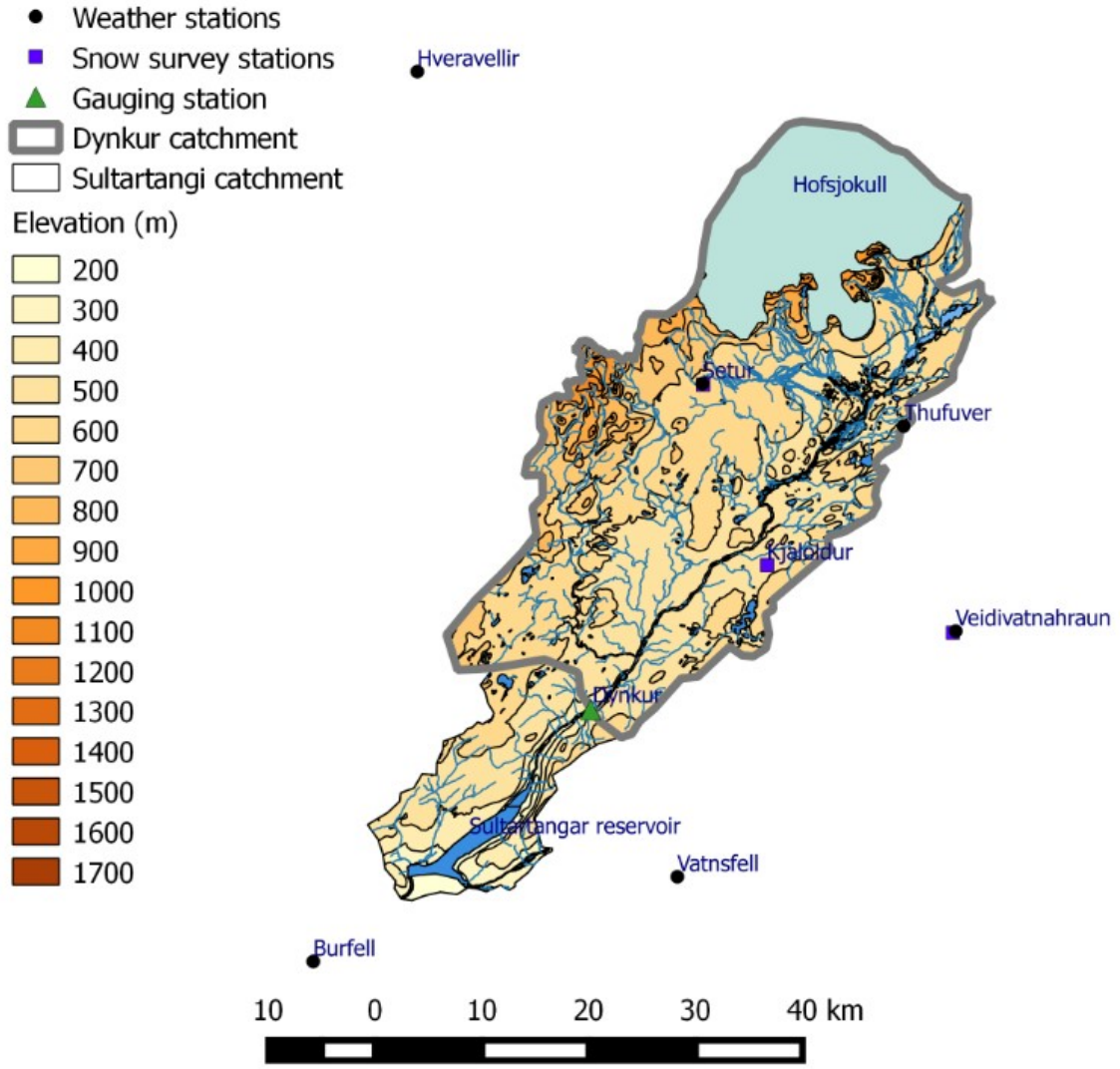

Figure 2.2 Overview of the catchment areas and the location of measurement stations. (Based on data from National Land Survey of Iceland).

Table 2.1 Catchment area with respect to Upper Þjórsá River, estimated from coordinates provided by Landsvirkjun

Catchment	Area (km^2)
Sultartangi	1709
Dynkur	1441

The study site is relatively flat, with some rolling hills and a proportionally small mountainous area in the north-west part of the catchment called Kerlingarfjöll. Further information about the catchments characteristics are presented in Table 2.2 and Figure 2.2.

It is difficult to describe accurately all the features in a river catchment when performing a hydrological modeling of a catchment. However, these different features play an important role in the hydrology of a catchment such as elevation, vegetation, lakes, soil and other spatial variations in the landscape. The main features of concern for this study were dependent on the hydrological model that was used to perform simulations.

All spatial data except for the coordinates of Sultartangi catchment were downloaded from the National Land Survey of Iceland web page. Elevation data, area of glacier within the catchment and area of lakes were derived from the following data packages: IS50V_VATNAFAR_24122014_ISN93, HAEDARLIKAN_LMI and IS50V_HAEDARGOGN_24122014_ISN93 (National Land Survay of Iceland, n.d.). The program QGIS was used to view, edit and analyze the data.

Table 2.2 Dynkur catchment characteristics (Based on data from National Land Survey of Iceland)

Characteristics	**%**
Moss and scrubs	9.2
Unvegetated sand and sandbars	3.4
Unvegetated lava	30.1
Semi vegetated grass land	15.6
Glacier	21.6
Riparian meadows	2.5
Wetland	5.3
Lakes	0.7

Figure 2.2 describes the elevation distribution for a non-glacier area and a glacier area separately. The non-glacier area is 79% of the catchment area and the glacier area is 21%. The largest part of the catchment lies within the elevation boundaries from 500 to 700 MASL, around 80% of the non-glacial area and around 63% of the catchment area when the glacier is included. This area is where the largest portion of the spring melt originates.

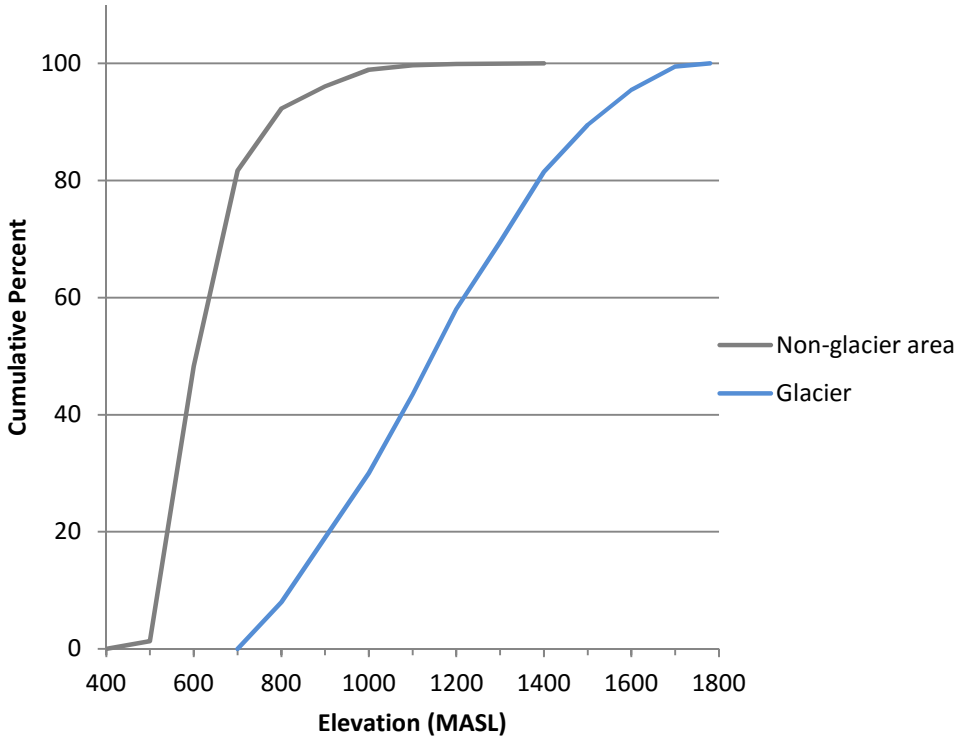

Figure 2.3 Cumulative elevation distribution for a non-glacier and glacier area.

2.2 Areal distribution of meteorological values

For hydrological simulations it is important to have a good estimation of the areal distribution of meteorological values within a catchment. Temperature difference within a catchment the size of the Dynkur is mostly dependent on elevation. Spatial distribution of precipitation is much more difficult to estimate than the temperature, especially if rain gauges are few and unevenly spread over the area. Making a logical estimation of precipitation distribution for Dynkur catchment depends on the location and density of the rain gauges.

Two most commonly used methods to estimate areal precipitations are the Thiessen method and the isohyetal method. Normally the isohyetal method is a more accurate approach to determine the average precipitation for an area. However, it depends on the insight of the hydrologist and demands careful attention to landscape and other variables affecting the spatial variability of the precipitation. The Thiessen method involves dividing the area into polygonal sub areas with rain gauges as center points. Each sub area in the catchment is used as weight to estimate average areal precipitation. The Thiessen method generally does not represent areal precipitation in mountainous areas well (Viessman & Lewis, 2003). Which method one chooses, the Thiessen method or the isohyetal method, depends on the topography and the distribution of the rain gauges. For Dynkur catchment only two rain gauges are within the catchment and both are in same elevation zone between 600 and 700 MASL. They are also relatively close to each other. With only two rain gauges within the catchment, it is hard to justify the use of the isohyetal method, thus the Thiessen method was used.

Accumulated precipitation was evaluated for all the weather stations used in the study over the study period and is presented in the results. Information about distribution of accumulated precipitation gives insight into local precipitation and could help to justify whether the estimated areal precipitation is logical or not.

2.3 Physics of the snow cover

A temperature index model like the HBV model does not describe the physics of the snow cover accurately, but simply assumes that the melt rate is proportional to temperature. However, it is beneficial to understand the basic physics of the snow cover when using a temperature index model, to understand the uncertainties and limitations of the approach. In general terms snow melt occurs when net energy input into the snow cover is enough for solid water to increase in temperature and melt. The energy balance equation for a snow cover is expressed,

$$\Delta Q = Q_i - Q_r + Q_a - Q_s + Q_h + Q_e + Q_m + Q_g \quad (4)$$

where Q_i is incident solar radiation, Q_r is reflected solar radiation, Q_a is incoming atmospheric and terrestrial longwave radiation, Q_s is longwave radiation emitted by the snow cover, Q_h is sensible heat transfer, Q_e is the latent heat transfer, Q_m is heat transfer due to mass changes, Q_g is heat transfer across soil-snow interface and ΔQ is the change in the heat storage of the snow cover (Anderson, 2006). Figure 2.4 illustrates the terms of the energy balance eqation.

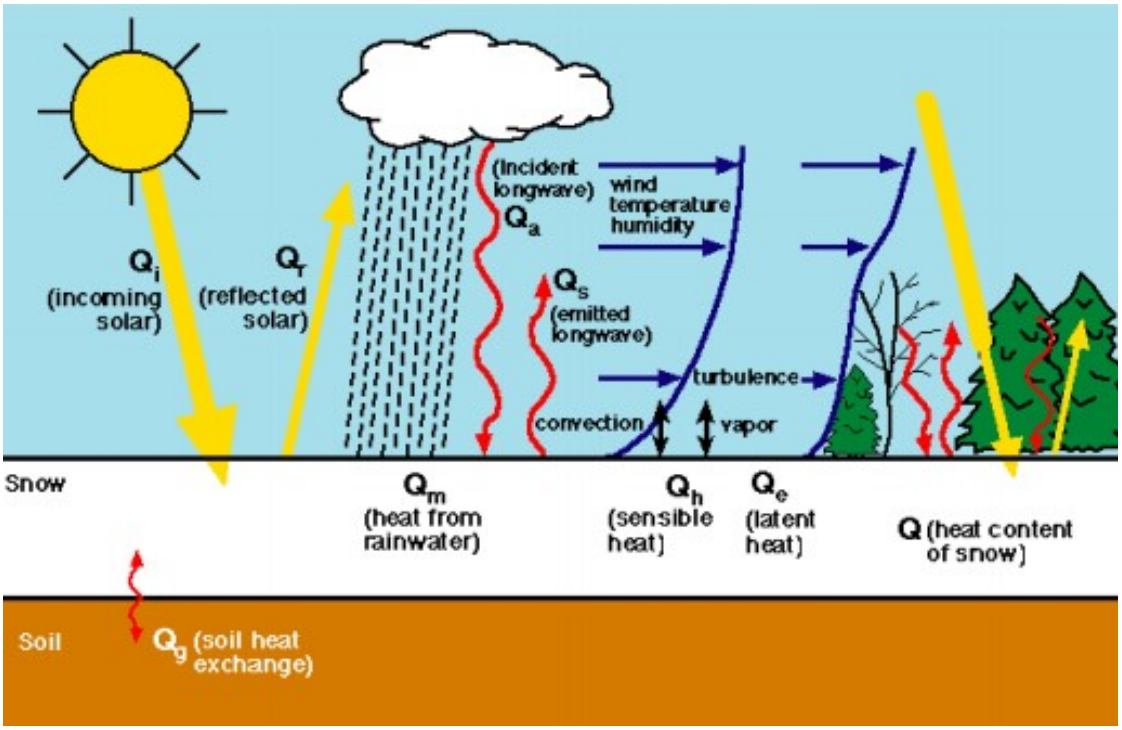

Figure 2.4 Summary of the energy terms affecting the snow cover (Anderson, 2006).

Snow melt occurs in three phases. A warming phase before melting starts the snowpack is warmed up to a point where it is isothermal at 0^0C. A ripening phase where the absorbed energy is used to melt the snow. The melted water is retained in the snowpack by surface

tension forces. When the melted water volume has reached a limit the snowpack cannot retain more water and the snowpack is said to be ripe. More input of energy leads to the output phase. The melted water seeps out of the snowpack and resulting in surface runoff, infiltration or evaporation (Boike, Roth, & Ippisch, 2003).

2.4 Spring runoff and snow measurement data

2.4.1 Runoff analysis

A large part of spring runoff in Upper Þjórsá River comes from snowmelt. Snow measurements have been done in a few places in the highlands of Iceland for over a decade. Normally they happen in the end of accumulation period, or in the middle of April. By finding a reliable connection between snow measurements and the total snowmelt volume, an estimate could be made regarding the volume of water stored in the snow cover based on snow measurements. If results show correlation between snow measurements and snowmelt volume, the snow measurements could provide a reference point in calibrating the snowpack in the hydrology simulations and thus improving spring flood simulations. Another advantage would be to use the correlation to obtain an empirical equation that could estimate the volume of water stored in Dynkur catchment that would later result as snowmelt.

To estimate the total snowmelt volume, the discharge data were plotted for the spring season along with temperature. The runoff was split into base flow, snowmelt and glacial melt. Figures 2.5 and 2.6 show how the runoff was split into different discharge components in 2012 and 2005. Figures for other years during the study period are represented in Appendix A. The snowmelt was calculated as,

$$Q_{melt} = Q_{total} - Q_{baseflow} - Q_{glacial} \quad (5)$$

where Q_{melt} is the total snowmelt, Q_{total} is the total runoff, $Q_{baseflow}$ is the base flow and $Q_{glacial}$ is the glacial melt.

Various approaches for base flow separation have been developed when actual base flow amount is unknown. For Upper Þjórsá River it is challenging to separate the base flow from the total discharge in an accurate way. Many base flow separation methods are based on evaluating hydrographs and identifying the point where direct runoff finishes with analysis of a recession and depletion curves. The runoff scheme in Upper Þjórsa River makes it difficult to make reliable estimation on the base flow by evaluating hydrographs. The reason for that is that the main runoff components in Upper Þjórsá River over spring and summer seasons are: snow melt and base flow over spring season, snow melt, glacial melt and base flow over the interface between spring and summer runoff, and finally glacial melt and base flow in the summer. This means that the base flow recession cannot be observed from hydrographs after spring discharge since there is always another discharge component included in the water volume. Other factors influencing the base flow are the response time of the aquifer system, infiltration rate to the groundwater, type of soil and condition of soil, to name a few.

Two different methods were chosen for Upper Þjórsá River. The simplest base flow separation method is to assume that base flow remains constant regardless of the total discharge. A straight line was drawn from the point where surface runoff starts and until

the snow melt was assumed to be finished. The discharge under the constructed line was defined as the base flow. This method is inaccurate and only provides rough estimations on base flow. If this method happens to give a realistic results for base flow it would mean that the response time of the aquifer system is very slow.

The second method was to use a two parameter recursive digital low pass filter developed by Eckhardt in 2005 sometimes called ‘‘Eckhardt filter‘‘ (Eckhardt, 2012),

$$b_k = \frac{(1-BFI_{max})a*b_{k-1}+(1-a)BFI_{max}y_k}{1-a*BFI_{max}} \quad (6)$$

where b is base flow (m^3/s), k is the time step number, a is filter parameter, y is the total stream flow (m^3/s) and BFI_{max} is maximum base flow index. BFI_{max} was calculated from long term discharge data and is the long term ratio of base flow to total stream flow (Eckhardt, 2012). Both base flow separation methods are presented in Figure 2.5 and 2.6

To estimate when snow melt receded and glacial melt started, the discharge and temperature plots on Figures 2.5, Figure 2.6 and the Figures in Appendix A were observed. This involved evaluating how the runoff responded to temperature. In general terms, when temperature was between 0 and 4°C the main runoff component was considered to be snowmelt in May and June. When the temperature exceeded 4°C at Setur it was estimated that glacial melt would start to contribute.

The elevation of the glacier goes from around 750 MASL at the base to 1780 MASL at the top, according to data from National Land Survey of Iceland. A weighted average elevation is 1150 MASL. The altitude difference between Setur and the average glacier elevation within the catchment is around five hundred meters. If it is assumed that the average temperature lapse rate is 0.6°C/100 m the average temperature difference would be around 3°C between Setur and average elevation of the glacier. In most cases melting is well correlated with temperature. From these estimations it is assumed that for glacier melt to make a quantitative contribution to discharge the temperature at Setur would need to be at least 4°C.

As the area of snow cover decreases during spring the snow melt rate decreases and the melt contribution to the discharge reduces. When the snow cover starts receding the volume from snowmelt reduces dependent on the distribution off the snow cover, temperature and other meteorological factors. To simplify matters it was assumed that the snowmelt receded linearly and that it receded at the same rate every year. Figure 2.5 and Figure 2.6 show the slope of estimated snowmelt depletion. The slope of snowmelt recession is the interface where snowmelt stops and glacial melt takes over.

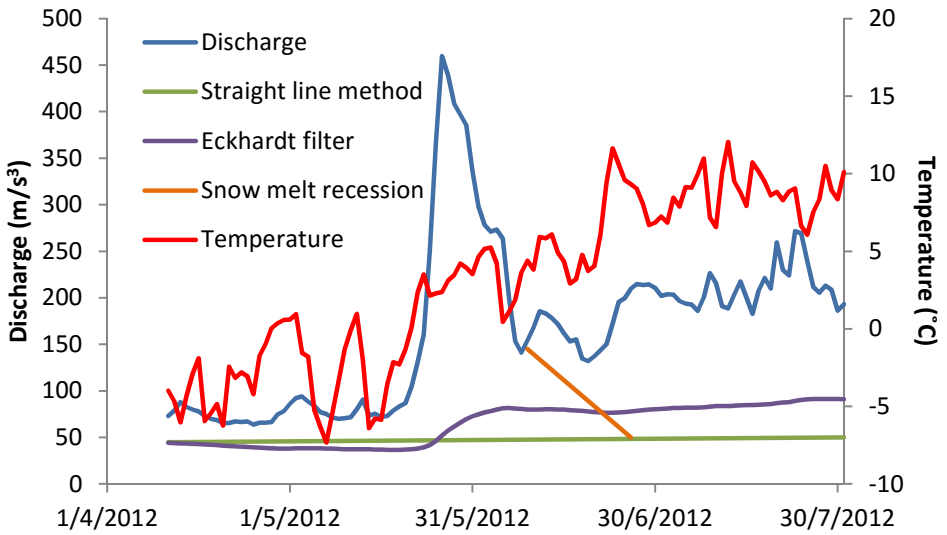

Figure 2.5 Hydrograph showing the discharge measured at Dynkur station, temperature measured at Setur and two variation of computed base flow.

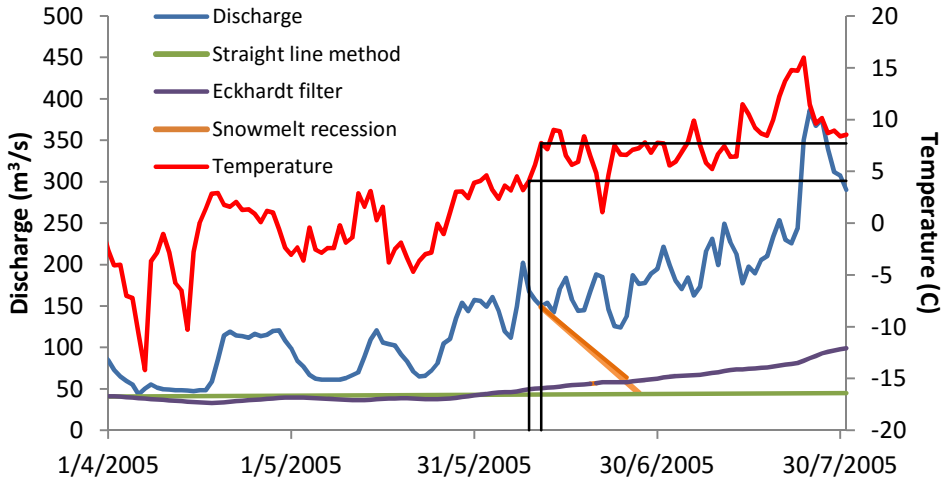

Figure 2.6 Hydrograph showing the discharge measured at Dynkur station, temperature measured at Setur and two variation of computed base flow. The black lines show the interval where discharge decreases but temperature increases, an indication that the snow cover is receding.

The main challenge was to evaluate when glacial melt started, how fast the snowmelt recession was, and the contribution of snowmelt to the base flow. The time when the snowmelt started to recede was determined mainly by observing the hydrograph and evaluating the evolution of temperature. Sometimes it was relatively easy to identify when the snowmelt was starting to recede, at other times it had to be evaluated in terms of the temperature. If the temperature had risen to 4 or 5°C and the hydrograph was not responding significantly it had to be assumed that the glacial melt was taken over.

Figure 2.5 and 2.6 show an example on how the runoff components were split for two spring season with different characteristics. For example, in Figure 2.5 a distinctive flood peak is observed. The temperature interval during the spring flood is between 0°C and 5°C,

indicating that the main portion of the discharge is coming from the snow cover in lower elevations rather than from the glacier. The example in Figure 2.6 on the other hand, does not show a distinctive flood peak. For spring seasons that do not produce an obvious flood peak a closer attention is made between changes in temperature and response of the hydrograph. An interval is marked with black lines in Figure 2.6 where the temperature rises considerably without response in the hydrograph. Until that time the discharge is increasing and decreasing along with temperature.

The same approach was used to estimate the snowmelt volume other years over the study period. As the approach is rather subjective the goal was to keep consistency between years. The approach is far from being perfect and is only an attempt to give a rough estimation on the snowmelt volume.

2.4.2 Correlation between runoff and snow measurements

The snow measurements have involved measuring snow depth and density and from these variables it is possible to estimate the snow water equivalent (SWE) for a specific location. Further explanations on these snow measurements such as locations and time of measurements are presented in Chapter 3.3. When the snowmelt volume had been estimated an attempt was made to link the snowmelt volume with measured SWE each year. The snowmelt volume and SWE was plotted and a regression analysis done.

From SWE data and total snowmelt volume an empirical regression equation was obtained. If a strong linear regression is observed, that is if coefficient of determination r^2 is high, the SWE measurements could serve as predictors for total snowmelt volume. An empirical regression equation could be used to predict future snowmelt volume based on SWE measurements done in the end of spring. In addition, strong correlation would indicate that SWE measurements could be used to represent the SWE in hydrological simulations.

Since snow measurements have been done in a few different locations a multiple regression analysis was also done with SWE measured at each location as an independent variable and snowmelt volume as a dependent variable. From the linear regression and multiple regression analysis a simple model was obtained to estimate the snowmelt volume based on SWE measurements.

2.5 HBV model

The runoff hydrology of the river catchment was simulated using HBV model (Hydrologiska Byrans Vattenbalans-avdeling or Hydrological Bureau Waterbalance-section) (SMHI, 2012). The model was originally developed in the 70´s at the Swedish Meteorological and Hydrological Institute (SMHI) to help with hydropower operations (Bergström, 1976). The model is used in runoff forecasting, flood simulations, water resource evolution and evolution of climate change among other things. Today it is reported that it has been applied in over 40 countries around the world, sometimes in modified versions (SMHI, 2012).

The Swedish Meteorological Institute (SMHI) developed a Graphical User Interface for the HBV model called IHMS (Integrated Hydrological Modeling System). It will be referred to as the HBV model in this study as is the case in the HBV/IHMS manual.

The HBV model is a semi-distributed conceptual rainfall runoff model used for continuous calculation of runoff. The input data have been kept as simple as possible where usually only observed precipitation and temperature are used. The use of wind speed, vapor pressure and estimates of potential evaporation is optional. Monthly average values are normally used for evapotranspiration and daily values adjusted to mean daily temperature. When computing snow melt and snow accumulation, temperature is the main parameter. It is also possible to have vapor pressure, rain and wind speed as an affecting values on the snow routine. The output is normally average daily runoff (SMHI, 2012). This means that the highest instantaneous flood peaks are not simulated.

Figure 2.7 shows a schematic structure of the HBV model for one sub-basin. There are four main storage components in the HBV model: snow zone (same for glacier), soil zone, upper zone and lower zone.

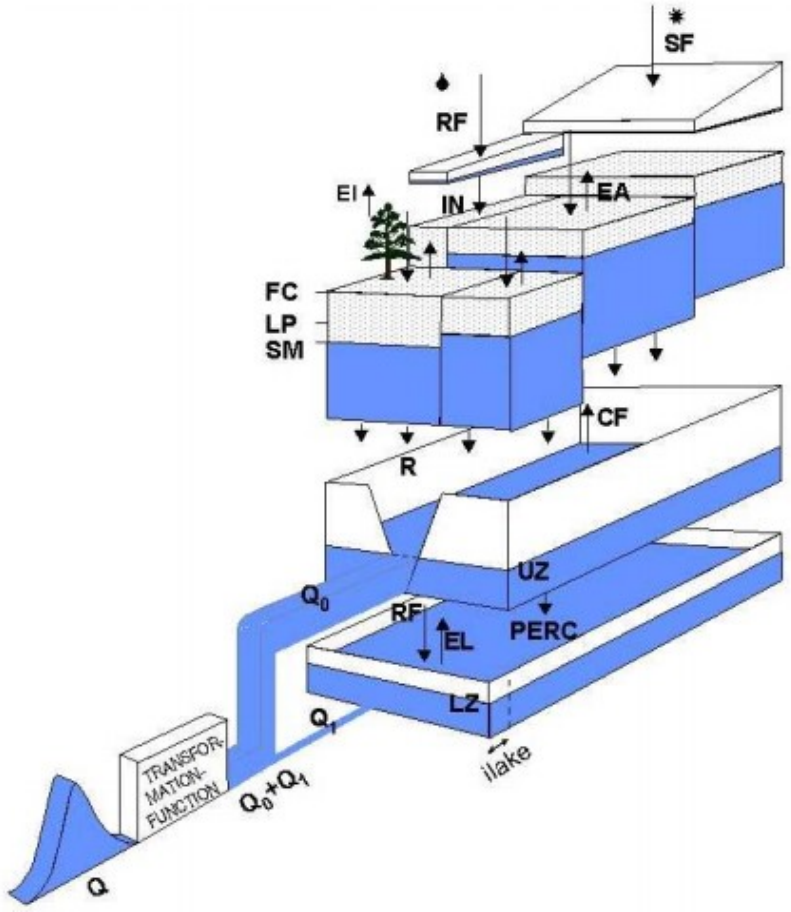

Figure 2.7 General structure of the HBV model. SF is snowfall, RF is rainfall, IN represents the contribution from rain or snow into the soil routing. EA is actual evaporation, EI is evaporation from forest zones and EL is evaporation from lakes. FC, LP, and SM are parameters that describe the soil moisture and will be explained later on. R is the contribution from the soil routing to the upper zone, CF is the maximum capillary flow from the upper zone to the soil moisture zone. PERC is the percolation capacity from upper to lower zone. UZ is upper zone, LZ is lower zone (groundwater), Q_0 is discharge from upper zone and Q_1 from lower zone. (SMHI, 2012).

2.5.1 Snow routine

The HBV model treats the catchment as a single unit. However, it computes precipitation, snow melt and accumulation for each elevation- and vegetation zone within sub-basins. In the HBV model the precipitation and temperature is adjusted to altitude with lapse rate parameters *pcalt* and *tcalt*

$$P = (1 + pcalt * h)p_m \quad (7)$$

$$T = (1 + tcalt * h)t_m \quad (8)$$

where T is the observed temperature (°C) adjusted to altitude, P is computed precipitation (mm), h is the altitude difference elevation zone and weighted mean of the weather stations, t_m is measured temperature (°C) and p_m is measured precipitation (mm). A recommended value for *pcalt* is 0.1 and the lapse rate for temperature *tcalt,* is 0.6 (°C/100m). The *pcalt* parameter could be estimated according to measurements in the study area.

Each elevation zone can be subdivided into 3 subzones. These subzones can represent different snow distribution with in an elevation zone. A *sfdisfi* describes the distribution, where a 0 value gives an even snow distribution over the elevation zone but a value between 0 and 1 means that the snow accumulation will be distributed between the 3 subzones linearly.

The HBV model uses a temperature index method to calculate snow melt, glacial melt and snow accumulation. Snow accumulation and separation between snow and rainfall is done by using a threshold temperature. It is possible to use a parameter *ttint* to describe the transition when precipitation is assumed to be a mix of rain and snow. If *ttint* is used the threshold temperature is extended to an interval where the upper end is 100% rain and lower end is 0% rain (SMHI, 2012).

There are separate snowfall (*sfcf)* and rainfall (*rfcf*) correction factors for observed precipitation. Measured precipitation is often effected by observation losses mostly related to wind. Snow measurements are generally more effected by wind then rain (SMHI, 2012).

The snow routine is based on a simple degree-day snowmelt relation with a threshold temperature (*tt*) close to 0°C to define the time when snow melt starts,

$$Snow\ melt\ =\ cfmax * (T - tt) \quad (9)$$

where *T* is the observed temperature (°C) adjusted to altitude by the program, *cfmax* is the melting factor ($mm^oC^{-1}\Delta t^{-1}$) and *tt* the threshold temperature that tells when snow melt starts. It is possible to use a different threshold parameter (*dttm*) to account for when precipitation falls as rain or snow. To account for difference in shortwave radiation between seasons, where more sun is in summer than winter, the *cfmax* can be described with two parameters. *Rmfhigh* is the snow melt factor in June 21st and *rmflow* is the snow melt factor in December 21st. The snow melt factor then increases linearly from December 21st until June 21st when it starts to decrease again.

The snowpack retains water to a certain extent. This is described in the model by a retention coefficient *whc*. When the temperature drops again the retained water refreezes in the snowpack according to the formula,

$$Refreezing\ melt\ water\ = cfr * cfmax * (T - tt) \quad (10)$$

where *cfr* is a refreezing factor.

For glacier zones, the same formula is used as for snow melt but with a different melting factor,

$$Glacier\ melt\ = gmelt * (T - tt) \quad (11)$$

where *gmelt* is the melting factor for the glacier ($mm^{o}C^{-1}\Delta t^{-1}$).

The glacier melt is only applied when there is no snow in the glacier zone (SMHI, 2012).

2.5.2 Soil moisture routine

Input data for the soil moisture routine is precipitation, potential evapotranspiration and snow melt. The output is actual evapotranspiration, soil moisture and groundwater recharge. The soil moisture routine is the main part controlling runoff formation. The soil moisture routine is based on three parameters, β, *lp* and *fc*. β controls the contribution to the response function (runoff coefficient) from rainfall or snow melt. *Lp* is a soil moisture value that tells when the actual evapotranspiration has reached potential value and is given as a fraction of *fc*. *fc* is the maximum soil moisture storage and is in mm. Figure 2.8 describes the soil moisture routine (SMHI, 2012).

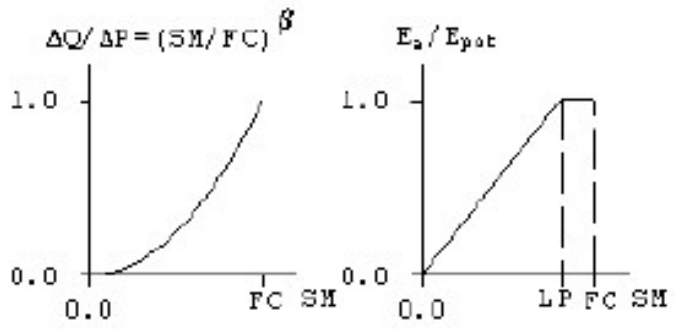

Figure 2.8 Description of the soil moisture routine (SMHI, 2012).

SM is the computed soil moisture storage, ΔP is contributed rainfall or snowmelt, ΔQ is contribution to the response function (effective rainfall), E_{pot} is potential evaporation (mm), E_a is computed actual evapotranspiration (mm).

The contribution to runoff is less when the soil is dry than when it is wet. The soil routine also affects the actual evaporation, as it decreases when the soil dries out.

2.5.3 Potential evaporation

Potential evaporation can be accounted for in two different ways in the HBV model. Long term mean values of potential evaporation can be used as input to the HBV model and is the traditional method. It is therefore assumed that inter annual variations in actual evaporation is more closely dependent on soil moistere than on the variations on inter annual potential evaporation. The model allows for adjustment to the potential evaporation for weather variations in temperature using a factor *etf*. Potential evaporation is then adjusted according to the formula,

$$E_{pot} = E_0(1 + etf * \partial t) \quad (12)$$

where *dt* is deviation of temperature from normal and E_0 is input monthly mean value (mm). Monthly mean values thus increase when actual temperature increases above normal temperature. It is also possible to use an elevation adjustment parameter *ecalt* to allow increase or decrease of potential evaporation dependent on elevation (Berglöv, German, Gustavsson, Harbman & Johansson, 2009).

An alternative method is to calculate the potential evaporation as being proportional to air temperature. The model then calculates the potential evaporation using a simple variation of Thornthwaites equation,

$$E_{pot} = athorn * stf(t) * T \ (= 0 \ if \ T < 0) \quad (13)$$

where *T* is the observed temperature (°C) adjusted to altitude, *athorn* is a conversion factor and *stf(t)* is to describe seasonal variations in the relation between evaporation and temperature (Berglöv, German, Gustavsson, Harbman & Johansson, 2009). The monthly factors used in Thornthwaite method were developed for catchments in Scandinavia and might not be directly applicable outside of Scandinavia (SMHI, 2012).

2.5.4 Response routine

Excess water from the soil moisture zone is transformed to runoff in the response routine. It also accounts for direct precipitation and evapotranspiration in lakes and river areas. The response function consisted of an upper and lower reservoir. The upper reservoir is a non-linear reservoir and the lower is a linear reservoir as is shown in Figure 2.9. Quick flow (over land flow) is computed from the upper reservoir and slow flow from the lower reservoir. Water from the upper reservoir percolates to the lower reservoir which represents the groundwater storage that contributes to base flow (SMHI, 2012).

The yield from the soil moisture routine goes to storage in the upper reservior. As there is water in the upper reservoir it percolates down to the lower reservoir depending on the parameter *perc* (mm/day). With high yield for the soil routine the upper reservoir contibutes directly to discharge as long as yield is higher than the parameter *perc* (SMHI, 2012).

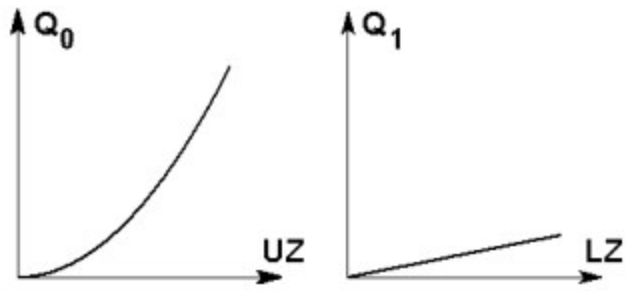

Figure 2.9 Description of the response routine (SMHI, 2012).

The outflow from the upper non-linear reservoir is computed,

$$Q_0 = k * UZ^{(1+alfa)} \quad (14)$$

where Q_0 is the outflow from the upper reservoir (mm), UZ is the amount in upper reservoir (mm), k is the recession coefficient for the upper reservoir and alfa is a measure of non-linearity of the reservoir.

The outflow from the lower reservoir is computed,

$$Q_1 = k_4 * LZ \quad (15)$$

where Q_1 us the outflow (mm), LZ is the amount in the lower reservoir (mm) and k_4 is the recession coefficient for lower reservoir (SMHI, 2012).

2.5.5 Transformation function

The generated runoff from the response routine is distributed over time steps through a transformation function using one free parameter, *maxbaz*. The transformation function is a simple filter technique that uses a triangular distribution of the weights as shown in Figure 2.10, to transform runoff from the response routine (SMHI, 2012).

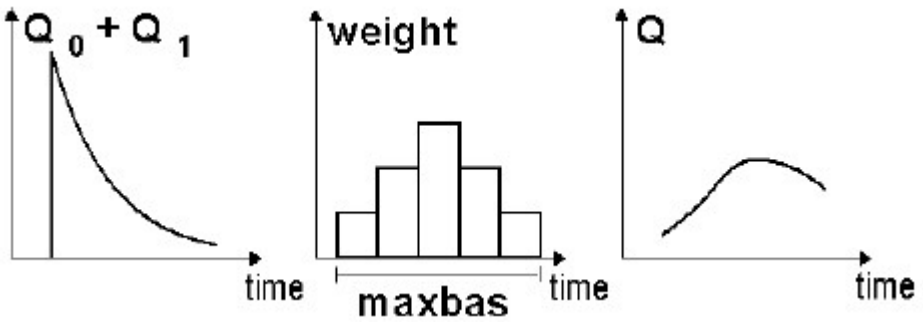

Figure 2.10 Description of the transformation function (SMHI, 2012).

2.5.6 Evaluating efficiency

Three efficiency criteria were used to evaluate the HBV simulation performances.

1. Nash-Sutcliffe efficiency coefficient,

$$E = 1 - \frac{\sum_t (QC - QR)^2}{\sum_t (QR - Q_{mean})^2} \quad (16)$$

where QC is simulated discharge, QR is recorded discharge and QR_{mean} is recorded mean discharge over the simulation period. E criteria was introduced by Nash and Sutcliff (1970) and is often used in hydrological modeling (Berglöv, German, Gustavsson, Harbman & Johansson, 2009). The closer that E is to 1 the better is the efficiency of the model.

2. The logarithmic Nash-Sutcliffe efficiency coefficient,

$$E_{log} = 1 - \frac{\sum_t (QC_{log} - QR_{log})^2}{\sum_t (QR_{log} - QR_{log,mean})^2} \quad (17)$$

where QC_{log} is the logarithm of computed discharge, QR_{log} is the logarithm of recorded discharge and $QR_{log,mean}$ is the logarithm of mean recorded discharge. Most weight is given to high flow using the normal E. Thus E_{log} better reflects the performance for intermediate and low flows (SMHI, 2012).

3. Accumulated difference between observed and simulated discharge,

$$Acc.dif. = \sum_t (QC - QR)\, C_t \quad (18)$$

where C_t is coefficient to transform mm over the basin. This criteria helps to indicate if the model overestimates or underestimates the total discharge volume (SMHI, 2012).

The efficiency criteria help to evaluate the accuracy of the model and to get an overview of the model performance. Visual inspection of the simulation and observed hydrograph is also very important in judging the model results (Berglöv, German, Gustavsson, Harbman & Johansson, 2009).

2.6 Model Calibration

The simulations were calibrated with measured discharge data from Dynkur gauging station. Prior to calibration, the discharge data were checked both for missing data and any unreliable values. The observed discharge has been quality marked: good, estimated and suspected. Values marked as estimated and suspected were checked and if they were evaluated as unreliable they were deleted from the time series. Only obvious unreliable values were deleted and almost all of them were during winter.

The model was calibrated for a seven year period and then validated over four year period. The calibration period started at 1.10.2003 and ends 1.10.2010. The validation period starts when calibration ends and stops in 31.12.2014. After an optimum parameter set had been obtained for the whole period each year was evaluated and the snow cover readjusted in accordance with measured SWE. Since it is difficult to measure snow precipitation accurately with automatic rain gauges, the measured SWE might provide a good reference point. Adjusted snowpack might improve simulations for the spring discharge which is a difficult period to model accurately.

With the HBV model only manual calibration is available. Parameters were calibrated by trial and error in the following order,

1. Volume parameters; *rfcf*, *sfcf.*

2. Parameters that affect snow accumulation and melt. Dependent on snow melt method; *cfmax*, *rmfhigh*, *rmflow*. To adjust threshold when melting starts*; tt* and *dttm*. Water holding capacity; *whc*.

3. Soil parameters, *fc*, *β*, *lp*, *athorn*.

4. Response parameters; *khq*, *k4*, *maxbaz, perc*.

The parameters were calibrated and the results were evaluated with efficiency criteria that were described in previous chapter and by observing the hydrograph. The purpose of calibrating the HBV model was to seek an optimal parameter set that represents the catchment. However, experience has shown that there is no unique parameter sets with optimum solution but several parameter sets that give similar results during a calibration period. When predicting runoff in the future, these different parameter sets might give different results (Seibert, 1997).

The model output is tuned using the models parameters. There are various ways of estimating model parameters e.g. by using tables from prior estimates and calibrations. However, the parameters may not represent the true process value of the catchment that results in uncertainties in the prediction of the model. These uncertainties can reduce likelihood of success when making predictions with the model (Abebe, Ogden & Pradhan, 2010). To reduce the uncertainties the parameter set is tested on an independent discharge data.

3 Data

3.1 Input data

Meteorological data for the catchment were obtained from six automatic weather stations in, or in the vicinity of the catchment. These weather stations are owned by Landsvirkjun and have been in operation from 10 to 20 years (Icelandic Met Office, n.d.). The type of meteorological data that were used in the study was precipitation, temperature, wind and humidity. The Icelandic Met Office (IMO) provided all the meteorological data time series that were used.

Snow measurements have been done in two locations within the catchment at Setur and Kjalöldur and one at a relatively short distance from the catchment at Veiðivatnahraun. Most of the snow measurements were done once a year between the middle of March to the beginning of May, prior to spring floods. The snow and discharge measurements were obtained from Landsvirkjun.

The gauging station for Dynkur catchment is close to Dynkur waterfall. The discharge was measured with stage measuring instrument where water surface elevation is measured and discharge computed from stage-discharge relations. Since 2005, the discharge resolution for the time series has been 15 minutes, while before 2005 a mean daily discharge was produced. The coordinates for the catchment were obtained from Landsvirkjun and adjustments were made so that Dynkur is the discharge outlet point for the HBV model.

Discharge data from Dynkur gauging station goes back to 1988. Temperature measurements in the catchment area started in 1993, measurements from rain gauges in the area started in September 2003 and snow measurements at Setur started in 2002. Hydrological simulations were limited to the precipitation time series and therefore the main time of interest was the period between 2003 until 2015. The meteorological stations and snowpack measurements locations are shown in Figure 2.2 and information about these measurements locations are in Tables 3.1 and 3.2.

Table 3.1 Weather stations locations used in the hydrological modeling (Icelandic Met Office, n.d.)

Weather Station	St. number	Location	MASL	Since
Búrfell	6430	64°07.010', 19°44.691'	249	1993
Setur	6748	64°36.258', 19°01.116'	693	1997
Vatnsfell	6546	64°11.735', 19°02.800'	539	2004
Þúfuver	6760	64°34.509', 18°36.051'	613	1993
Veiðivatnahraun	6657	64°23.706', 18°30.286'	647	1993
Hveravellir	6935	64°52.005', 19°33.733'	641	1996

Table 3.2 Location of the snow measurements (Sigurðsson & Jóhannesson, 2014)

	Locations	MASL	Since
Setur	64°36.258', 19°01.116'	693	2002
Veiðivatnahraun	64°23.706', 18°30.286'	647	1995
Kjalöldur	64°33,459', 19°57,596'	590	1975

Rain gauges were normally installed a few years after the weather stations, except for Vatnsfell. Long term monthly potential evapotranspiration values for the catchment were obtained from a research paper conducted by Markús Á. Einarsson (1972) about evapotranspiration in Iceland.

3.2 Data verification

Measurements from precipitation gauges are known to have random and systematic errors. The causes of systematic errors in the gauges are wind field deformation around the gauges, wetting of the inner wall of the gauge and evaporation of the water accumulated (Nespor & Sevruk, 1998). Wind induced error for rain depends on wind and rain intensity and has been estimated to be around 30% on average for rain and for snow around 80-100% (Sigurðsson, 1990; Sigurðsson & Jóhannesson, 2014). No wind corrections were performed on the data instead a correction factor was used in the program to adjust the rainfall.

Almost all time series that are created by instruments such as precipitation measurements from automatic weather stations are affected by a percentage of missing values (Simolo, Brunetti, Maugeri & T.Nanni, 2009). For the automatic weather stations in the highlands, missing values are most likely because of malfunctions in the appliances, due to frozen water on appliances or some other technological reasons. For the HBV model to run properly, missing values in time series needed to be filled in.

Many interpolation methods have been developed for estimating missing observations in a climatic time series. Most of them have been to evaluate monthly or yearly values, while methods to evaluate daily values are scarce and show considerable errors. For precipitation it is even more difficult to estimate missing values because of large space and time variability of precipitation (Simolo et al., 2009). Large difference in measured precipitation can occur between stations due to elevation and other spatial features in the landscape that result in higher precipitation in one place than in another.

Time series that were used for the hydrological simulation all had missing observation periods. Figure 3.1 and Figure 3.2 show the missing data for precipitation, temperature and discharge. Only short periods are missing for temperature while for precipitation longer periods are missing. Missing precipitation data are almost always during the winter months and could be explained by climatic scenarios causing malfunction in rain gauges. Precipitation time series for Setur is missing almost three years between 1.12.2011 and 1.10.2014 and measurements at Vatnsfell don’t start until 1.12.2004.

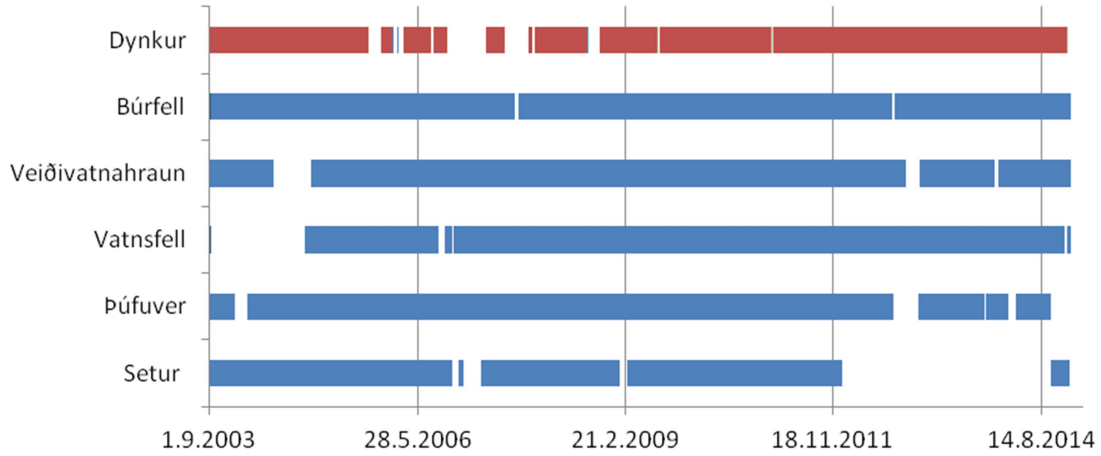

Figure 3.1 Missing precipitation and discharge data plotted on a time line. Blue color represents observed precipitation data red color observed discharge data period and blanks represents missing data in the time series.

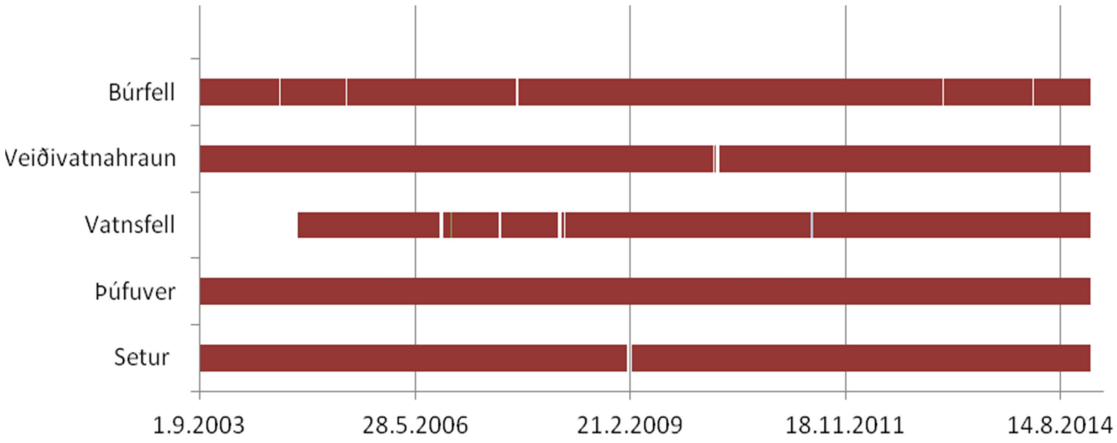

Figure.3.2 Missing temperature data plotted on a time line. Red color represents observed temperature data and blanks represents missing data in the time series.

The gauging station had some discontinuity in the time series, with an exceptionally bad period in 2007 when the station was damaged in flooding. Smaller discontinuities in the discharge time series were normally during winter and a likely reason is ice in the river that causes disturbance in the data. There can also be malfunctions in the instruments. The quality of the discharge data affects the calibration, where low quality discharge data will result in inaccurate calibrated simulations.

Many different methods have been developed to estimate missing precipitation values. Among common methods are the Inverse Distance Weighting Method (IDWM), the normal-ratio method and a simple average method (Teegavarapua & Chandramoulia, 2005). Using a simple average method was recommended by McCuen (1998) if the annual precipitation value at each of the rain gauges differed by less than 10%. If the annual value exceeded the 10% from annual precipitation value of the missing data station, the normal-ratio method was recommended. The equation for normal ratio method,

$$P_x = \frac{1}{n}\sum_{i=1}^{i=n}\frac{N_x}{N_i}P_i \quad (19)$$

where P_x is the estimated missing rain gauge value at station x, n is the number of nearby stations, P_i is the precipitation at the i_{th} replacing station, N_x and N_i are the normal annual precipitation value for the x and i_{th} station.

Another method called the Correlation Coefficient Weighting Method (CCWM) resembles the IDWM but instead of using distance as weights, they are replaced by the correlation coefficient. The correlation coefficient is calculated between any two data sets obtained from two locations (Teegavarapu, 2012). The missing rain gauge value is estimated by,

$$P_x = \frac{\sum_{i=1}^{n} P_i * R_{xi}}{\sum_{i=1}^{n} R_{xi}} \quad (20)$$

where P_x is the estimated value, R_{xi} is the coefficient of correlation, P_i is the observation value at station i.

Both the normal ratio method and the CCWM were tested on data sets from two different stations and the Root Mean Square Error (RMSE) used to evaluate and compare these methods. The RMSE is given by,

$$RMSE = \sqrt{\frac{1}{n}\sum_{i-1}^{N}(G_i - Y_i)^2} \quad (21)$$

where n is number of stations, G is observed value and Y is prediction value. Results are presented in Chapter 4.1.2.

3.3 Snow survey

The snow survey at Setur, Kjalöldur and Veiðivatnahraun have involved snow depth measurements over a profile using snow stakes for measurement reference and density measurements of snow to calculate the snow water equivalent (SWE). In Kjalöldur six snow stakes were implemented in 1975 with average spacing of 20 m between stakes. In 2003, 11 new snow stakes were installed at Kjalöldur in a new location with 100 m spacing over a 1 km stretch. In Veiðivatnahraun 20 snow stakes were implemented in 1995, forming a cross that measures a profile from north to south and west to east. Landsvirkjun also had snow stakes put up at Setur, first in 2002, when 20 stakes were put west to east with 100 m spacing. In 2003, another 10 snow stakes were implemented north to south also with 100 m spacing (Sigurðsson & Jóhannesson, 2014).

An overview of snow measurements in the highlands in Iceland were presented in a report by Sigurðsson and Jóhannesson (2014). SWE and snow density measurements were presented in the report. The results from snow density measurements and snow water equivalent (SWE) are summarized in Figure 3.3 and Figure 3.4. The period from 2002 to spring 2014 is of special interest. No measurements were done 2003, 2007 and 2013. The measurements in 2014 were done in January when the snowpack was still accumulating snow, and therefore does not represent total spring melt and has limited value for this study.

Since snow measurements started at Setur, records show that the site accumulates the largest amount of snow, i.e. compared to Veiðivatnahraun and Kjalöldur. The difference in measured SWE between these locations is large, in that Setur has on average two times more SWE than Kjalöldur and five times more SWE than Veiðivatnahraun, but it varies a lot between years. Measured SWE in Veiðiðvatnahraun has been limited during the study period with little snow measured, compared with other locations. For three years, there was not sufficient snow to dig a snow pit in Veiðivatnahraun.

The average snow density for the snow profiles spreads over relatively wide span or from 145-760 kg/m^3 where half the values are between 420-515 kg/m^3. For snow profiles deeper than 75 cm, the average snow density for these profiles was between 385-605 kg/m^3 (Sigurðsson & Jóhannesson, 2014). Figure 3.4 shows that the snow profile for Veiðivatnahraun is normally much smaller compared to the other locations, and two years it had no snow when measurements were supposed to be taken.

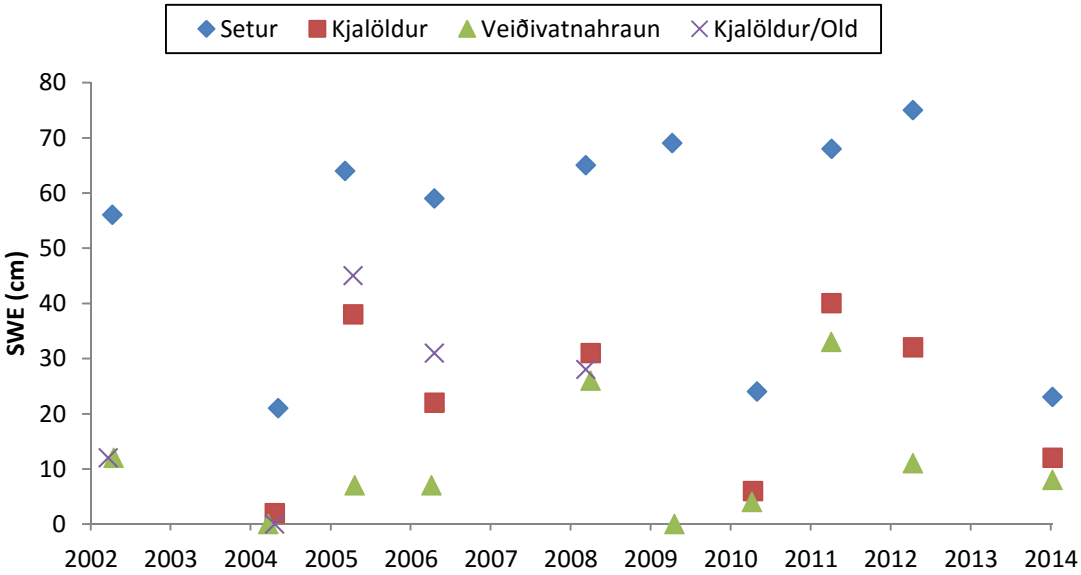

Figure 3.3 Calculated Snow Water Equivalent (SWE) for the snow cover on the bases of snow depth measurements for Setur, Kjalöldur, Kjalöldur old snow stakes location and Veiðivatnahraun (Sigurðsson & Jóhannesson, 2014).

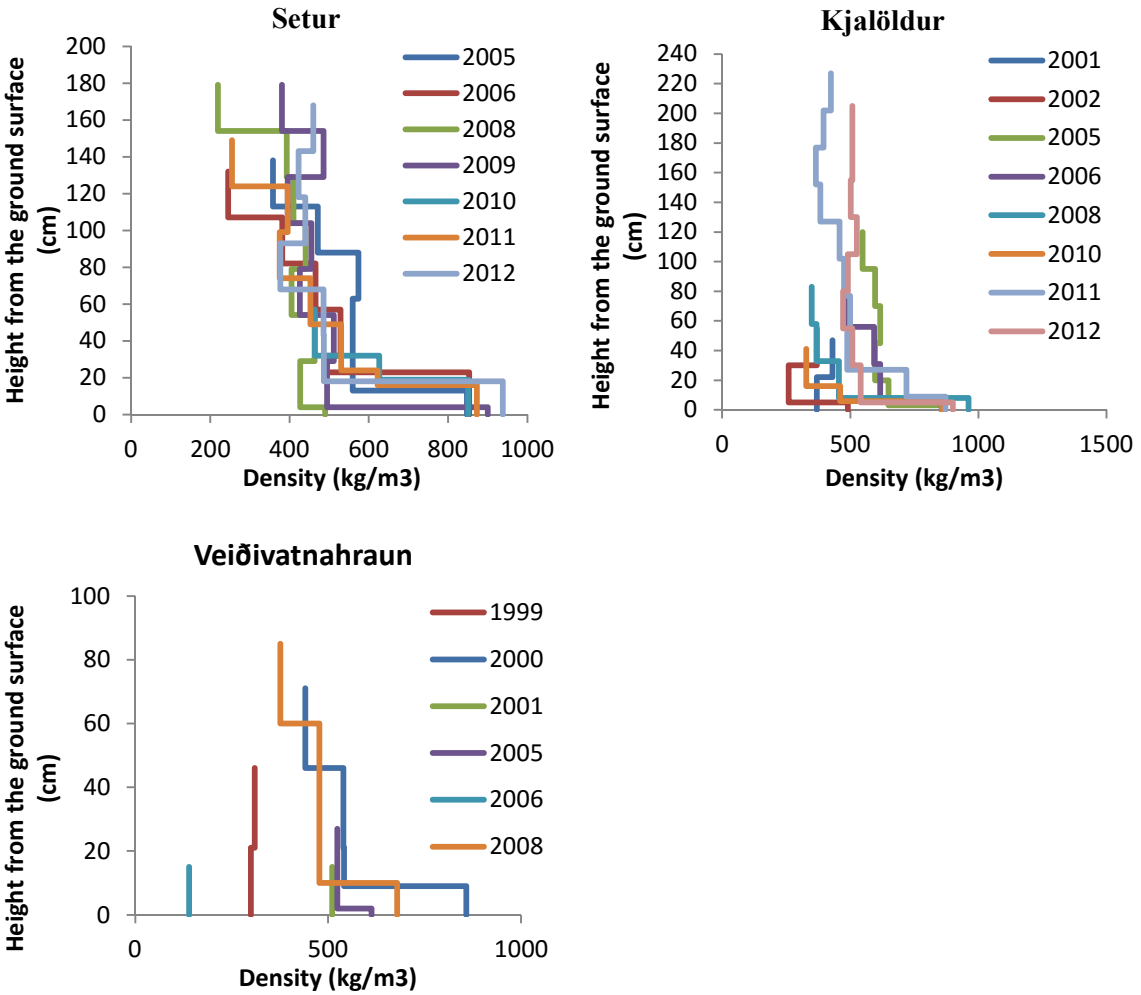

Figure 3.4 Snow density measurement for snow profiles in Setur (top left), Kjalöldur (top right) and Veiðivatnahraun (bottom) (Sigurðsson & Jóhannesson, 2014).

It was evaluated if there was a connection between SWE data and spring discharge and if it could be used as a reference point to adjust the snowpack in the HBV model. The density measurements were only used in discussion. It was evaluated if difference in simulations results was observed between years with thick ice layer at the bottom of snowpack and years with thin ice layer. The ice layer is observed from Figure 3.4, for example the thickest ice layer over study period at Setur was in 2006, where over 20 cm layer with density over 800 kg/m^3.

4 Results and Discussion

4.1 Data analysis

4.1.1 Runoff

The runoff in Upper Þjórsá River for Dynkur catchment was analyzed for the period between 1998 and 2014 Figure 4.1 shows the mean daily flow and maximum annual flood during that period. It also shows the standard deviation of the mean flow. The highest standard deviation is during winter from January to March. That is when the large winter floods occur. During the winter season the average flow is at minimum and the main runoff component comes from base flow. In winter the temperature drops well below zero in Dynkur catchment area and ice forms in the river. The river ice can cause disturbances in the river gauging system, which are observed as gaps in the runoff time series or unusual runoff values, such as runoff well below normal winter base flow. Most of the gaps (time series data that were missing) or data that had values marked as suspicious, were observed in the winter season. This was noted when hydrological simulations were performed.

The spring runoff season starts as soon as the temperature rises enough for the snow melt to start to contribute to the runoff. Figure 4.1 shows that on average the spring melt starts in middle of April; that is when rising slope on the hydrograph starts. The spring season is considered to finish when most of the snow in the non-glacier catchment area has melted. On average, the spring is from middle of April until June/July. That was the period of main interest for the study, which chiefly aimed to analyze the spring runoff. The main focus was on finding out what would be the expected total discharge volume related to snow accumulation during winter and to be able to simulate the spring melt with the greatest possible accuracy.

Summer runoff season was defined as the period when the glacial melt has become the dominant factor in the runoff and most of the snow has melted. Figure 4.2 shows the relations between the mean daily flow and the mean daily temperature. It is difficult to define when spring runoff finishes and summer runoff starts, or when glacial melt takes over the snow melt as the main runoff component. In general, the glacial melt starts to contribute to discharge early June and has become the dominant discharge component in late June, depending on the annual snowpack and the temperature. The glacial melt usually starts to increase when the average daily temperature at Setur reaches 4 to 6°C.

The autumn runoff season starts after most of the glacial melt has finished by mid-September and ends in early November. Flooding in autumn is mainly caused by rain storms. There is little snow on the ground during these events and therefore no snowmelt to be added to the discharge. In autumn the standard deviation is the lowest over the year and the maximum annual flood never occurs during the autumn period.

The two largest annual maximum floods from 1998 to 2014 occurred during the winter season. Seven maximum annual floods were in spring, six in summer, four in winter and none in autumn.

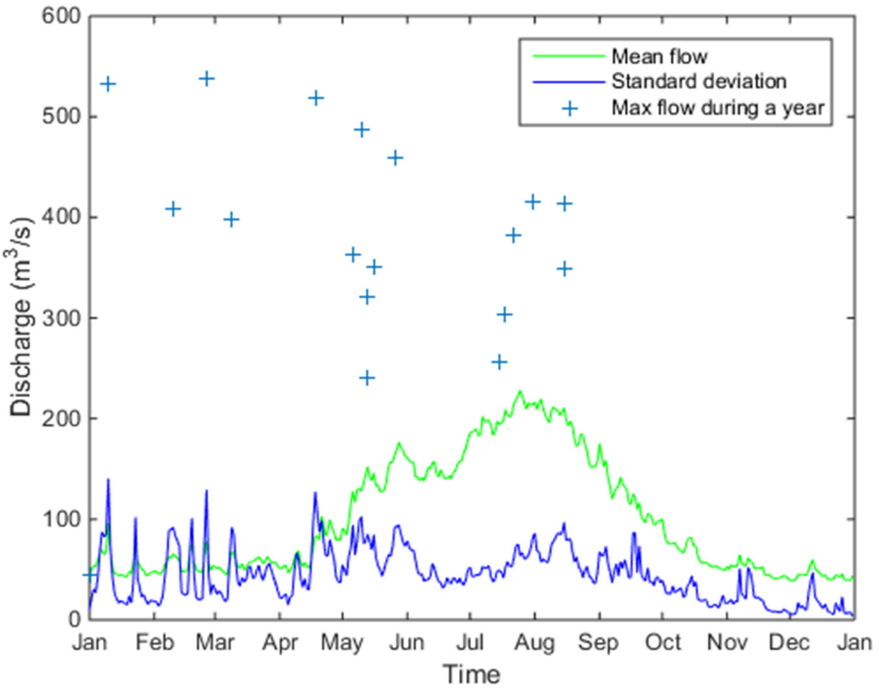

Figure 4.1 Mean daily flow, standard deviation and annual maximum flow in Upper Þjórsá River between 1998 and 2014 (gauging station at Dynkur).

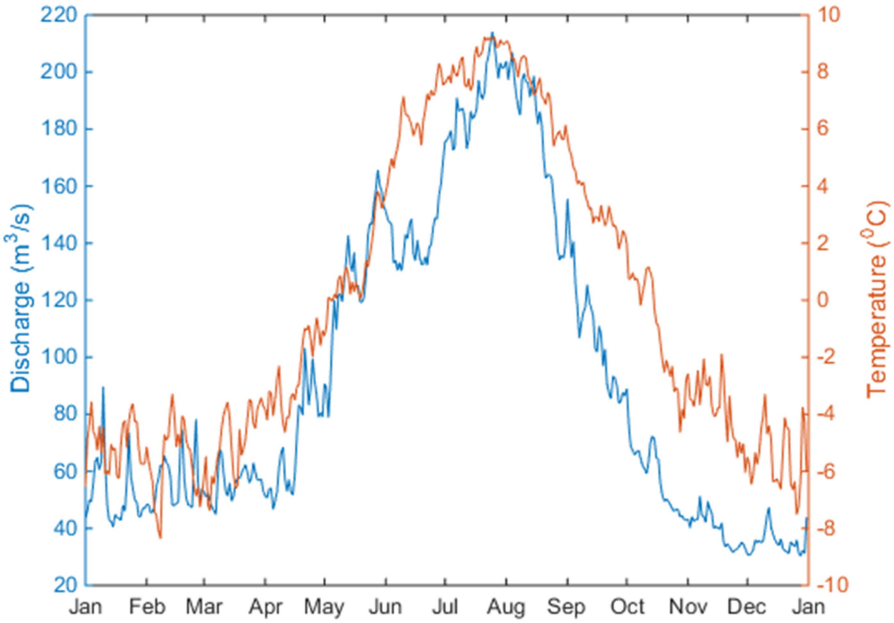

Figure 4.2 Mean daily flow and temperature 1998-2014. Flow measured at Dynkur and temperature at Setur.

4.1.2 Precipitation and temperature

The precipitation time series for the period from September 2003 and to end of 2014 have significant discontinuities in them with periods of missing data. These data gaps needed to be filled before running the HBV model. Normal Ratio method (NRM) and Correlation Weighting Method (CCWM) which were presented in Chapter 3.2 were tried on the time series from 2004 to 2008 to predict precipitation for rain gauges at Setur and Vatnsfell. The comparison between the CCWM and the NRM showed slight advantage to NRM. The missing precipitation data for specific stations were replaced using the NRM. Table 4.1 shows the predictions efficiency when using NRM and CCWM. The efficiency was measured with root mean squared error (RMSE). The result show that for Vatnsfell the NRM gives a better estimation measured with RMSE, where RMSE for NRM was 3.3 but for CCWM was 4.1. For the rain gauge at Setur the RMSE measured similar results both for NRM and CCWM. Figure 4.3 shows comparison between observed and predicted precipitation values. The results are far from perfect and show the inaccuracy in predicting precipitation value for a specific rain gauge using other rain gauges in the vicinity.

Table 4.1 Prediction efficency measuerd with RMSE.

	NRM	CCWM
Vatnsfell	3.3	4.1
Setur	3.4	3.3

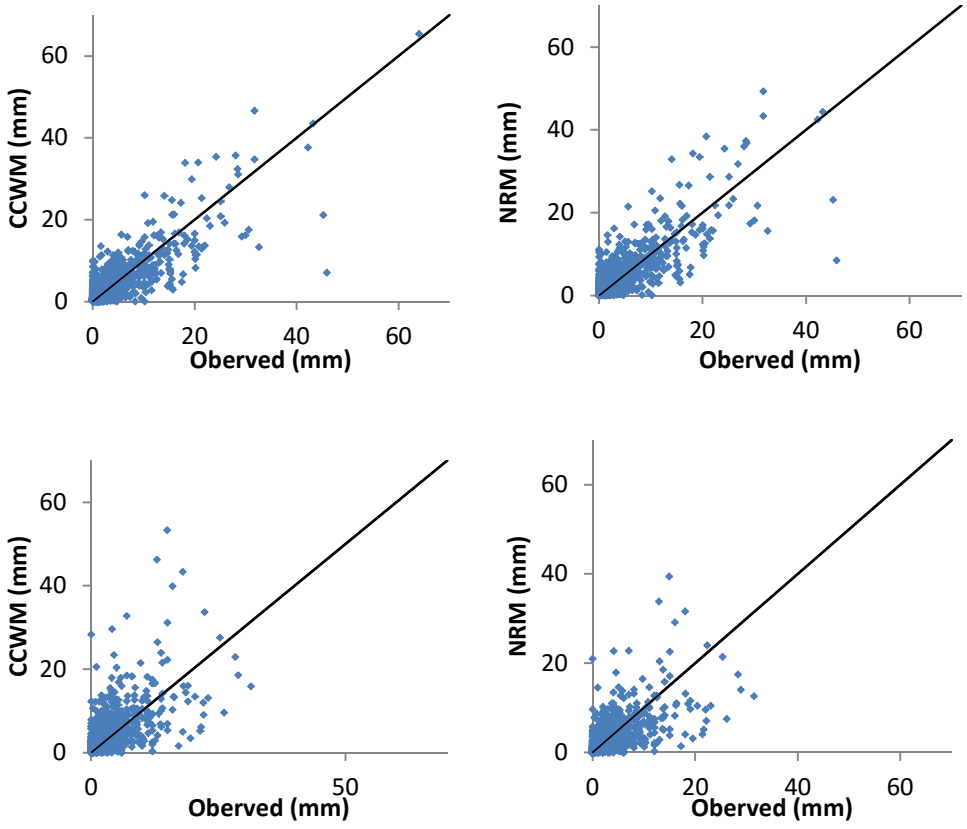

Figure 4.3 Comparison between observed and predicted precipitation values using both NRM and CCWM. The two plots above are for Setur and the two below are for Vatnsfell.

The longest period of missing precipitation value for Setur was from October 2011 to October 2014. For that reason the time series for Setur weather station was not used in the final simulations. Vatnsfell weather station did not start operation until December 2004 but simulations started in October 2003. However, the time series for Vatnsfell is fairly consistent during the rest of the period. Also, the rain gauge is in an elevation that represents a large part of the catchment. Therefore precipitation time series for Vatnsfell was used with replaced values for the first year. Vatnsfell is around 15 km away from the catchment boundary, which is shown in Figure 2.2.

Table 4.2 shows the results for average annual accumulated precipitation for the rain gauges used in the study. Rain gauges that were used for simulations where located at Þúfuver, Vatnsfell and Búrfell. The rain gauge at Setur was also used to test the sensitivity of the model if different rain gauges were used. According to Table 4.2 Þúfuver receives on average most precipitation and Vatnsfell the least.

Table 4.2 Average annual accumulated precipitation during the period 2004-2015 for six rain gauges in or in the vicinity of Dynkur catchment.

	Búrfell	**Setur**	**Vatnsfell**	**Veiðivatna-hraun**	**Þúfuver**	**Hveravellir**
Precipitation (mm)	934	1018	725	816	1109	770

Temperature is an important input variable for the hydrological simulations for Dynkur catchment. Energy input controls the rate of snow and glacial melt and temperature is usually well correlated with energy (Anderson, 2006). Since the largest discharge components for Dynkur catchment is glacial melt in summer and snowmelt in spring, temperature plays a crucial role in the hydrological simulations. Fortunately, the quality and continuity of the temperature time series relevant for the catchment are much better than for precipitation. Normally, measurements are only missing for day or two and have minimum effect on the simulations.

4.1.3 Snow and precipitation data comparison

Setur and Veiðivatnahraun have rain gauges in close vicinity to the snow stakes used to measure the snow depth which the SWE was computed from. Comparison between snow precipitation values from the rain gauges to SWE measurements done on location is presented in Figure 4.4. The accumulated precipitation when temperature was at or below 0°C was compared to the SWE measured on location. Precipitation can fall as snow at higher temperature than 0°C and rain can fall at lower temperature than 0°C. It was assumed that on average the threshold temperature was 0°C for rain/snow. The accumulated snow precipitation was normally around 50 to 70% of total accumulated precipitation over winter months from beginning of November to middle of April.

It is a great simplification to compare measured SWE to accumulated precipitation, since melting, rain and evaporation is not taken into account. Over the winter months evaporation is low and affects the snow cover minimally. Rain on the other hand plays a large role in the evolution of the snow cover. When it rains the melting increases as energy from the rain gets added to the snow cover. However, if the rain and the temperature does

not reach a certain threshold that puts the snow cover into a melting phase, the rain is stored in the snow and eventually freeze, adding to the water equivalent of the snow cover.

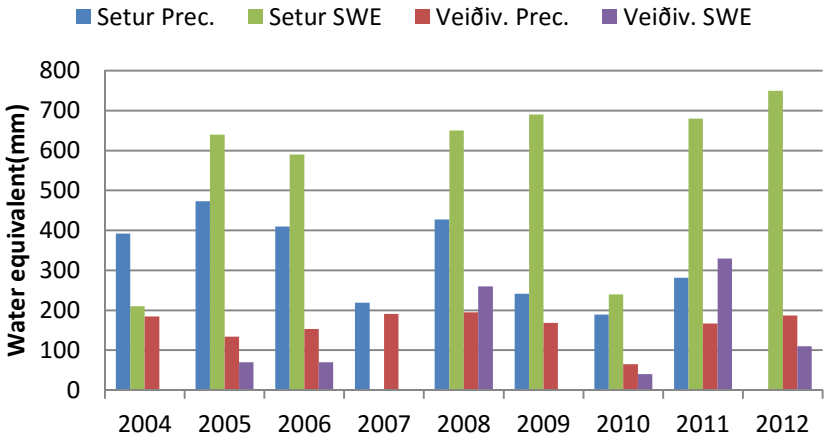

Figure 4.4 Accumulated precipitation from rain gauges when temperature is under or equal to 0°C and snow water equivalent (SWE) measured in Setur and Veiðivatnahraun.

Figure 4.4 shows that every year, except for 2004, the snow precipitation measured from the rain gauge in Setur was much less than the measured SWE in Setur. In 2004, snow measurements were done at the beginning of May, when the melting period had already started. That can explain why more precipitation was observed from the rain gauge at Setur than the SWE measured in 2004. Other years, the accumulated snow precipitation measured at the rain gauge at Setur was 20 to 60% less than SWE measurements on location showed. The fact that less snow is observed from the rain gauge could be explained by the inefficiency of rain gauges in capturing the precipitation when it is windy. This is a well known problem with rain gauges, especially when dealing with snow precipitation and wind.

The largest difference between measurements from rain gauge and on location at Setur was in 2011, where around 60% less water equivalent was observed from the rain gauge. Total accumulated precipitation (rain and snow) was around 430 mm which is still around 30% less than the measured SWE. That year a large winter flood occurred at the end of January which should reduce the SWE in Setur and reduce the difference between observation from rain gauge and measured SWE.

Average annual precipitation is around 20% less in Veiðivatnahraun than in Setur based on rain gauge measurements. According to SWE measurements, there is a great deal less snow accumulation in Veiðivatnahraun than in Setur. In Veiðivatnahraun, most years more snow precipitation was observed from the rain gauge than what the SWE measurement showed. Three reasons can explain this: the snow has melted, it has been redistributed with wind or the rain gauge overestimates the precipitation.

There is no obvious relationship between the accumulated snow precipitation measured at the rain gauges and SWE in both locations. In Setur, the rain gauge seems to underestimate by a large factor the snow accumulation and in Veiðivatnahraun the opposite is observed. The results show the unreliability of these rain gauges in measuring snow precipitation and

underline the importance of finding another approach to estimate the snow accumulation before spring melt start.

4.2 Spring runoff and snow measurements

Regression analyses were done to study the relationship between SWE measurements and the total volume of snowmelt (Q_{melt}) that delivers into the rivers during spring runoff. To compute the total volume of snowmelt, the flow was split into base flow and direct runoff, where the direct runoff was assumed to be mostly coming from snowmelt. The method that was used to split the flow into different runoff components is described in Chapter 2.4. Hydrographs in Appendix A show the spring runoff and the different runoff components for all the years that were studied.

Each site where the SWE measurements were carried out was evaluated individually with linear regression analysis, to see if the SWE measurements were representative for the catchment. If a coefficient of determination r^2 is high it indicates that the site is representative for the catchment and the measured SWE is likely to give a good prediction for the resulting snowmelt volume.

Since snow distributes unevenly over an area and the distribution varies from year to year, it is more likely that measurements from more than one location would better represent the snow accumulation of a catchment each spring. Introducing more variables to the regression analysis, a multiple regression analysis could be done. There are few key assumptions to keep in mind when applying multiple linear regression. One of them is that there should be little or no multicollinearity in the data. It is called multicollinearity when independent variables are not independent from each other. When independent variables are highly correlated with each other it is difficult to get reliable estimates on the coefficients of the regression equation and could adversely affect regression estimates (Franke, 2010).

In this study, SWE measurements from three different locations (Setur (S), Kjalöldur (K) and Veiðivatnahraun (V)) are presented as independent variables. The correlation between the independent variables was 0.19 between S-V, 0.41 between K-V and 0.69 between S-K. The r^2 value does not confirm or exclude the presence of multicollinearity. The independent variables are the same variable in a way that it describes the same thing but in a different location. Therefore, it is easy to assume that the independent variables are correlated to each other to some extent. However, the main purpose of using the multiple linear regression, was for prediction analysis and not causal analysis. The goal is just to get a regression equation that can predict future runoff volume based on snow measurements from all the three locations and not to study the cause or effect of individual independent variable. On that note a higher degree of multicollinearity is allowed and therefore used in this study. With longer time series a better estimation on the multicollinearity of the data would be possible.

Because of the problems involving in using the multiple linear regression analysis, another method was attempted to include all the measured SWE sites together. The mean SWE between the sites was computed and used as a single variable in a linear regression analysis. Both the mean SWE between Setur, Veiðivatnahraun and Kjalöldur (S-K-V) and between only Setur and Kjalöldur (S-K) was computed, since Veiðivatnahraun is not inside the catchment area. Figure 4.5 and 4.6 shows the results from the linear regression

analysis. Two different methods were used to compute the base flow, a straight line method (SLM) and Eckhardt filter method (EF). These are described in Chapter 2.4. Both methods are represented in the figures. The study period was from 2002 until 2012, but no snow measurements were done in 2003 and 2007.

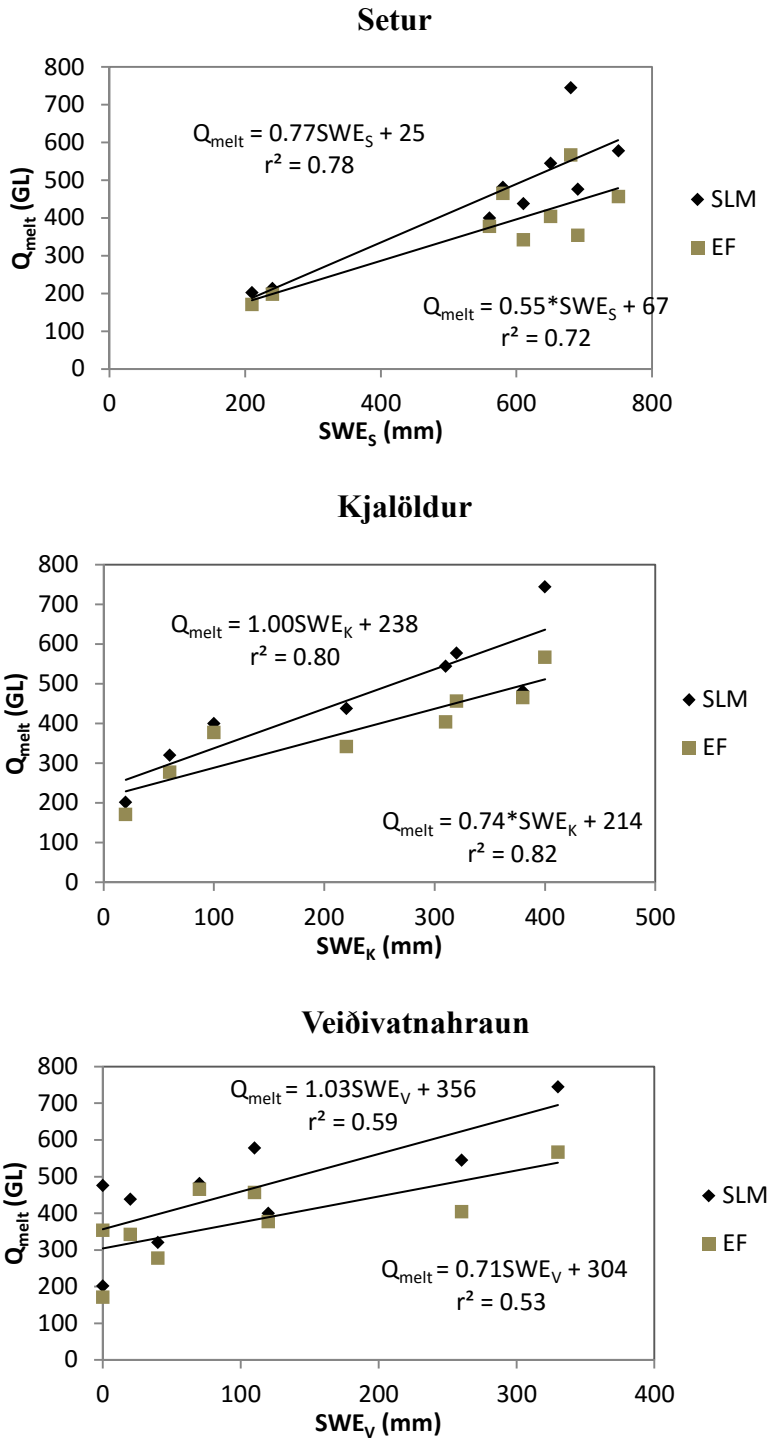

Figure 4.5 SWE measured at individual site plotted against Q_{melt} (total snowmelt).

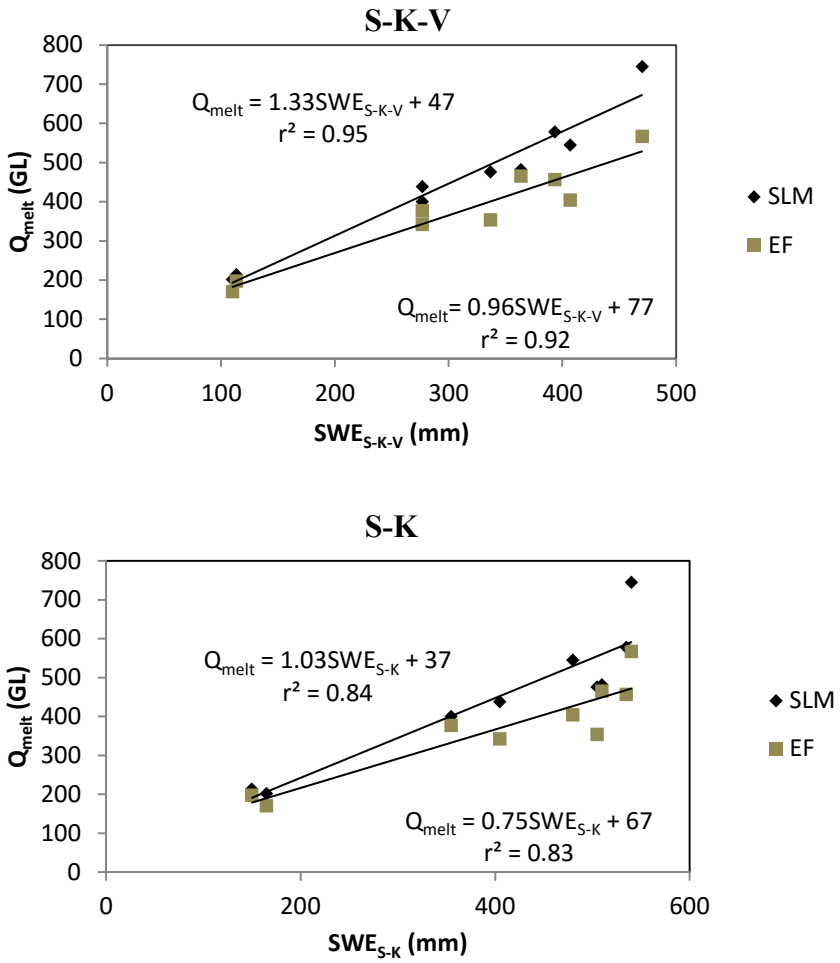

Figure 4.6 Mean SWE between Setur, Kjalöldur and Veiðivatnahraun (S-K-V)(top), and Setur and Kjalöldur (S-K)(bottom) plotted against Q_{melt} (total snowmelt).

Table 4.3 shows the coefficient of determination r^2, computed from linear regression for plots on Figures 4.5 and 4.6 and for the multiple linear regression. The results show that the data do fit to the regression line for all cases fairly well, except for Veiðivatnahraun. The coefficient of determination r^2, was between 0.59 to 0.95, lowest for Veiðivatnahraun. When more sites were presented together, r^2 increased. The r^2 is highest when the mean SWE between Setur, Kjalöldur and Veiðivatnahraun was used, where r^2 is 0.95, which is very high for a snowmelt regression model like this. From the graph with highest r^2 an empirical regression equation was obtained that can be used to predict the total snowmelt,

$$Q_{melt}\ (GL) = 47 + 1.33 * SWE_{S-K-V} \qquad (22)$$

where $SWE_{S\text{-}K\text{-}V}$ is the mean snow water equivalent (mm) between Setur, Kjalöldur and Veiðivatnahraun.

Multiple linear regression was done with Excel where snow measurements from Setur, Kjalöldur and Veiðivatnahraun were independent variables and the Q_{melt} the dependent variable. This is the multiple regression model that was obtained,

$$Q_{melt}\ (GL) = 77 + 0.21 * SWE_S + 0.71 * SWE_K + 0.58 * SWE_V \qquad (23)$$

where SWE_S is snow water equivalent (cm) measured in Setur, SWE_K is for Kjalöldur and SWE_V is for Veiðivatnahraun. R-squared was 0.97 with multiple regression. The multiple regression does not improve the fit by much compared with when the SWE_{S-K-V} was used.

Table 4.3 Coefficient of determination r^2 for plots on Figures 4.5 to 4.9.

Base flow type	Straight line	Eckhardt filter
Setur	0.78	0.72
Kjalöldur	0.80	0.82
Veiðivatnahraun	0.59	0.53
SKV	0.95	0.92
SK	0.84	0.83
MLR	0.97	0.93

Figure 4.7 shows the results when the total snowmelt (GL) was divided with the catchment area that is not covered by glacier and plotted against SWE_{S-K-V} and SWE_{S-K}. By dividing the total snowmelt (GL) by the catchment area, the average depth of total snowmelt is obtained. The result shows that the measured SWE is almost equal to total snowmelt (mm) with slope of the straight line close to 1. That indicates that the SWE_{S-K-V} and SWE_{S-K} is close to the area average SWE of the catchment. However, precipitation, evaporation and the volume of water that goes to groundwater during the melting period have not been taken into account. Precipitation adds to the direct runoff while evaporation and the volume that goes to groundwater reduce the volume that goes to the direct runoff.

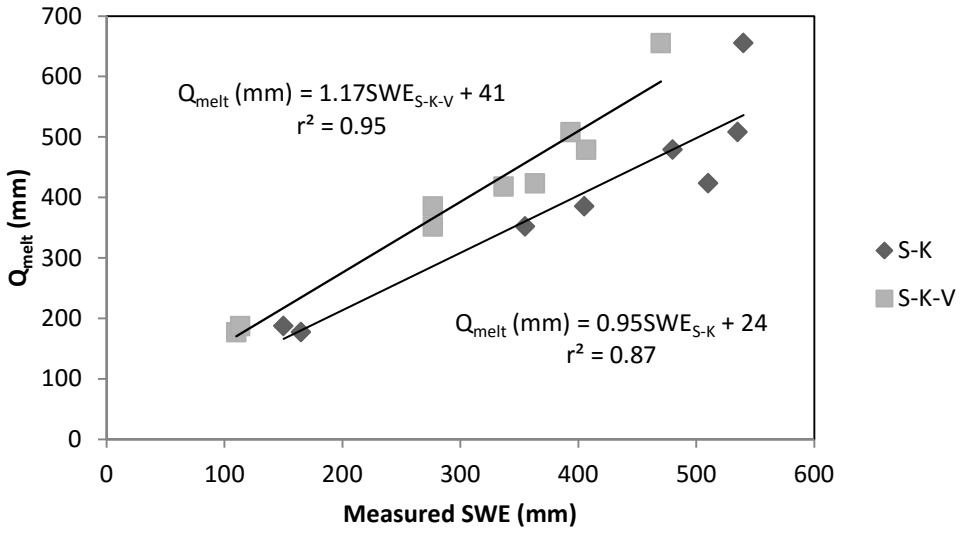

Figure 4.7 Total snowmelt with straight line base flow method and mean SWE at Setur, Kjalöldur and Veiðivatnahraun.

The high r^2 value might give a false impression. It is a very good fit, but there are great uncertainties involved, both in the computation of the total snowmelt and the mean SWE. The main uncertainty regarding computation of total snowmelt was to evaluate the

interface when glacial melt started and snow melt finished. The method used to compute the total snowmelt was mainly by evaluating the hydrograph for each spring and compare the hydrograph response to temperature. The method is subjective and only gives a rough estimation. The main uncertainty regarding the measured SWE was to evaluate the evolution of the snowpack between different times of measurements when computing mean SWE between locations. The period studied is short or only nine years, which reduces the validity of the results. What is concluded from the results is that more snow measurement sites evaluated together can better represent the snowpack and the resulting snowmelt.

The results show that there is a correlation between SWE measurements and the volume of spring runoff. The correlation improves when more than one measurement site is presented together. From the regression analysis empirical equations were obtained that can estimate the volume of snowmelt that is stored in Dynkur catchment based on SWE measurements. Since there is a correlation between the SWE measurements and spring runoff, it would indicate that the SWE measurement could be used to adjust the SWE in hydrological simulations. Since simulating snow accumulation in a catchment can be tricky, a reference point to adjust SWE in the end of accumulation period would be useful. The results from regression analysis indicate that using $SWE_{S\text{-}K\text{-}V}$ or $SWE_{S\text{-}K}$ could provide a reference point to calibrate the snow pack to. This was done with the HBV model and the results are presented in the following chapter.

4.3 HBV model

4.3.1 Model calibration and validation

Calibrations were done to obtain an optimum parameter set that describes the hydrology of the catchment and simulates runoff. After a parameter set was obtained the modeled snow accumulation was evaluated each year and compared to snow measurements. The calibration period was from 1.9.2003 until 1.10.2010. The validation period, where the parameter set that was obtained from calibration was tested on an independent time period, was from 2.10.2010 until 31.12.2014.

The calibration was done by trial and error since only manual calibration was an option. Sixteen parameters were calibrated and are presented in Table 4.4. A few parameters were not calibrated and predefined values were used that were recommended in the HBV manual and are presented in Table 4.5.

Table 4.4 HBV model parameter ranges and optimized value obtained from calibration.

Parameter	Description	Unit	Range	Optimized value
Snow routine				
tt	Threshold temperature rain/snow	°C	-1 to 1	0
dttm	Threshold temperature for snow melt	°C	-1 to 1	-0.4
cfmax	Melting factor	$mm^oC^{-1}\Delta t^{-1}$	1-10	5
gmelt	Melting factor for the glacier	$mm^oC^{-1}\Delta t^{-1}$	1-15	10
rfcf	Rainfall correction factor	-	0.7-1.5	1.1
sfcf	Snowfall correction factor	-	0.7-1.5	1.2
whc	Water holding capacity	-	0-0.5	0.4
Soil routine				
fc	Maximum soil moistere storage	mm	100-1000	540
lp	Threshold for reduction of evaporation	-	0.2-1	0.9
β	Shape factor	-	1-4	2.3
athorn	Conversion factor to calculate potential evaporation	-	0.15-0.3	0.2
Response routine				
alfa	Measure of non-linearity of the reservoir	-	0.1-1.5	0.2
khq	Recession coefficient for upper response box	1/day	0.08-0.6	0.43
k4	Recession coefficient for lower response box	1/day	0.0001-0.1	0.0001
perc	Percolation from upper zone to lower	mm/day	0.1-5	3
maxbaz	Transformation function	-	0-5	0.3

Table 4.5 Predefined parameters values used in the HBV model.

Parameter	Description	Unit	Value
cflux	Capillary flow from upper zone to soil moisture zone	mm/day	0.05
pcalt	Precipitation lapse rate	-	0.1
stf	To describe seasonal variations in the relation between evaporation and temperature	-	2
tcalt	Temperature laps rate	°C/100m	0.6
ttint	Describes the transition when precipitation is assumed to be mix of rain and snow	°C	3

Figure 4.8 and Figure 4.9 show comparison between observed and simulated mean daily discharge over calibration and validation period. Appendix B shows figures of simulated and observed daily discharge for all years, both calibration and validation period. During calibration period the efficiency measured from day to day with Nash-Sutcliffe (*E*) criteria was 0.82. A value of 1 would mean a perfect comparison to observed discharge. According to the HBV manual (2013), *E* normally ends up somewhere between 0.8 and 0.95 if the quality of the input data are good. The efficiency of the model is presented in Table 4.6.

Most weight is given to high flow using the normal E criteria. Thus, E_{log} was also computed, which better reflects the performance for intermediate and low flows.

Table 4.6 Efficiency of simulations measured with Nash-Sutcliffe and logarithmic Nash-Sutcliffe criteria.

	E	**E_{log}**
Calibration	0.82	0.84
Validation	0.70	0.79

The spring and summer discharge is fairly well simulated during the calibration period. It fails to simulate large winter flood peaks and underestimates the glacial melt during peak discharge. The calibration period was seven years, but a large part of 2007 had gaps of missing data.

A validation was done to test the parameters obtained from calibration on independent data that the parameters have not been calibrated to. Normally, when the parameters are tested on an independent data the efficiency of the model reduces. In this case, the efficiency of the model decreased from 0.82 over calibration period down to 0.70 over the validation period. The validation period was only four years, which is a short period to perform a validation on parameter set, but the time span was dependent on the length of the study data. When the model fails to simulate a large event and the simulation deviate by a large factor from observed value, it can have a large impact on the measured efficiency of the model when the time period is short. However, the efficiency did not fall too far or from 0.82 to 0.70 which is reasonable.

Figure 4.9 shows that the largest simulation error was during spring where the discharge was underestimated substantially by the model. It can be explained by the model failure to simulate the spring flood peaks in 2011. Figure 4.9 also shows that in contrast to the calibration period it overestimates the glacial melting during summer peak discharge. These are general assumptions for the entire period. Individual years need to be studied to identify scenarios that explain failure to simulate spring melt and the difference between glacial melt between validation and calibration periods. The model performance will be further discussed in Chapter 4.3.4. One way to increase the model efficiency over validation period is to study the uncertainty and sensitivity of the parameter set used by the model.

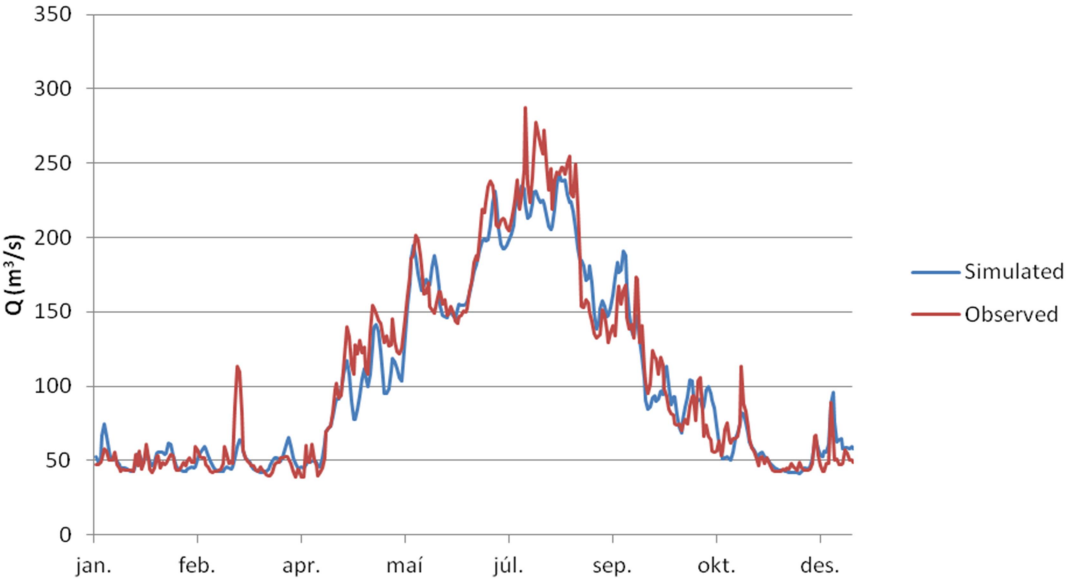

Figure 4.8 Observed and simulated mean (daily) discharge over calibration period 1.9.2003 to 1.10.2010.

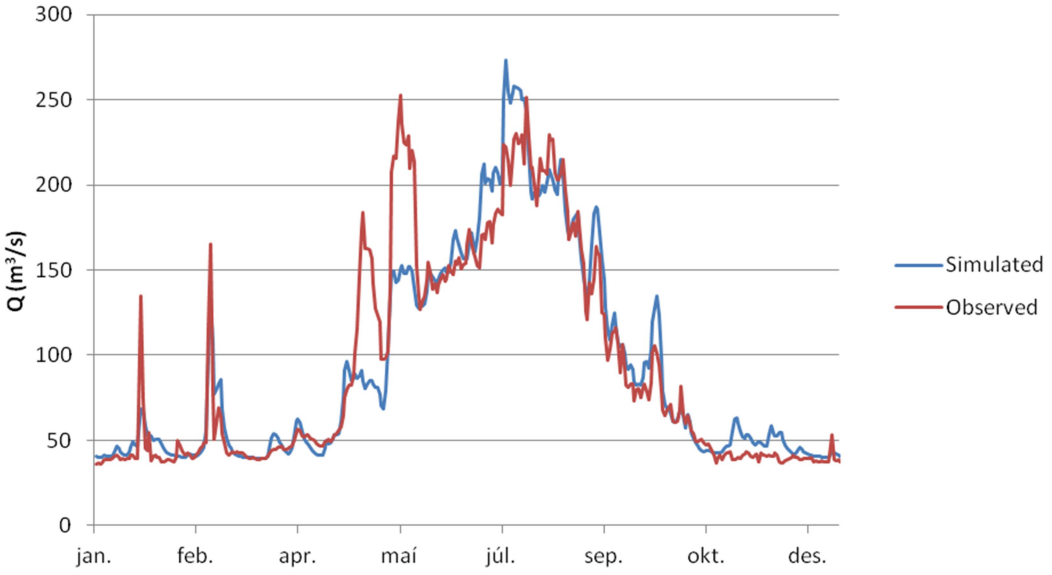

Figure 4.9 Observed and simulated mean (daily) discharge over validation period 2.10.2010 to 31.12.2014.

4.3.2 Sensitivity analysis

The sensitivity of the HBV model parameters was evaluated after an optimum parameter set was obtained. One parameter was allowed to vary at a time on the interval range presented in Table 4.4 and the change in efficiency measured with Nash-Sutcliffe criteria was recorded. The sensitivity of one parameter that was not calibrated, the temperature lapse rate (*tcalt*), was also tested. Figure 4.10 shows the sensitivity of the HBV model with respect to changes in the model parameters.

The HBV model simulation for Dynkur catchment is least sensitive to parameters in the soil routine and good results could be obtained from wide range of parameter values. The most sensitive parameters are in the snow routine where all the parameter except *whc,* reduces the Nash-Sutcliffe efficiency quite fast after changing the parameters from optimum value. The parameters in the snow routine control the volume to the main discharge components for Upper Þjórsá River, which are glacial melt and snow melt, and therefore it is not a surprise that these parameters are sensitive. It is interesting to observe that the rainfall correction factor (*rfcf*) was less sensitive than the snowfall correction factor (*sfcf*). The *sfcf* adjusts the precipitation that falls as snow and therefore adjusts the simulated SWE. As discussed before, it is difficult to measure accurately the snow precipitation in rain gauges. Since the *sfcf* is a sensitive parameter it might improve simulations if *sfcf* was calibrated each year to SWE measurements done in the end of snow accumulation period.

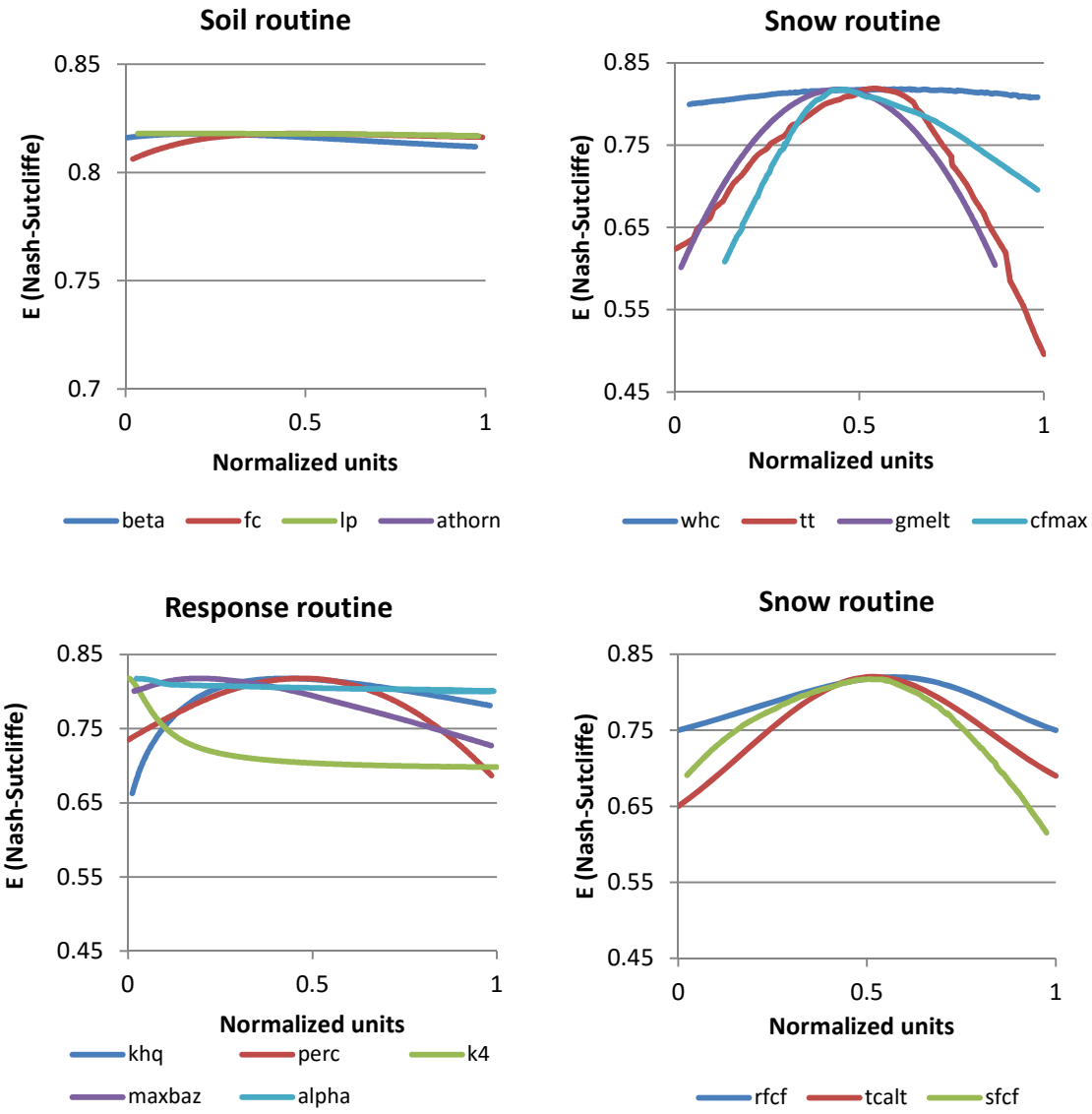

Figure 4.10 Sensitivity of the HBV model to selected parameters.

Other sensitive parameters are the ones that affect the temperature in the snow routine: threshold temperature (*tt*) and the temperature lapse rate (*tcalt*). The *tt* parameter is calibrated but the *tcalt* is kept as a constant. Recommended values for *tcalt* are between 6 and 7 C°/km, which is the average adiabatic lapse rata for moist air. However, the temperature lapse rate varies on seasonal and daily basis (Gardner et al., 2009). The snow accumulation and the snow melt rate are quite sensitive to the temperature lapse rate and it is a simplification of the actual state to keep the parameter as constant. The biggest part of the non-glacier snow accumulation area in Dynkur catchment is within a relatively small elevation range, between 500 and 800 MASL. Thus, the temperature lapse rate has less effect in that area since the weather stations are also in same elevation, than in more mountainous areas. However, the elevation of Hofsjökull spans a greater range, or from 800 to 1750 MASL and as a result the glacial melt rate is more sensitive to the temperature lapse rate. An improvement could possibly be made to the model by studying the temperature laps rate in the area, especially for Hofsjökull, and then implementing it into the model.

The recession parameter *k4,* in the response routine controls the outflow from the lower response box (groundwater). To be able to maintain the discharge volume from groundwater over low flow periods the *k4* parameter needed to be very low. As a result the base flow computed by the program was close to a constant over the simulation period. To maintain the base flow, *perc*, parameter that controls the rate of water that seeps down to the groundwater was calibrated. Calibrate these two parameters to get a correct base flow was a straight forward move, and even though they are quite sensitive, they are also well defined where tight range of parameter values can give good results.

It is interesting to see that the recession parameter *khq*, in the response routine that controls the outflow from the upper response box, is not all that sensitive on a quite wide range. The values for *khq* from 0.6 to 0.2 do not affect the Nash-Sutcliffe efficiency by a great deal. This could be explained by the diversity of the runoff response of the catchment. By having a high recession constant better results are gained for quick flows and lower constant fits with slower flows. Rainstorms normally have a quick response while the response from glacial melting is slower. The temperature slowly increases over the summer and so does the glacial melt, until it peaks in July/August.

The response from the lower response box is very slow, but quite fast in the upper response box. It was observed that as a result it was difficult to simulate the interflow, the water that does not go to the groundwater but flows through the soil and has a response time between the base flow and the direct runoff.

4.3.3 Snow adjustment

The snow routine in the HBV model computes snow accumulation and snow melt for each elevation zone. The model also computes the area-average SWE for the entire catchment. The aim was to evaluate if there was a relationship between the area-average SWE computed by the model and the SWE measured at Setur, Kjalöldur and Veiðivatnahraun with a regression analysis.

For each year over calibration period, the simulated SWE was calibrated with snowfall correction factor *sfcf* so it would give optimum results, measured with Nash-Sutcliffe efficiency criteria and inspected visually from the hydrographs. The results where plotted

on a scatter plot and a regression analyses were done to estimate the relationship between optimum simulated SWE and the measured SWE. From the regression analyses an equation was obtained that could be used to use SWE measurements to adjust the snowpack in the HBV model. Figure 4.11 shows the results from the regression analysis and the regression equations obtained.

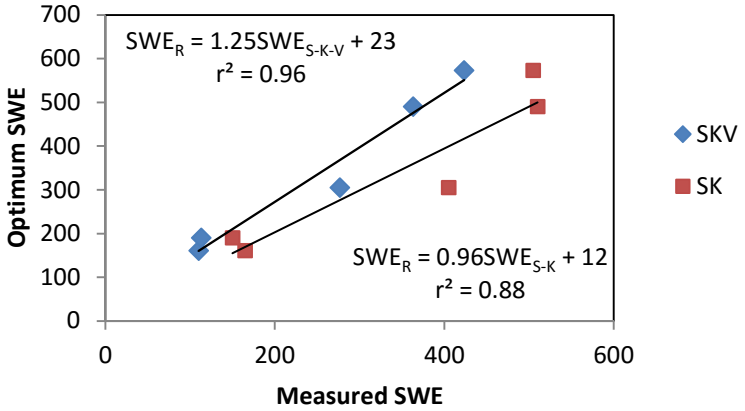

Figure 4.11 Optimum SWE from simulations compared with measured SWE, both mean SWE between Setur, Kjalöldur and Veiðivatnahruan and mean between Setur and Kjalöldur

Regression equation that was obtained by using $SWE_{S\text{-}K\text{-}V}$ showed a better fit of the two equations, with a r^2 quite high or 0.96. Therefore, simulated SWE was adjusted to the SWE equation,

$$SWE_R = 23 + 1.25 * SWE_{S-K-V} \quad (24)$$

where SWE_R is snow water equivalent computed from regression equation. The simulated SWE was adjusted in the model on the same day as the snow measurements were done. Results are presented in Table 4.7 and 4.8.

Table 4.7 Comparison of the original calibration and the one carried after the simulated SWE has been adjusted to SWE_R over the calibration period.

	Original		**Adjusted SWE**	
	E	**E_{log}**	**E**	**E_{log}**
2004	0.825	0.787	0.833	0.792
2005	0.837	0.869	0.858	0.873
2006	0.729	0.841	0.729	0.841
2008	0.877	0.907	0.877	0.907
2009	0.837	0.844	-	-
2010	0.811	0.818	0.831	0.831
Average	0.819	0.844	0.826	0.848

Table 4.8 Comparison of the original calibration and the one carried out after the simulated SWE has been adjusted to SWE_R over the validation period.

	Original		Adjusted SWE	
	E	**E_{log}**	**E**	**E_{log}**
2011	0.484	0.649	0.612	0.783
2012	0.818	0.751	0.906	0.789
2013	0.692	0.853	-	-
2014	0.860	0.905	-	-
Average	0.714	0.790	0.767	0.833

The results show that most years, adjusting the simulated SWE to the SWE_R improves the efficiency measured with the Nash-Sutcliffe criteria. In 2006 and 2008, the SWE_R was almost the same as the simulated SWE with original parameters. Thus, no snow adjustment was done for those years. Little improvements could have been made in 2008 since the simulated SWE was very close to the optimal SWE value and the year showed good results in general. However in 2006, the simulated SWE showed too large a snowpack at the end of spring. This can also be observed in Figure 4.11, where the data point that is furthest away from the regression line is the data from 2006. No snow measurements were done in 2009 in Kjalöldur, and it is therefore not possible to adjust the simulated SWE for that year. Measurements from Setur indicate that the simulated SWE from original calibration underestimate the snow accumulation considerably in 2009 and with more snow the simulation would improve the results that year.

During validation years, snow measurements were only available in 2011 and 2012. Both years the SWE_R improved predictions considerably and the total Nash-Sutcliffe efficiency improved from being 0.71 to 0.77 over the validation period. A longer time period is needed for more conclusive results.

Figure 4.12 shows the same scatter plot as Figure 4.11, but data from 2011 and 2012 has been added to the plot. The added data maintains a similar fit and the regression coefficient only increases a fraction. The slope of the regression line is close to 1 when using measurements from S-K and the intersection is lower than measurements from S-K-V. That indicates that the snow measurements from S-K are closer to represent the area-average SWE of the catchment than S-K-V and therefore should be evaluated if measurements from S-K should be used instead of S-K-V. It is likely that if number of snow measurement sites would be increased inside or close to the catchment a better estimation on the area-average SWE would be obtained which might improve the results further. The main outlier on Figure 4.12 is the snow measurements from 2006. That year was the only year in which snow measurements and optimum adjusted snow in the model showed little relationship.

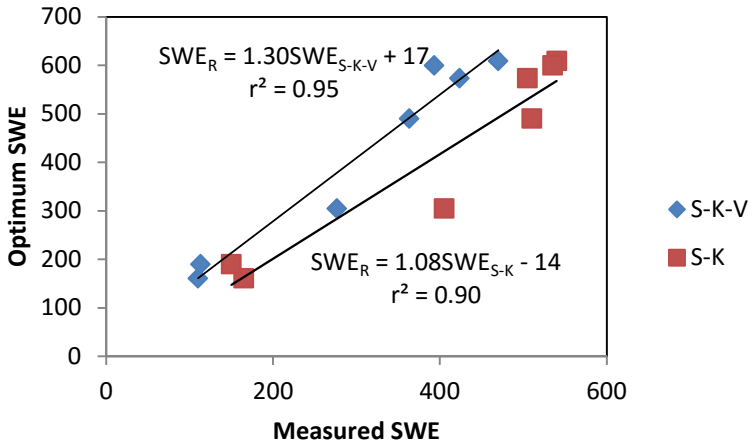

Figure 4.12 Optimum SWE from simulations compared with measured SWE. Data added from validatin period.

A relationship between snow measurements and simulated snow in the model was established with a regression equation. The results show that most years, adjusting the SWE to measured SWE improves the efficiency measured by the Nash-Sutcliffe criteria. For water resource management, is also important to study the volume error as well as the precision of hydrograph response. More detailed analysis of the results is presented in the following chapter, where other factors are studied.

4.3.4 Model performance

The HBV model performance was evaluated for each year in terms of snow accumulation and the spring discharge. Each spring was evaluated separately to try to identify when the model fails and when it succeeds in simulating spring floods efficiently, and what could be the reason for success or failure. Results from original calibration were studied and also when the simulated snow accumulation had been adjusted to snow measurements, as discussed in the previous chapter.

The most sensitive routine in the HBV model was the snow routine. Two main factors influence the snow routine: the snow volume and the snow melt rate. An attempt was made to improve the snow volume simulations by adjusting the snowpack to measurements. In the HBV model the melt rate is controlled by a degree-day factor (melt rate factor) and air temperature. According to Anderson (1976), three explicit scenarios were identified where the relationship between snow melt and air temperature deviates from their calibrated average relationship:

1. Periods with high temperatures and little wind. In this case the temperature index model overestimates the snow melt rate as the amount of sensible heat is small.

2. Periods with low temperatures, clear sky and aged snow. Aged snow normally has lower albedo and hence the melt generated by solar radiation is more than the temperature index model simulates.

3. Periods with warm temperature, high humidity and strong winds. The model underestimates the snow melt due to large amount of sensible and latent heat fluxes.

In Iceland high temperature and little wind is a rare event especially in spring conditions making Scenario 1 an unlikely cause for air temperature and snow melt to deviate from calibrated average relations. Low temperature, clear sky and aged snow as described in Scenario 2 is not an uncommon scenario in Iceland and could cause the snow melt factor to increase. The same goes for Scenario 3, however it is more likely that warm temperature occur in late spring and over summer, hence influencing the glacial melt rate rather than the snow melt rate.

Since the model should be used for predictive studies on runoff for Upper Þjórsá River, the validation period is an important factor to test the model. It is one thing to get good results from calibrations, but another for the model to simulate runoff on data that the model parameters have not been calibrated to.

Calibration period

The calibration period was from 2004 to 2010 as previously discussed. Figures 4.13 to 4.15 show the simulations and observations of the discharge and snow, over the calibration period. The graphs on the figures show the simulated and observed snow water equivalent (SWE) and discharge (Q), simulated snow cover area (SCA) and accumulated difference between simulated and observed discharge. The simulation period that was used to present the spring runoff was from the beginning of April until the end of June. Table 4.9 shows the efficiency of the model simulations over spring measured with Nash-Sutcliff criteria.

Table 4.9 Comparison of the original calibration and the one carried after the simulated SWE has been adjusted to SWE_R over spring from April to end of June.

	Original		Adjusted SWE	
	E	**E_{log}**	**E**	**E_{log}**
2004	0.69	0.62	0.73	0.62
2005	0.58	0.66	0.74	0.68
2006	0.63	0.81	0.63	0.81
2008	0.87	0.94	0.87	0.94
2009	0.60	0.77	0.80	0.87
2010	0.42	0.57	0.57	0.69

Figure 4.13 shows the main simulations results for the years 2004 and 2005. The first year of simulation was 2004. The snow measurements were done at the beginning of May that year, much later than in other years and the snow melt had already begun. The simulations show that almost half of the snow in the catchment had already melted when measurements where done. The snow measurements indicate a below average snowpack that year, when compared with other years. Only the measurements in 2010 show smaller snowpack during the study period. No snow was measured in Veiðivatnahraun and the measured SWE was only two cm in Kjalöldur.

The efficiency computed by Nash-Sutcliffe criteria measured improvements after the snowpack was calibrated to measured SWE and the accumulated difference between observed and computed discharge was reduced. The hydrograph in 2004 on Figure 4.13 shows that the observed discharge before the snow melt started was much smaller than the simulated discharge. In fact, it was conspicuously low or around 20 m^3/s, when normally the discharge (base flow) is around 34-40 m^3/s. This indicating, that the water measurement during that period might contain some errors. Therefore the accumulated difference for 2004 was computed after the snow melt starts, as is shown on the accumulated difference plot for 2004 on Figure 4.13.

The snow measurements from 2005 indicate a relatively large snowpack. At Setur the snow measurements show that SWE was around average, but at Kjalöldur it was the second largest over the calibreation period. The snow density was high and thick ice was meaured at the bottom of the snow profile both at Setur and at Kjalöldur. Simulations give a fairly good results and efficiency of the model improved after the SWE was adjusted, the accumulated difference was reduced as well. The flood peaks are a bit too high and the recession after the first two flood peaks to steep. One reason could be that a deep snowpack dampense the flood peak and that the model is inefficent in simulating that scenario.

Another reason could be that the model is inefficient in simulating the interflow during springmelt. The interflow is the flow that is not a surface runoff and not a base flow but the water between that seaps throught the soil and has the response time between base flow and direct runoff. The reason for the inefficency of simulating the interflow is the large difference between response time of the lower response box (groundwater) and the upper reponsce box (direct runoff). To account for the base flow over the whole year, the recession constant for the base flow recession had to be very low to maintain the relatively

high base flow over winter months. For that reason the base flow is close to a constant in the model; it does not vary more than 10% annually.

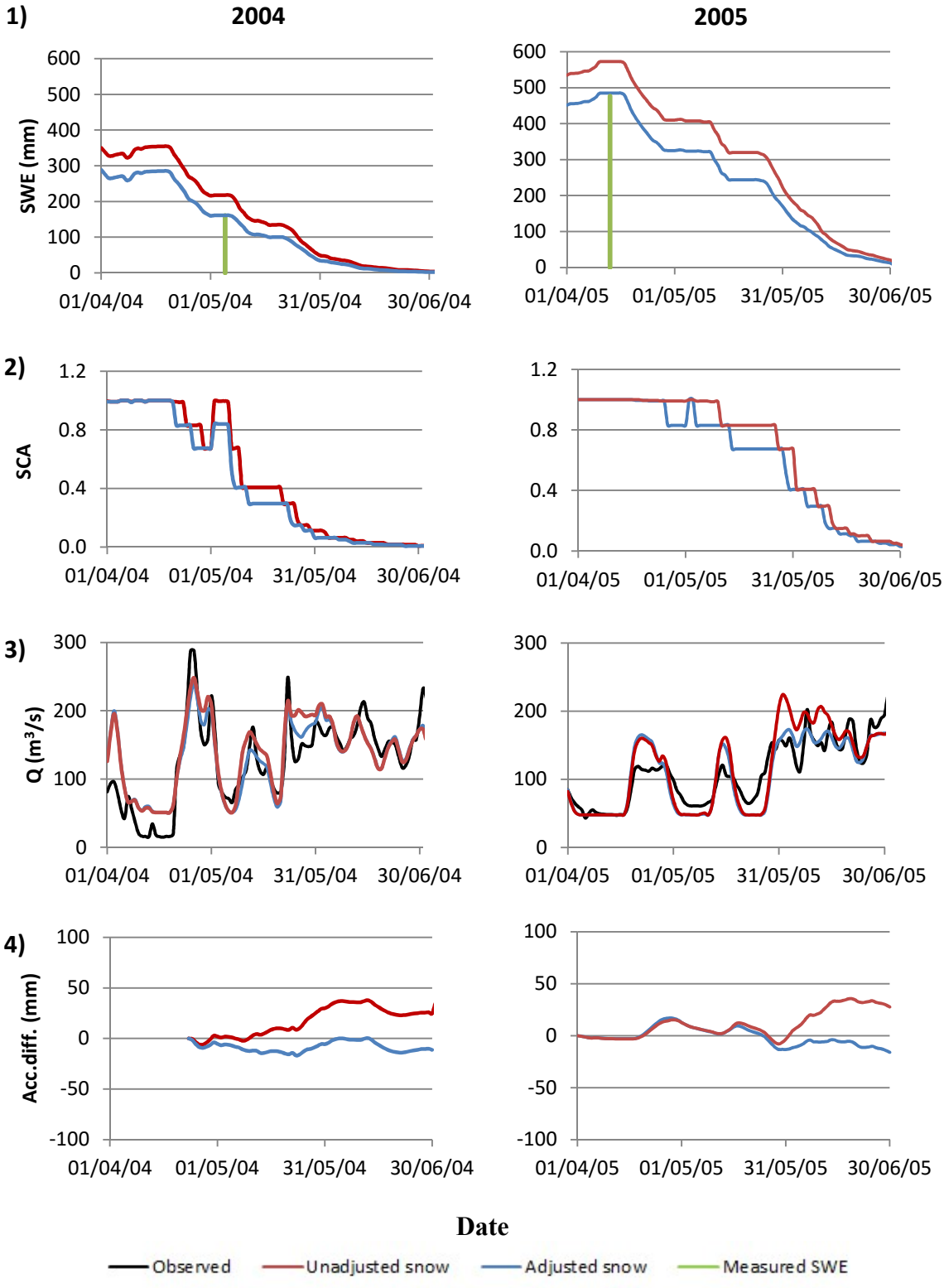

Figure 4.13 Simulation and observation of the runoff and the snow for spring 2004 and 2005 (calibration period): 1) Snow water equivalent (SWE); 2) Snow cover area (SCA); 3) Discharge (Q); 4) Accumulated difference between observed and simulated discharge.

Figure 4.14 shows the main results from simulations over the springs 2006 and 2008. In 2006 the snow measurements showed average snow accumulation. The snow measurements were done in the middle of April, two weeks before snow melt started. A thick ice layer was at the bottom of the snowpack at Setur and a small ice layer at Kjalöldur. Little snow was observed at Veiðivatnahraun. The Nash-Sutcliffe efficiency of the model was 0.63 for the spring and 0.73 for the whole year, which is below average. The simulated SWE with original parameter was the same as the SWE_R from Equation 24. Therefore, no snow adjustment was done for 2006. The accumulated difference plot in Figure 4.14, for 2006, shows that the simulated discharge volume is higher than observed volume. Four main factors influence the discharge volume: rain, evaporation, SWE and glacier melt. Glacier melt is not a large component until middle or late June.

The spring 2006 was sequential, May was dry and June was very wet compared to other years during the study period. The accumulated precipitation for May was around 55 mm and for June around 190 mm, but the average accumulated precipitation for May and June together was around 150 mm over the study period. It could be that the precipitation in June was overestimated for the catchment area. Computed evaporation over the spring 2006 was around 110 mm, while average computed evaporation over the spring period was 100 mm. The computed evaporation was above average, so it is unlikely that evaporation is being underestimated by a significant amount.

It is possible that the snow measurements in 2006 do not represent the average SWE for the catchment due e.g. snow distribution. Another reason could be that a higher portion of the snow seeped down to the aquifers compared to other years, thus not materializing as runoff until much later. The main factors influencing the flow rate down to the aquifers are the soil conditions and the dynamics of the snow cover. Less water seeps through frozen soil and thick ice layers in the snow cover could prevent water from reaching to the soil.

At last, errors could be in the SWE measurements. Thick ice layer was at the bottom of the snowpack in Setur, which does not support the theory of more water seeping to the aquifers. However, there was only a small ice layer in Kjalöldur. It is possible that the ice layer observed in the snow pit at Setur was localized. This would distort the SWE computed from the snow measurements, since the density of ice is higher than normal snow and the SWE is computed from the measured density of the snow pit. A smaller ice layer reduces the density resulting in lower SWE measured at Setur. For more accuracy in the SWE measurements, more than one snow density measurements should be done for each location.

A large part of 2007 discharge data were missing and no snow measurements were done that year and are therefore not presented in the results. In 2008 a large snowpack was measured. The measured snow density was smallest in 2008 over the whole period and no ice was at the bottom of the snow pack. That indicates that the weather had been stable over the winter, without many days of freeze/thaw cycles that could create ice layers in the snow pack. In general the spring was dry compared to other years and the accumulated precipitation was below average April, May and June.

The simulation showed very good comparison between computed and observed discharge. The measured SWE was very close to the simulated SWE with original calibration and therefore no snow adjustments were needed. Figure 4.14 shows the main results from simulations over the spring 2008. The efficiency measured with Nash-Sutcliffe criteria was

0.87 and with logarithmic Nash-Sutcliffe 0.94. This was the highest measured efficiency for all the years during calibration period. The accumulated difference plot on Figure 4.14 shows that there is little difference between simulated discharge volume and the observed, during the melting phase of the snowpack.

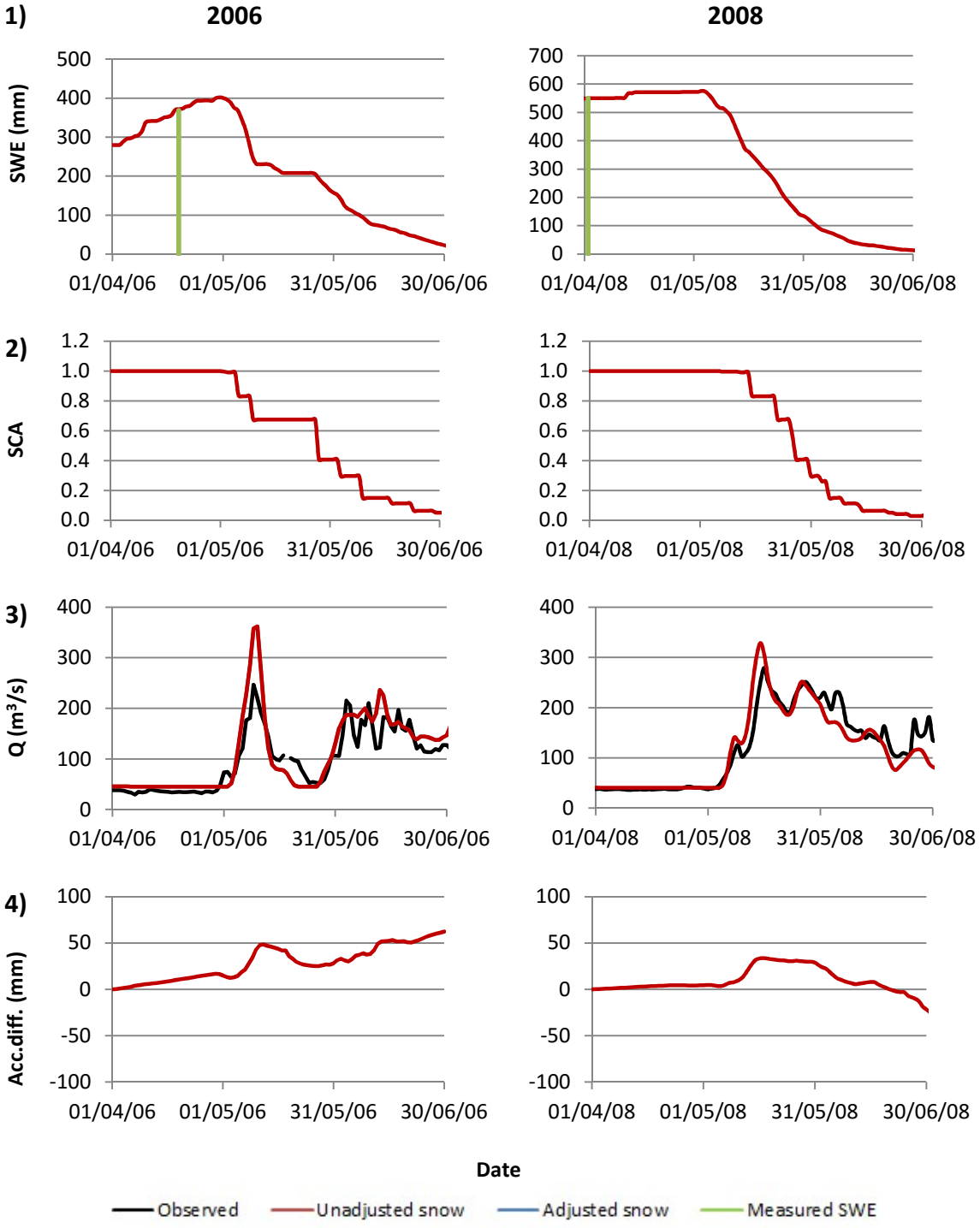

Figure 4.14 Simulation and observation of the runoff and the snow for spring 2006 and 2008 (calibration period): 1) Snow water equivalent (SWE); 2) Snow cover area (SCA); 3) Discharge (Q); 4) Accumulated difference between observed and simulated discharge.

Figure 4.15 shows the main results from simulations over the springs 2009 and 2010. There was no snow in Veiðivatnahraun in the spring 2009. However a deep snowpack was measured at Setur, the second highest over the study period. A small ice layer was at the bottom of the snow pit at Setur, otherwise the density of the snow layer was relatively low compared to other years. Unfortunately, there were no snow measurements done in Kjalöldur in 2009. Since it was important to have all the sites representing the snow cover, missing one site meant that it was not possible to adjust the SWE to measurements in 2009. Simulation without adjusting the SWE showed poor results and it was obvious that the snow accumulation was underestimated.

Since snow measurements were missing for Kjalöldur, the simulated SWE was adjusted until the optimum results were obtained. From these results, simulated SWE was recorded and used as SWE_R in Equation 24 to compute the $SWE_{S\text{-}K\text{-}V}$. From $SWE_{S\text{-}K\text{-}V}$ it was possible to compute what the SWE in Kjalöldur needed to be. The optimum simulated SWE was 510 mm, which means that to get the same $SWE_{S\text{-}K\text{-}V}$, the SWE in Kjalöldur would have needed to be around 350 mm or 49% smaller than the measurements in Setur showed. The SWE measured at Kjalöldur showed on average 50% lower SWE value than at Setur over the study period, so a value 350 mm fits quite well. After the simulated SWE was calibrated, the results were very good. The model efficiency measured with Nash-Sutcliffe was 0.8 instead of 0.6 before snow adjustment and accumulated difference improved significantly. The accumulated difference plot on Figure 4.15 shows that there is not much difference between simulated discharge volume and the observed, during the melting phase of the snowpack after the snow is adjusted.

In 2010 the snow measurements showed results similar to those of 2004, where the snowpack was relatively small. The measurements were carried out at the beginning of May, when the snow melt had already started. The density of the snowpack was high. At Setur the density was measure to be 762 kg/m^3, that is 50% higher than the average. The high density is most likely because of a melting phase two weeks earlier. Simulations for spring 2010 were the worst over the calibration period, as it failed to simulate the peaks during the spring flood. The model improved after snow adjustments, Nash-Sutcliffe efficiency was 0.57 and the accumulated difference improved just a bit. It is not clear what causes the model failure in simulating the flood peaks during these scenarios but it is related to insufficient amount of snow melt in the model.

As discussed before three main reasons can cause the melting to deviate from average calibrated relation to air temperature. None of those reasons seem to be an obvious influence on the first flood peak in middle of April 2010. The temperature was between 2-3°C and the average wind speed was around 7 m/s. A likely cause would be an underestimation on the areal precipitation. What supports this theory is that even though little precipitation is measured at rain gauges used for simulation, especially rain gauges east side of the catchment, the rain gauge in Hveravellir measured a relatively high precipitation. Hveravellir is located around 30 km north-west of the catchment; its rain gauge is not used in actual simulations but only to replace missing values in other rain gauges. It is possible the rain storm was localized mostly on the west side of the catchment where there are no rain gauges to measure the precipitation.

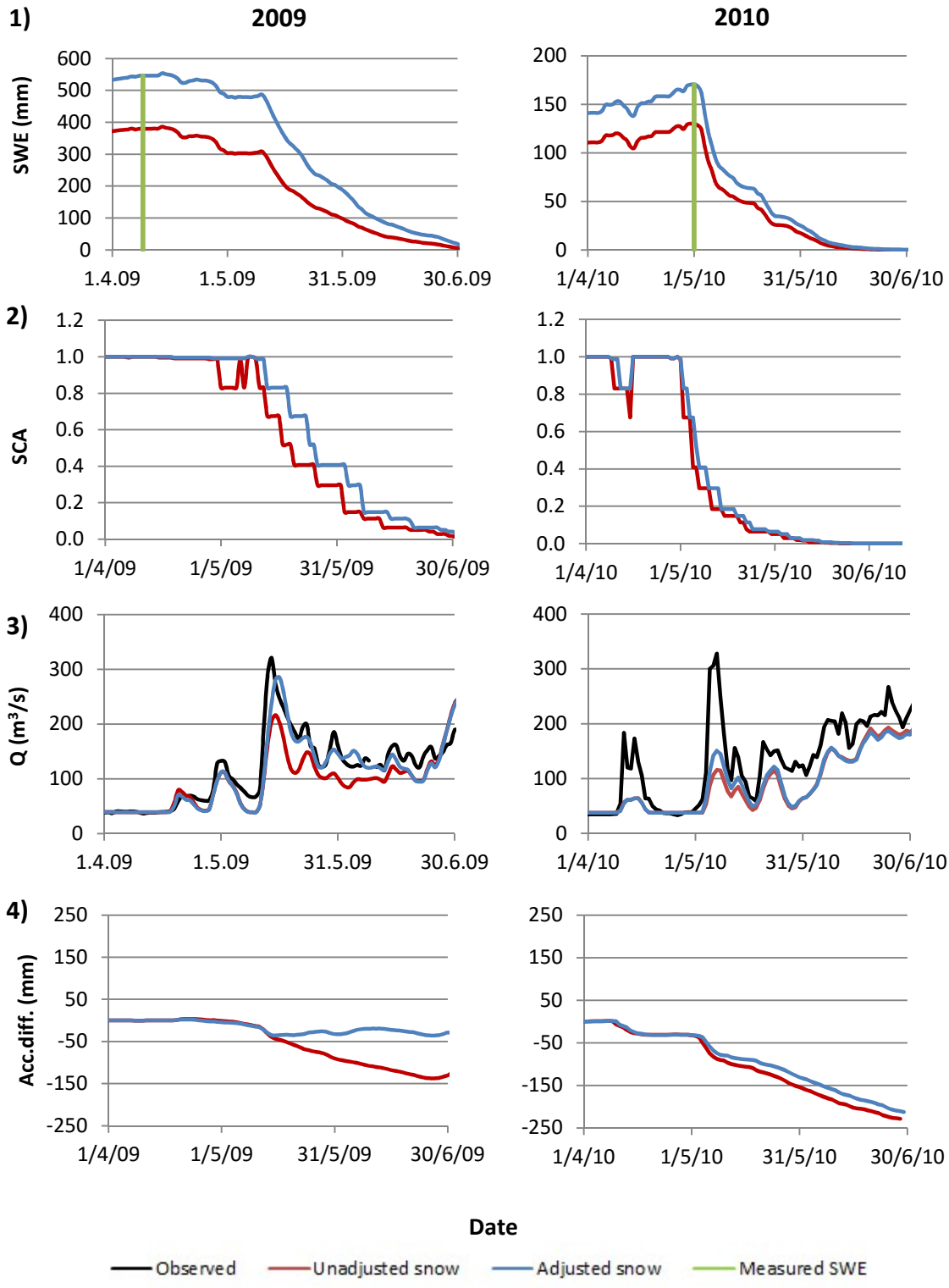

Figure 4.15 Simulation and observation of the runoff and the snow for spring 2009 and 2010 (calibration period): 1) Snow water equivalent (SWE); 2) Snow cover area (SCA); 3) Discharge (Q); 4) Accumulated difference between observed and simulated discharge.

There was no precipitation leading up to the second flood peak at beginning of May 2010, the humidity was relatively high, the wind speed low and temperature around 5°C. If there was a clear sky and aged snow with low albedo, it could explain the large deviation from the calibrated melt rated. On April 14th 2010, the Eyjafjallajökull volcano erupted, spewing large amount of volcanic ash into the atmosphere. Ash distributed over the area could affect the melt rate as it reduces the albedo of the snow and increases the radiation absorbing capacity of the snow. From the hydrograph in 2010 it can also be observed that the discharge continues to be underestimated after the simulated snow is gone. The main discharge component in summer is base flow, precipitation and glacial melt after the spring melt finishes. Glacial melting is also modeled with a melting factor, and when the glacier is covered with volcanic ash, the glacial melting rate may have increased.

It was observed that after the eruption in Eyjafjallajökull, glacial melt increased in many glacial rivers in Iceland. When the thickness of the volcanic ash over an area is the right amount it is believed that it increases the melting, but with increased thickness it isolates the glacier (Zophaníusson, 2010). Figure 4.16 shows simulations after the snow melt factor had been increased by 50%. It is obvious that increased melt factor improves the simulations considerable.

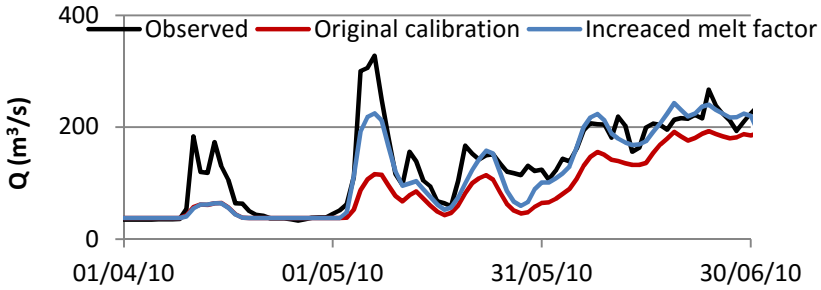

Figure 4.16 Hydrograph of simulations in 2010 where the melt factor has been increased.

The years that gave the best simulation results during the calibration period were 2008 and 2009. In both years there was a thin layer of ice measured at the bottom of the snowpack in Setur compared to other years and the climate relatively dry. Frozen soil and ice lenses affect the runoff response and water volume that infiltrates the soil. In every year except 2006, the adjusted SWE improved simulation results. This gives good hope that the SWE measurements could be used to adjust the snowpack in the model, which is a valuable tool when other methods to compute the SWE for a catchment give variable results.

Validation period

It was important to study the model performance over the validation period and to see if the snow measurements could improve the results on independent data. Snow measurements were not available in 2013 during the validation period. In 2014 the snow measurements were only done in early January, half-way through the snow accumulation period, and could not be used as a reference to adjust the SWE in the model. Hence, only two years of the validation period was it possible to adjust the SWE in the model to the measured SWE, which was unfortunate. Figures 4.17 to 4.19 show the simulations and observations of the discharge and snow, over the validation period. Table 4.10 shows the efficiency of the model simulations over spring measured with Nash-Sutcliff criteria.

Table 4.10 Comparison of the original parameters and the one carried after the simulated SWE has been adjusted to SWE_R over validation period from April to end of June.

	Original		Adjusted SWE	
	E	**E_{log}**	**E**	**E_{log}**
2011	-0.19	-0.25	0.37	0.6
2012	0.63	0.56	0.91	0.74
2013	0.57	0.74	-	-
2014	0.62	0.77	-	-

Figure 4.17 shows the main simulations results for the years 2011 and 2012. Spring 2011 had on average the highest measured SWE over the whole study period. In Setur, the snow was around average, but in Kjalöldur it was the highest measured SWE over the study period and the same was observed in Veiðivatnahraun. The snow density was relatively low, or around 460 kg/m^3 and an average thickness of the ice layer was measured at the bottom of the snow pack. The model was not able to simulate the flood peaks and had the worst results over the whole study period with Nash-Sutcliffe efficiency of -0.19 with original parameters and 0.37 after the snow pack was adjusted. The accumulated difference was by far the highest over the study period in 2011. It had negative accumulated difference of close to 400 mm for original parameters and 180 mm when adjusted to snow measurements. Even though there are other factors that can influence the discharge volume also, it is clear that the main discharge component that the model fails to simulate is the snowmelt.

It is evident that not enough energy was put into the snowpack system so the model cannot melt enough snow to produce these flood peaks. A likely cause is an underestimation on radiant energy flux into the snowpack. Another reason could be related to the snowpack dynamics and different phases of snow melt that the model fails to simulate. It takes time for the snowpack to become isothermal, especially when the air temperature is close to zero. A large snowpack needs larger quantity of energy to become ripe and ready to melt. Large snow packs can also retain larger quantities of water. Once it finally becomes ripe it releases a large quantity of liquid water that has been building up in the snowpack. Finally, it is possible that too much water is going to the groundwater storage box in the model. With a thick ice layer at the bottom of snowpack it could prevent water to seep through the ground and resulting in higher portion of water as direct runoff. It was tested to limit the water going to groundwater box, it only increases the runoff by a small portion. Figure 4.18 shows the hydrograph when the flow down to the groundwater box has been stopped compared with normal simulation.

There is a second flood peak resulting from snow melt which starts on May 20th and recedes around June 5th 2011. The model also fails to simulate the flood peek during this period and grossly underestimates the snow melt again. Melt generated by solar radiation could explain the failure of the model to account for the rate of snow melt. The temperature during this period is between 0 and 4°C, the humidity is around 80% and precipitation was little, with only occasional showers. Another volcanic eruption occurred in Grímsvötn on May 21st, also spewing ash over a large area. It is likely that the volcanic ash has an impact on the snow melt factor as discussed before, increasing the melt rate of

the snow. It was tested how much the melt factor had to increase to be able to sustain the second flood and it need to increase between 300 and 400%.

In reality the melting factor is not a constant, it varies with sun radiation and other factors discussed previously. By incorporating the melting into one factor, it is assumed that it is well correlated with the air temperature, which it usually is. It is likely that the melting factor of the snow and ice is more variable after the volcanic eruptions in 2010 and 2011. According to Magnús Sigurðsson (2013) the impacts of ash fall on glacial melting becomes minimal after about a year. The ash fall can have an influence on the melt factor from day to day. As soon as it snows over the ash layer the melting factor decreases temporarily. The ash can also be distributed by wind long after eruption. This could complicate the snow melt modeling.

According to Sverrir Guðmundsson et. al. (2012), May and June 2011 where one of the coldest months measured on Langjökull, a glacier approximately 50 km west of Hofsjökull, and an unusual amount of snow fall was observed. The ash fall was not observed in Langjökull until June 11th, eleven days after the eruption finished. The ash reduced the reflection considerably and as a result the snow melt increased. Dynkur catchment is located midway between Langjökull and Grímsvötn and could have seen ash fall sooner than Langjökull. Looking at the hydrograph, it looks like it was affected by the ash fall right away, as this seems to be the most likely cause for the high flood peaks.

Snow measurements for 2012 showed second highest average SWE measurements during the study period, only 2011 exceeded in snow amount. Snow density was around average or 500 kg/m^3, and the thickness of the ice layer was above average at Setur. Results from simulations were good and the simulated discharge was well comparable with observed discharge with efficiency of 0.91 measured with Nash-Sutcliffe criteria. The hydrograph on Figure 4.17 for 2012 shows that before spring melt starts the observed discharge was between 70 and 90 m^3/s for over a month. There is no logical explanation for such high discharge during this period, since the temperature rarely goes over 0°C and normal base flow during winter/spring season is around 40 m^3/s. There can be errors in the water measurements due e.g. ice and ice jams in the river, affecting the water levels at the gauge. If the assumption is correct that the discharge gauge overestimates the discharge from the middle of April until spring melt starts, then the accumulated difference would show better results as well as the logarithmic Nash-Sutcliffe efficiency criteria.

The accumulated difference plot for 2012 on Figure 4.17 shows that after the SWE was adjusted, the accumulated difference was reduced by a significant amount. The Nash-Sutcliffe efficiency was also improved by a large factor. The simulation results for 2012 showed the best results over the validation period.

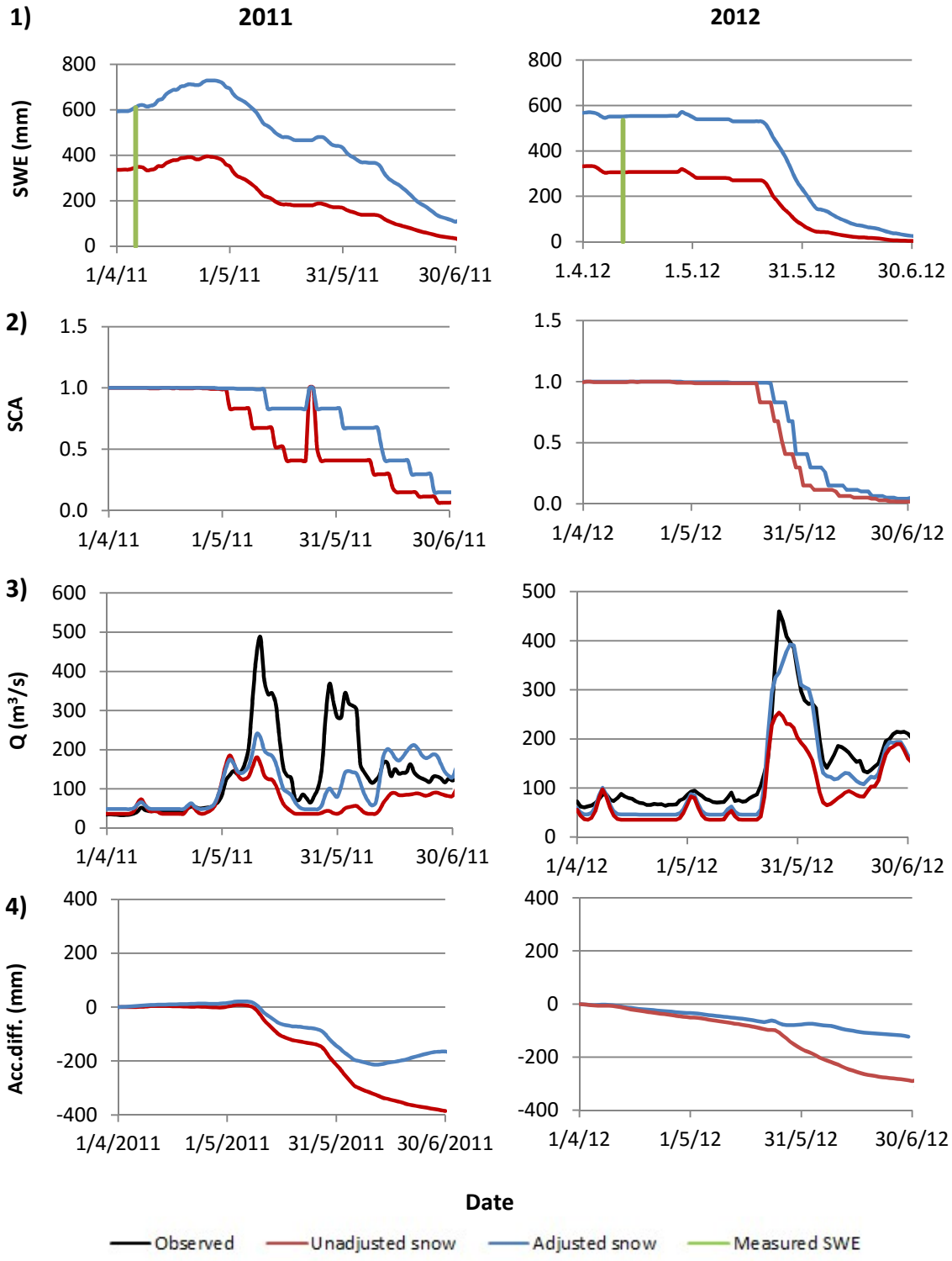

Figure 4.17 Simulation and observation of the runoff and the snow for spring 2011 and 2012 (validation period): 1) Snow water equivalent (SWE); 2) Snow cover area (SCA); 3) Discharge (Q); 4) Accumulated difference between observed and simulated discharge.

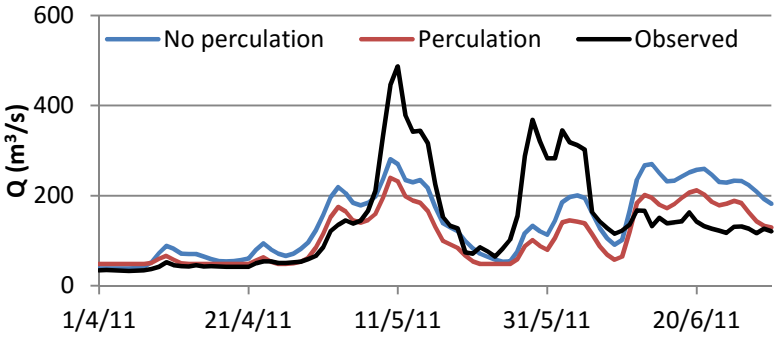

Figure 4.18 Hydrograph for spring 2014 where the flow down to the ground water box has been restricted and is compared to normal simulation and observed discharge.

Figure 4.19 shows the main simulations results for the years 2013 and 2014. As mentioned above, snow measurements were missing for 2013 and 2014. Both 2013 and 2014, the runoff volume over the year was well below average and in 2014 the power company Landsvirkjun had to limit their delivery of energy because of low water supply (Landsvirkjun, 2015). Simulated SWE was well below average for 2013, and was close to the simulated SWE in 2010. The snow accumulation was somewhat higher in 2014, but still below average.

The spring runoff started late in 2013, or in the middle of May. The model was not able to simulate the flood peak in spring 2013 and the model efficiency was measured to be 0.58 with Nash-Sutcliffe criteria. The model misses the largest flood peak in the end of May. The rapid increase in runoff was due to a rain storm and snow melt. During rain storms, the model often underestimates the response time and dampens the flood peaks. As was discussed in Chapter 4.3.2, it is difficult to apply the same recession coefficient on all scenarios, in particular on a river catchment that is as diverse as the Dynkur one. The areal precipitation could also be underestimated. The accumulated difference plot for 2013 on Figure 4.19 shows that the discharge volume was underestimated and most likely the simulated SWE was too little. With snow measurements that year it is possible that the simulations could have been improved.

The simulations for 2014 were relatively good; the model simulates the main flood peaks quite well. The Nash-Sutcliffe efficiency was 0.62 and the logarithmic efficiency 0.77. The accumulated difference plot on Figure 4.19 shows that the discharge volume is perhaps underestimated, which could be because of underestimation on snow accumulation. The model overestimates the glacial melting in end of June. The same was observed for 2013. The glacial melting is sensitive to the temperature lapse rate as discussed in Chapter 4.3.2. The temperature on the glacier might be overestimated if there are meteorological scenarios where the temperature lapse rate is lower than 0.6°C/100m.

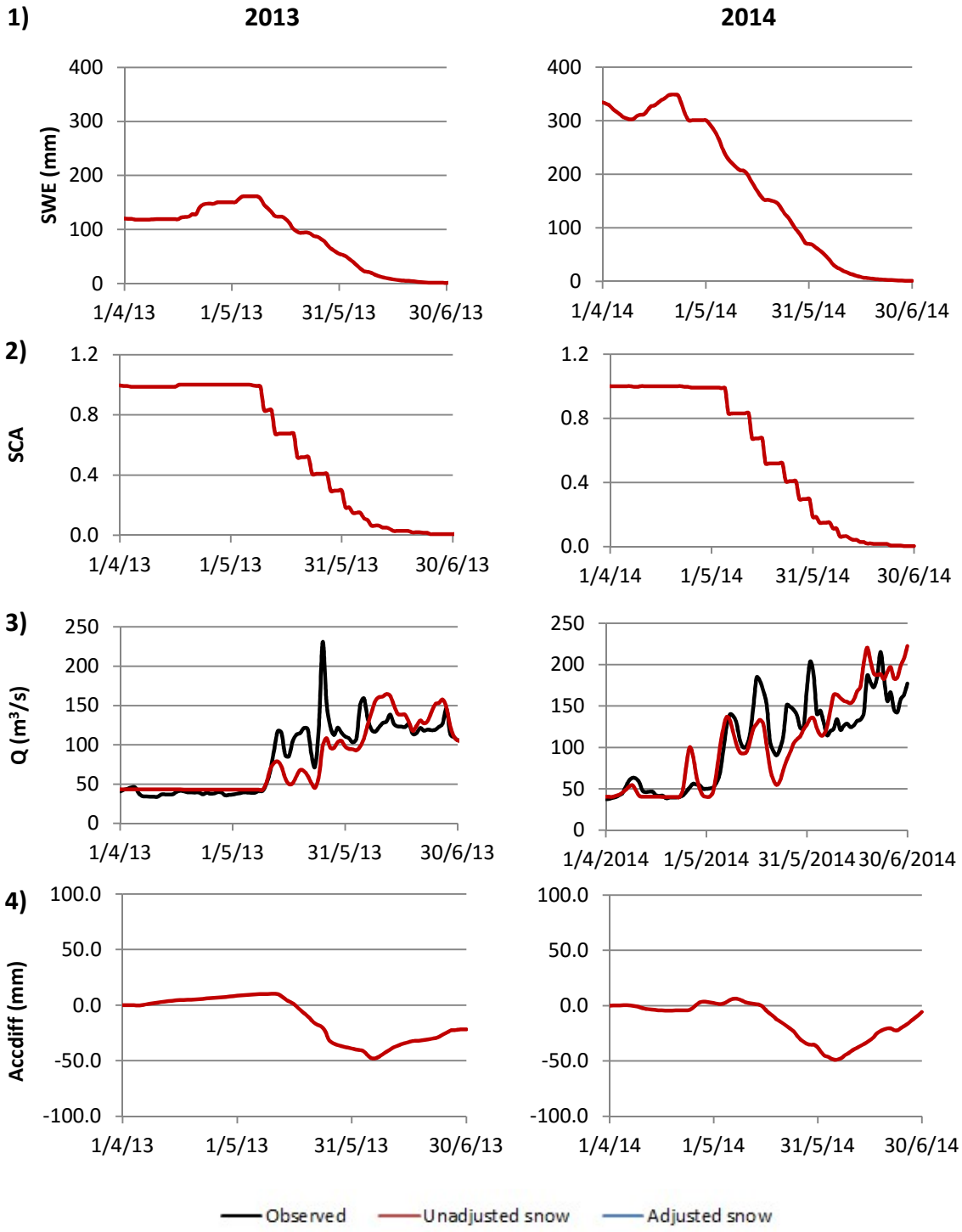

Figure 4.19 Simulation and observation of the runoff and the snow for spring 2013 and 2014 (validation period): 1) Snow water equivalent (SWE); 2) Snow cover area (SCA); 3) Discharge (Q); 4) Accumulated difference between observed and simulated discharge.

The snow measurements improved both the model efficiency measured with Nash-Sutcliffe criteria and the accumulated difference for both 2011 and 2012 during the validation period. Unfortunately, no snow measurements were available for 2013 and 2014. The results are positive regarding using snow measurements as reference points to adjust the snowpack in hydrological simulations for Dynkur catchment.

The simulations are relatively good most years. Two years are an exception, 2010 and the following year 2011. In 2010 the snowpack was very small. The model fails to simulate the high frequency flood peaks. In 2011 the snowpack is very large compared to other years. The model fails to simulate both flood peaks during the spring. In order to find explanations for these failures to simulate the flood peaks, both weather conditions and the dynamics of the snowpack need to be studied as well as the effect of volcanic ash on the snow melt rate. In both years a volcanic eruption occurred close to the catchment, which likely increased the melt factor.

4.3.5 Limitations

An automatic calibration has become a common option for many hydrological computer programs. It was not included in the program version used in this study. It would have helped considerably to find optimum parameter sets with automatic calibrations and more parameter sets could have been tested. More calibrations would be needed to evaluate the uncertainty of parameters. Many parameter sets could give the same results but might return different prediction values, some more accurate than others. Automatic calibration with an objective function with two or three efficiency criteria would have been ideal to find the optimum parameter set that would sufficiently represent the catchment. The objective function describes the weight of each efficiency criteria, e.g. most weight might be put on Nash-Sutcliffe and then on accumulated difference.

A longer study period would give more reliable results. The calibration period is from 2003 until 2010, with more than half of 2007 missing because of missing data from the discharge gauge in Dynkur. The validation period is four years, from 2011 to 2015. There are also long periods of missing precipitation data that affect the quality of the input data. The snow data available are inconsistent, measurements are done at different times during spring from the middle of Mars to the beginning of May, and for some years they are missing. It would be best if the snow measurements would be done just before spring melt (middle of April normally) and all locations would be measured in the same time period (same week).

Only two rain gauges are inside the catchment area and a few others located 10 to 30 km away from the catchment. To represent a catchment the size of the Dynkur one, the rain gauges are too few and sparse. The model is a conceptual model and treats the catchment as a lumped catchment, which is a great simplification of the actual situations. The model uses average daily values to simulate the average daily flow. Therefore it can never represent the different rain storms, with different duration that fall in different locations within the catchment and cause variable response in the hydrographs.

Dynkur catchment is a complex system and difficult to model. It accumulates a fair amount of snow and in the summer the main discharge component is glacial melt. The minimum base flow, normally at the end of winter, is relatively large. That results in a rather high portion of water from snow, and rain needs to percolate down to the groundwater box to

maintain the base flow over dry periods. It is possible that the model in some years overestimates the amount of snow that goes to the groundwater box since less water might seep through the soil when there is ice covering the ground. The program version used does not include the option of accounting for frozen soil and the effects it might have on runoff and the percolation rate down to the groundwater.

If the model were to be used for forecasting the input data (temperature and precipitation) must be unbiased, compared to those that were used for the calibration. The model should be updated regularly to remove bias and minimize random errors (Anderson, 2006). The relation between SWE measurements and the area-average SWE computed by the program should also be updated every year to improve predictions and validate their connection.

4.4 Discussion and future work

The spring season is often a crucial time when managing a water resource for energy production in an optimum way. Accurate prediction on runoff based on simulations could be a valuable tool for water management. It is by no means a simple task to perform hydrological modeling of a river catchment like Dynkur catchment. It is a complex system with discharge components from base flow, snow melt, glacial melt and runoff from rain events. Snow accumulation and snow melt play a crucial role in the quality of the simulations over spring season. One of the goals was to separate the discharge components to study the snow accumulation and snow melt and the relationship between the snowmelt volume and the snow measurements.

Separating the discharge components was a crucial step to get a realistic relationship between the snowmelt volume and the snow measurements. It is difficult to estimate how accurate the computed snowmelt volume is, mainly because of the difficulty in estimating when the snow melt finishes and glacial melt takes over. It was done mainly by observing the hydrographs and comparing them to the response to temperature. The time when snow melt was considered to be finishing and the time when the simulated snow cover was depleting was compared. Snow accumulation and the evolution of the snowpack were simulated with the HBV model. The results from simulations were compared with the hydrographs where the discharge components were separated.

Figure 4.20 shows the hydrograph for spring 2005 and the simulated SWE the same year. When these graphs are compared and the day analyzed when the snow melt recession starts, the simulated SWE is between 50 and 90 mm and the snow cover area is between 10 and 20%. When the snow cover area is between 10 and 20% of the catchment area not covered with glacier, it means that the snow line is in an elevation zone between 700 to 900 MASL in the model. Figure 2.3 describes the elevation zones at Dynkur catchment. The source of the glacier is in between 700 and 800 MASL and 90% of the catchment area not covered with glacier is below 800 MASL.

It is likely that when the snow line reaches the same elevation as the glacier, the glacial melting slowly takes over and becomes the main discharge component. All the years except in 2011, the same thing was observed. Table 4.11 shows the state of the simulated snow pack at the start of snow recession and at the end.

Table 4.11 Status of the simulated snow cover in the HBV model the same day as the start of the snow recession is estimated in computation on total snow melt.

	Start		End	
	SWE (mm)	SCA	SWE (mm)	SCA
2004	60	0.15	13	0.03
2005	76	0.15	13	0.03
2006	75	0.15	27	0.06
2008	77	0.15	21	0.04
2009	60	0.11	14	0.04
2010	56	0.15	27	0.06
2011	322	0.67	114	0.15
2012	92	0.15	44	0.06

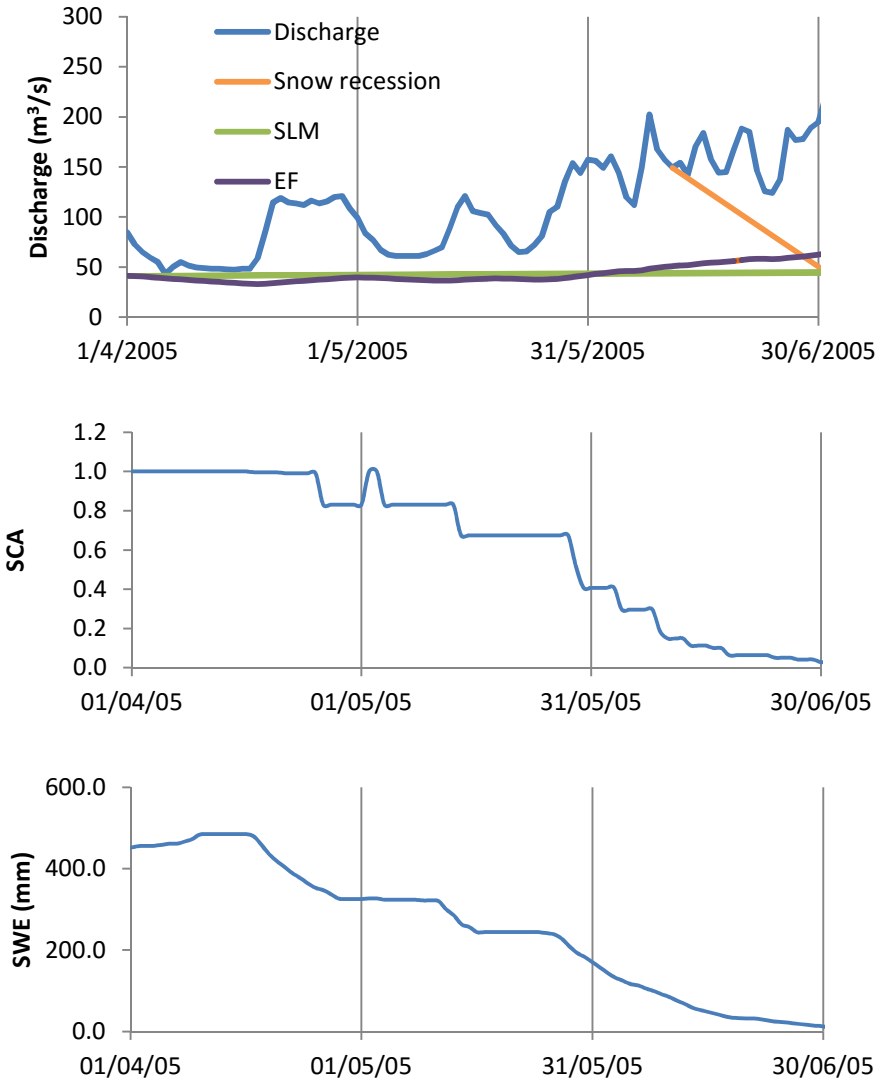

Figure 4.20 Top graph shows hydrograph for spring 2005 and the different discharge components. Middle graph shows the simulated SCA. Lower graph shows simulated SWE.

The results suggest that the timing of when the snowmelt recedes, is consistent with simulation results. The slope of the snow recession line is difficult to estimate and approximating it as a straight line leaves large uncertainties. Further studies are needed to make better estimation on the runoff component coming from snow melt. One method also could be to observe other similar catchment areas that do not have a glacier within its zone. Stóra- Laxá River catchment area located next to Dynkur catchment could be used in that purpose.

Accurate estimation on the snowmelt volume could provide an important variable if a study on the timing of the spring melts would be done. After snowmelt volume has been estimated, predictions on when snow melt will start and finish would be valuable for water management. One possible method to estimate the timing of spring floods is with a multiple regression analysis. It is possible to study the timing of e.g. the start of the snowmelt and when half of the snowmelt volume has finished. Independent variables in such a model could be e.g. temperature, precipitation and SWE in the end of snow accumulation season and the dependent variable; the onset of the snowmelt (Clow, 2010).

The snow measurement provided a valuable point of reference to adjust the simulated SWE in this study. It would be interesting to continue with the research with collection of more snow data. For example, more snow measurements over the melting period would be interesting to analyze, to study the relations between the decrease of SWE on location and the resulting increase in runoff over a spring period.

In Norway, hydrologists have been using the HBV model for hydrological simulations, where they have developed a method to adjust the SCA to remote sensing from satellites. Instead of dividing the catchment into elevation zones for the precipitation and temperature, the catchment is divided into a grid. The SCA can then be calibrated to satellite images on days with no clouds. This has improved the spring flood simulations on average and proved a good reference to adjust the snowpack (Lundholm, Johansson, Malnes, & Solberg, 2008).

The quality of the data should be evaluated, especially the precipitation where spatial precipitation might not be representing the catchment area sufficiently. Rain gauges used are sparse between and the quality of their measurements is not always accurate, especially when dealing with wind and snow. Long periods of missing precipitation data also affect the quality of input precipitation in the model. A research was conducted in Norway to improve measurements from automatic rain gauges to measure snow. An adjustment function was developed to adjust wind induced solid precipitation loss for automatic rain gauges (Wolff, Isaksen, Petersen-Øverleir, Ødermark, Reitan & Brækkan, 2015). If such an equation could improve snow precipitation measurements, it would be valuable for hydrological studies in the Icelandic highlands.

The quality of the snow measurement data is also questionable. The snow data available are inconsistent, the measurements were not always done in the end of snow accumulation period, sometimes the melting period had already started, and some years are missing. With time, longer time series of snow measurement will be obtained that could improve both the prediction efficiency of the HBV model, and snowmelt volume prediction in start of spring. Longer period should be studied to get more conclusive results.

Improvements could possibly be made to the response routine. The percolation rate down to the groundwater box is controlled with one parameter, *perc*. The parameter is a constant and the same for the whole catchment. In reality the rate of percolation depends on the soil or surface characteristics. It can also depend on the season, as frozen soil has different characteristics to an unfrozen soil. Therefore it is a large simplification to assume the same percolation rate over the entire catchment. The response from the lower box (groundwater) is very slow compared to the upper box (direct runoff). As a result, the model often does not simulate the interflow over spring melt sufficiently. The runoff response was also often too slow when simulating large rain events in winter or the rain input insufficient, hence underestimating the flood peaks. One idea would be to calibrate the model for different seasons or splitting the catchment up, where separate parameters would be for the glacier zone and another for non- glacier zone.

5 Conclusion

The study presented an analysis of Dynkur catchment, with the aim evaluating the hydrology of the catchment over the spring season. The focus was on estimating the snow accumulation, the spring melt and to simulate the runoff. The spring runoff is an important factor in the hydrological resource management for hydropower companies. There is a valuable resource stored in the snow cover and with reliable prediction on the quantity of water stored in the snow and accurate simulations on spring runoff, improvements can be made in the resource management.

Snow measurements from three locations were studied. The results show that the snow measurements from an individual location do not give us a clear enough indication of the total volume of snowmelt. However, when all sites are made to represent the SWE of the snow cover, a much better results are obtained. In the case where the mean SWE was computed from snow measurements from Veiðivatnahraun, Kjalöldur and Setur, and used in the linear regression analysis, the correlation was 0.95 between SWE and total snowmelt. This indicates that measurements from these locations are good representatives for the snow accumulation of the catchment and could be used together to predict the total volume of snowmelt in the following spring. Increasing number of snow measurement sites inside or close to the catchment might improve the estimated snow accumulation of the catchment even further. Longer time series of snow measurements is needed to gain a better estimation of the relation between snow measurements and spring discharge.

Snow measurements should always be conducted at least once a year in the end of accumulation period. The accumulation period normally ended in middle of April during the study period. It is important that the snow measurements in all location are measured within the same timeframe e.g. one week in middle of April all locations should be measured. To improve the quality of the snow measurements the snow density should be measured in more than one snow profile at each measurement site. Errors in snow density measurements or a snow profile that does not represent the snow density in the area sufficiently can lead to large errors in the SWE estimated from measurements.

Precipitation is one of the main input data in the HBV model and determines the simulated snow accumulation. Automatic rain gages often fail to measure snowfall sufficiently. Therefore it was analyzed whether the snowpack could be calibrated to some reference point, such as the SWE measurements that have been done in the catchment. As the correlation analysis suggested, the mean SWE from all snow measurement locations are good representatives for the snow accumulation of the catchment. SWE measurements from Veiðivatnahraun, Setur and Kjalöldur provided valuable data that the SWE computed by the model could be adjusted to. When the SWE in the model was adjusted according to the relation to the measured SWE, the efficiency improved and the accumulated difference between observed and computed discharge reduced on average.

The HBV model simulated the discharge year fairly well. The most difficult and inefficient season to simulate was the spring season. Most years the model simulated the spring quite well, but there were notable exceptions. For two springs the model returned inadequate

results, underestimating the melting considerably. The failure of the model to simulate these events was most likely related to meteorological scenarios and volcanic eruptions that affect the albedo of the snow cover. These scenarios cause the relationship between snow melt and air temperature to deviate from their calibrated average relationship.

References

Anderson, E. A. (1976). *A Point Energy and Mass Balance model of a Snow cover*. Tech. Rep. 19, NOAA, Silver Spring, Md.

Abebe, N. A., Ogden, F. L. & Pradhan, N. R. (2010). Sensitivity and uncertainty analysis of the conceptual HBV rainfall–runoff model: Implications for parameter estimation. *Journal of Hydrology, 389*(3-4), 301-310.

Aghakouchak, A. & Habibi, E. (2010). Application of a Conceptual Hydrologic Processes. *International Journal of Engineering Education, 26*(4), 963-973.

Anderson, E. (2006). *Snow Accumulation and Ablation Model – SNOW-17.* Silver Spring: NWS.

Berglöv, G., German, J., Gustavsson, H., Harbman, U. & Johansson, B. (2009). Improvement HBV model Rhine in FEWS, Final report. *Hydrology,* (112).

Bergström, S. (1976). *Development and application of a conceptual runoff model for Scandinavian catchmnet.* Norrköping: SMHI RHO.

Boike, J., Roth, K. & Ippisch, O. (2003). Seasonal snow cover on frozen ground: Energy balance calculations of a permafrost site near Ny-A lesund, Spitsbergen. *Journal Of Geophysical Research, 108*(D2), ALT 4-1 - ALT 4-11.

Crochet, P. (2014). *Probabilistic daily streamflow forecasts based on the combined use of a hydrological model and an analogue method.* Reykjavík: Icelandic Meteorological Office.

Clow, D. W. (2010). Changes in the Timing of Snowmelt and Streamflow in Colorado: A Response to Recent Warming. *Journal of Climate , 23*, 2293-2306.

Eckhardt, K. (2012). Technical Note: Analytical sensitivity analysis of a two parameter recursive digital base flow separation filter. *Hydrology and Earth System Sciences, 16*, 451–455.

Einarsson, M. Á. (1972). *Evaporation and Potential Evapotranspiration in Iceland* . Reykjavík: Icelandic Meteorological Office .

Elder, K., Rosenthal, W. & Davis, R. E. (1998). Estimating the spatial distribution of snow waterequivalence in a montane watershed. *Hydrological Processes, 12*, 1793-1808.

Franke, G. R. (2010). *Multicollinearity.* Wiley International Encyclopedia of Marketing.

Friðriksson, R. F. & Ólafsson, H. (2005). Estimating Errors In Wintertime Precipitation Observations by Comparison With Snow Observations. *Hrvatski meteorološki časopis, 40*(40), 695–697.

Gardner, A. S., Sharp, M. J., Koerner, R. M., Labine, C., Boon, S., Marshall, S. J. et al. (2009). Near-Surface Temperature Lapse Rates over Arctic Glaciers and Their Implications for Temperature Downscaling. *Journal of Climate* (22), 4281–4298.

Grayson, R. & Bloschl, G. (2001). Spatial Modelling of Catchment Dynamics. In R. Grayson, & G. Bloschl, *Spatial Patterns,* pp. 51-81. Cambridge: Cambridge University Press.

Grunewald, T., Schirmer, M., Mott, R. & Lehning, M. (2010). Spatial and temporal variability of snow depth and ablation rates in a small mountain catchment. *The Cryosphere, 4*, 215-225.

Jonas, T., Marty, C. & Magnusson, J. (2009). Estimating the snow water equivalent from snow depth measurements in the Swiss Alps. *Journal of Hydrology, 378*(1-2), 161–167.

Khanal, A. (2013). *Inflow Forecasting for Nepalese Catchments.* Master´s thesis, Faculty of Engineering Science and Technology, NTNU.

Kokkonena, T., Koivusaloa, H., Jakemanb, A. & Norton, J. (2006). Construction of a Degree-Day Snow Model in the Light of the "Ten Iterative Steps in Model Development". In A.Voinov et al. (Ed.), *Proceedings of the iEMSs Third Biennial Meeting: Summit on Environmental Modelling and Software.* Burlington: Environmental Modelling and Software Society.

Kuchment, L. & Gelfan, A. (1996). The determination of the snowmelt rate and the meltwater outflow from a snowpack for modelling river runoff generation. *Journal of Hydrology, 179*(1-4), 23–36.

Kumar, M., Marks, D., Dozier, J., Reba, M. & Winstra, A. (2013). Evaluation of distributed hydrologic impacts of temperature-index and energy-based snow models. *Advances in Water Resources,* (56).

Landsvirkjun. (n.d.). *Búrfell Power Station*. Retrieved February 11, 2015, from Landsvirkjun: http://www.landsvirkjun.com/Company/PowerStations/BurfellPowerStation

Landsvirkjun. (2015). *Ársskýrsla 2014.* Retrieved June 20, 2015, from Landsvirkjun: http://arsskyrsla2014.landsvirkjun.is/orkuvinnsla/orkuvinnsla-2014

Lundholm, K., Johansson, B., Malnes, E. & Solberg, R. (2008). Evaluation of satellite images of snow cover areas for improving spring flood in the HBV- model. In Ó. G. Sveinsson, S. M. Garðarsson, & S. Gunnlaugsdóttir (Ed.), *Northern Hydrology and its Global Role. 2*, pp. 455-464. Reykjavík: Icelandic Hydrological Committee.

Madsen, H., Pedersen, C. & Borden, C. (2009). A Real-Time Inflow Forecasting and Reservoir Optimization System. *Waterpower XVI* (pp. 1-12). Spoken: PennWell Corporation.

McCuen, R. (1998). *Hydrologic Analysis and Design.* Englewood Cliffs: Prentice-Hall.

National Land Survay of Iceland. (n.d.). *Niðurhalssíða*. Retrieved from Landmælingar Íslands: http://atlas.lmi.is/LmiData/index.php

Nespor, V., & Sevruk, B. (1998). Estimation of Wind-Induced Error of Rainfall Gauge Measurements Using a Numerical Simulation. *Journal Of Atmospheric And Oceanic Technology, 16*, 450-464.

Orkustofnun. (n.d.). *Raforkuvinnsla eftir uppruna árið 2013*. Retrieved January 4, 2015, from Orkustofnun: http://www.orkustofnun.is/yfirflokkur/raforkutolfraedi/raforkuvinnsla-eftir-uppruna

Ortha, R., Staudingerb, M., Seneviratnea, S. I., Seibertb, J. & Zappac, M. (2015). Does model performance improve with complexity? A case study with three hydrological models. *Journal of Hydrology*, *523,* (147-159).

Pálsson, F., Guðmundsson, S. & Björnsson, H. (2012). *Áhrif ösku úr eldgosunum 2010 (Eyjafjallajökull) og 2011 (Grímsvötn) á leysingu á vatnasviðum Tungnaár, Köldukvíslar og Hálslóns.* Jarðvísindastofnun Háskólans.

Pisarenko, V. F., Lyubushin, A. A., Bolgov, M. V., Rukavishnikova, T. A., Kanyu, S., Kanevskii, M. F. et al. (2005). Statistical Methods for River Runoff Prediction. *Water Resources, 32*(2), 115–126.

Schöber, J., Achleitner, S., Kirnbauer, R., Schöberl, F. & Schönlaub, H. (2012). Impact of snow state variation for design flood simulations in. *Advances in Geosciences, 31*, 39-48.

Schöbera, J., Schneidera, K., Helfrichta, K., Schattana, P., Achleitnerd, S., Schöberlb, F. et al. (2013). Snow cover characteristics in a glacierized catchment in the Tyrolean Alps - Improved spatially distributed modelling by usage of Lidar data. *Journal of Hydrology, 519*, 3492–3510.

Seibert, J. (1997). Estimation of Parameter Uncertainty in the HBV Model. *Nordic Hydrology, 28*(4/5), 247-262.

Sigurðsson, F. H. (1990). Vandamál við úrkomumælingar á Íslandi. *Vatnið og Landið*, 101-110.

Sigurðsson, M. (2013). *Áhrif eldgosa eldgosa í Eyjafjallajökli Eyjafjallajökli og Grímsvötnum á orkuvinnslu Landvirkjunar.* Retrieved July 20, 2015, from Samorka: http://samorka.is/Apps/WebObjects/SW.woa/wa/dp?id=4336

Sigurðsson, O. & Jóhannesson, T. (2014). *Samantekt um snjómælingar.* Reykjavík: Icelandic Meteorological Office.

Simolo, C., Brunetti, M., Maugeri, M. & T.Nanni. (2009). Improving estimation of missing values in daily precipitation series by a probability density function-preserving approach. *International Journal Of Climatology, 30*, 1564-1576.

SMHI. (2012). *Intergrated Hydrological Modelling System, Manual, Version 6.3.* Swedish Meteorological and Hydrological Institute.

Teegavarapu, R. S. (2012). *Floods in a Changing Climate: Extreme Precipitation.* Cambridge: Cambridge University Press.

Teegavarapua, R. S. & Chandramoulia, V. (2005). Improved weighting methods, deterministic and stochastic data-driven models for estimation of missing precipitation records. *Journal of Hydrology, 312*(1-4), 191–206.

Thirela, G., Notarnicolab, C., Kalasa, M., Zebischb, M., Schellenbergerb, T., Tetzlaffb, A., Duguay, M., Mölg, N. Burek, P. & de Roo, A. (2012). Assessing the quality of a real-time Snow Cover Area product for hydrological applications. *Remote Sensing of Environment, 127*, 271-287.

Trujillo, E., Ramírez, J. & Elde, K. (2009). Scaling properties and spatial organization of snow depth fields in sub-alpine forest and alpine tundra. *Hydrological Processes, 23*(11), 1575–1590.

Viessman, W. & Lewis, G. L. (2003). *Introduction to Hydrology* (Vol. 5th edition). Upper Saddle River, New Jersey: Pearson Education, Inc.

Wolff, M. A., Isaksen, K., Petersen-Øverleir, A., Ødermark, K., Reitan, T., & Brækkan, R. (2015). Derivation of a new continuous adjustment function for correcting wind-induced loss of solid precipitation: results of a Norwegian field study. *Hydrology and Earth System Sciences , 19* (2), 951-967.

Zhang, L., Walker, G. R. & Dawes, W. R. (2002). Water balance modelling: concepts and applications. *Aciar Monograph series, 84*, 31-47.

Zophaníusson, S. (2010, 12 29). *Rennsli í ám á vatnsárinu 2009/2010.* Retrieved Juny 12, 2015, from Veðurstofa Íslands: http://www.vedur.is/vedur/frodleikur/greinar/nr/2076

Appendix A

Graphs that computations on total snowmelt volume were based on.

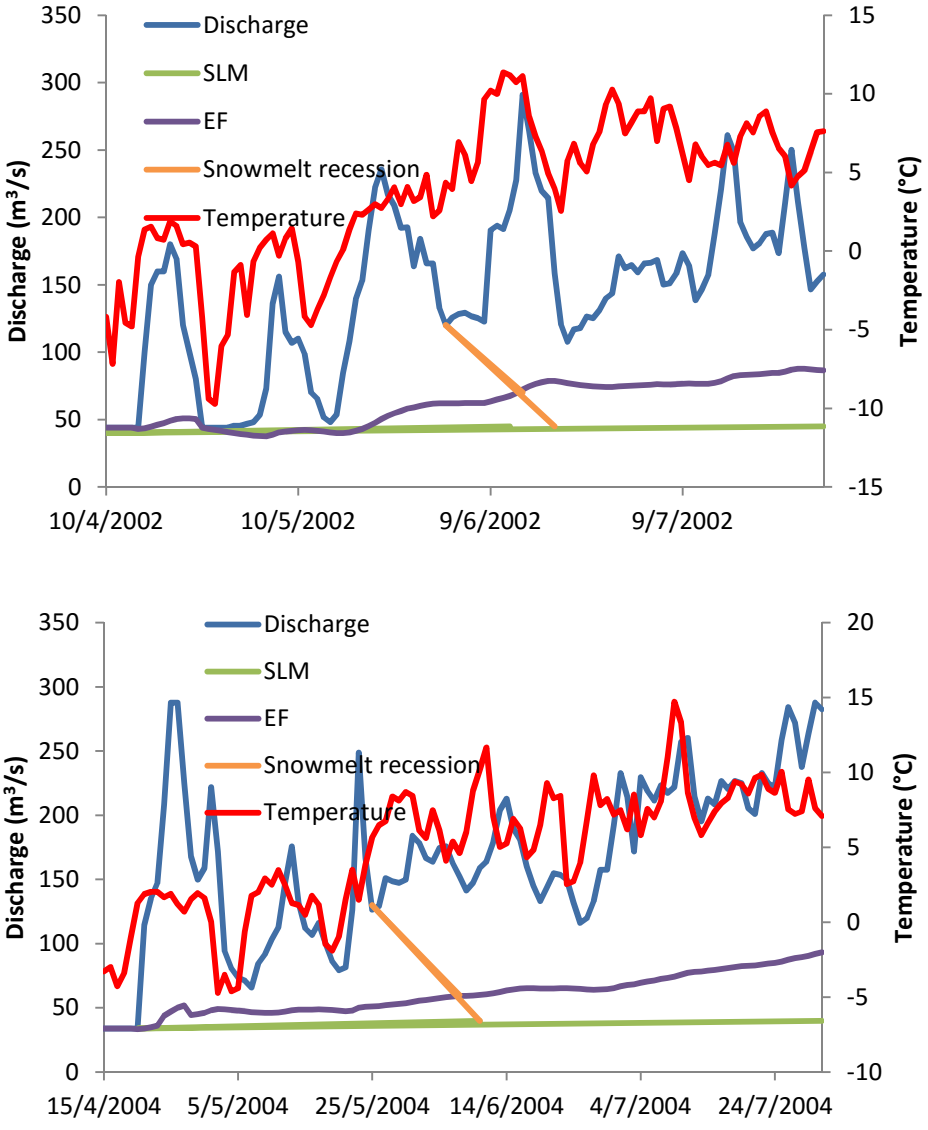

Figure A.0.1 Discharge and temperature over spring and summer 2002 and 2004.

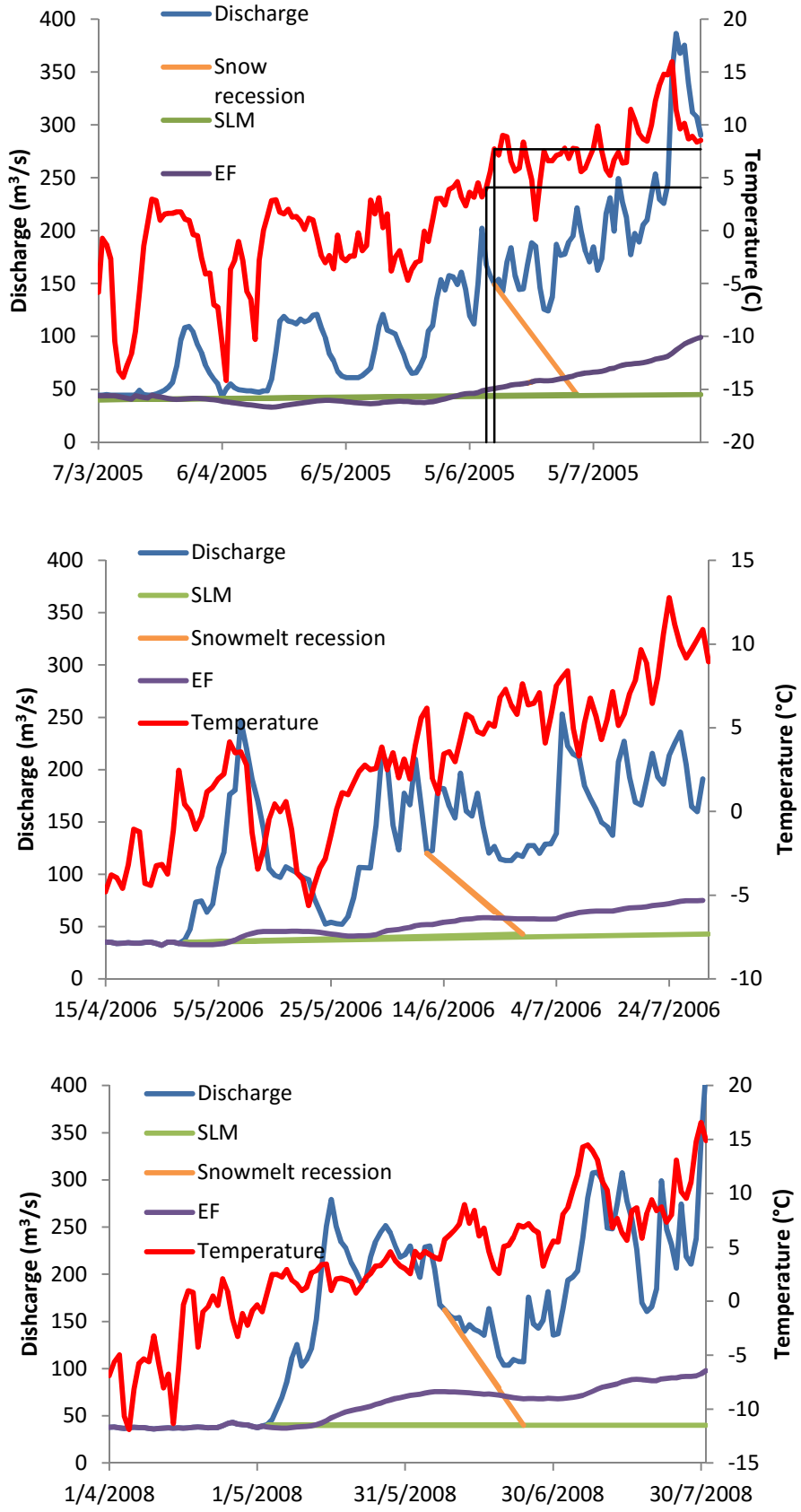

Figure A.0.2 Discharge and temperature over spring and summer 2005, 2006 and 2008.

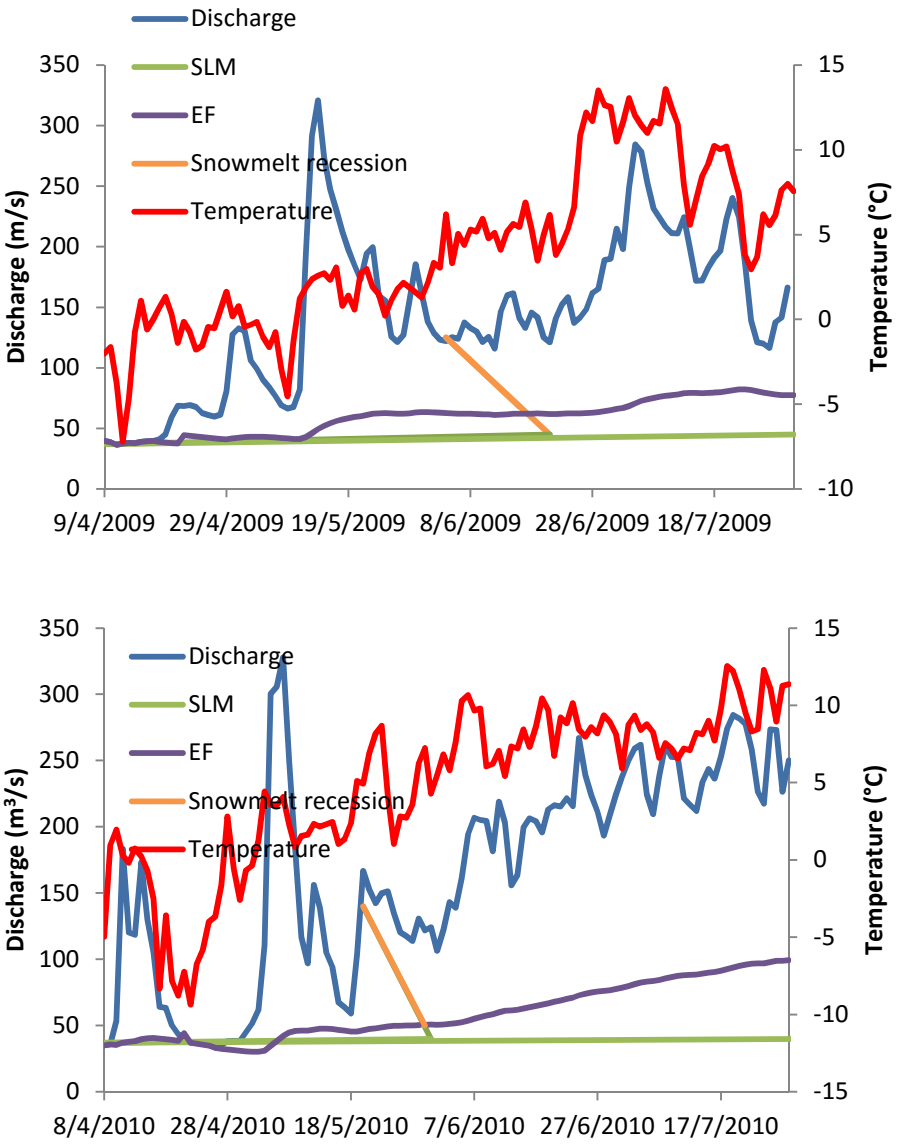

Figure A.0.3 Discharge and temperature over spring and summer 2009 and 2010.

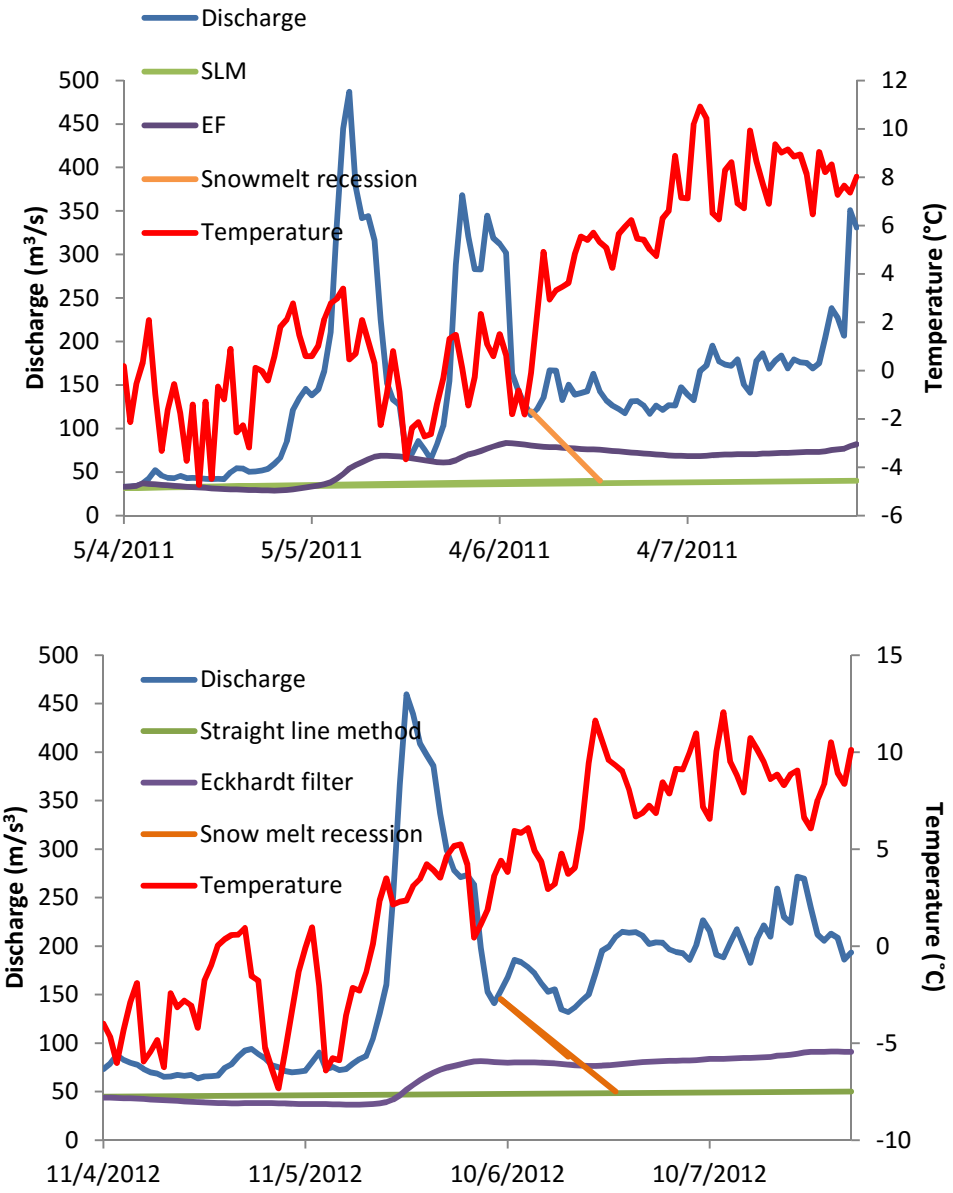

Figure A.0.4 Discharge and temperature over spring and summer 2011 and 2012.

Appendix B

Hydrographs from simulations and observations.

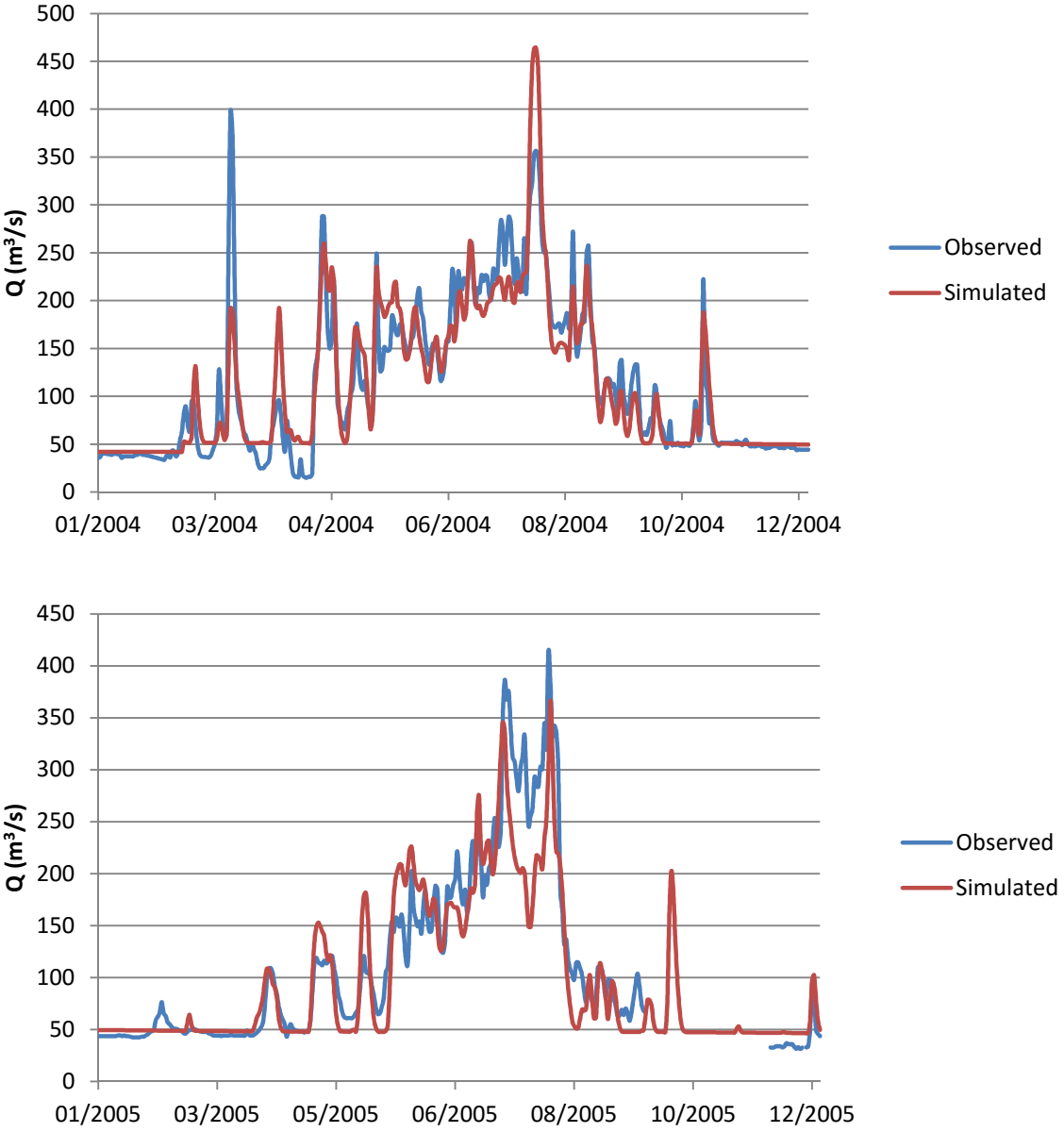

Figure A.0.5 Observed and simulated daily discharge for 2004 and 2005 (calibration).

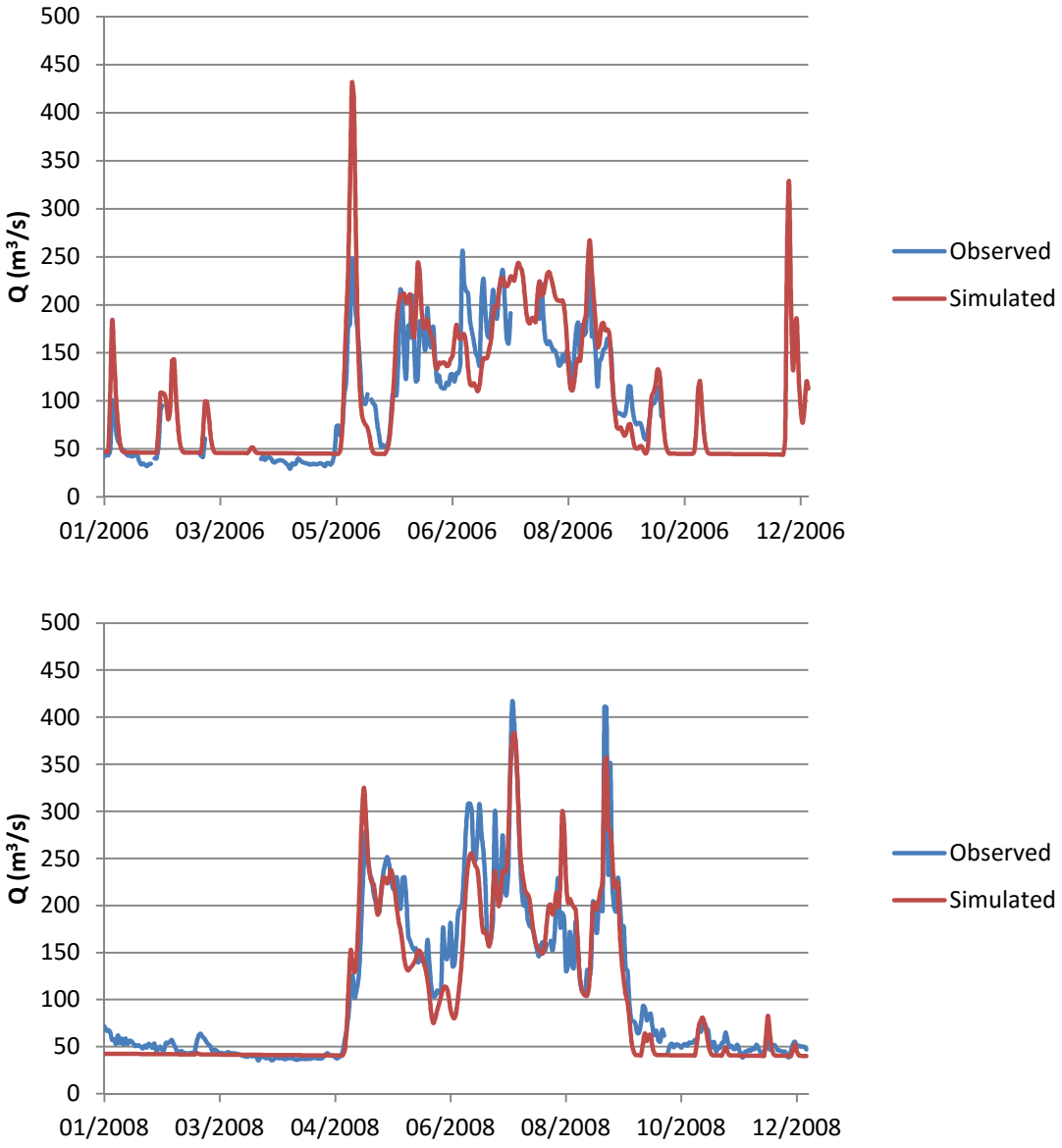

Figure A.0.6 Observed and simulated daily discharge for 2006 and 2008 (calibration).

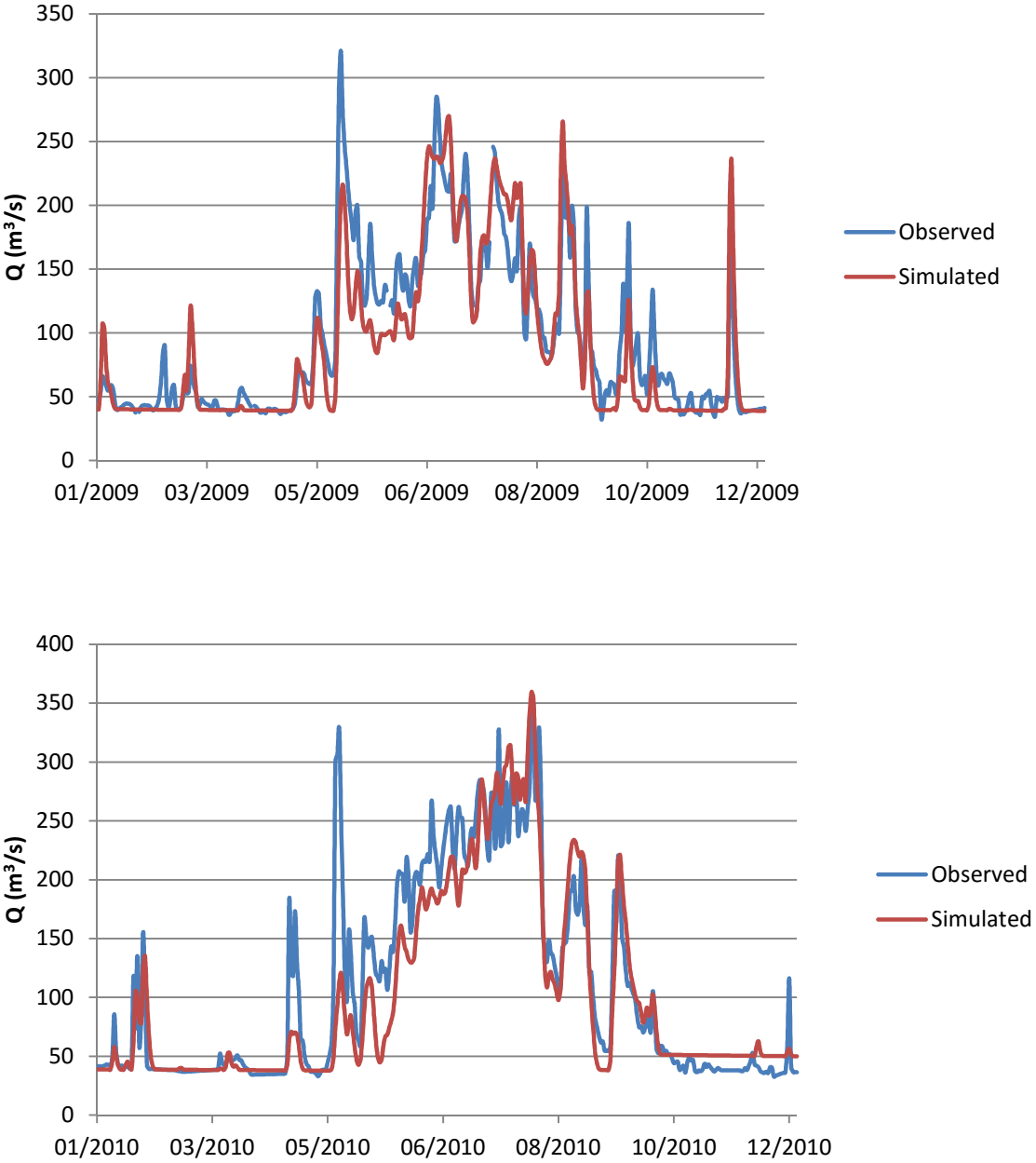

Figure A.0.7 Observed and simulated daily discharge for 2009 and 2010 (calibration).

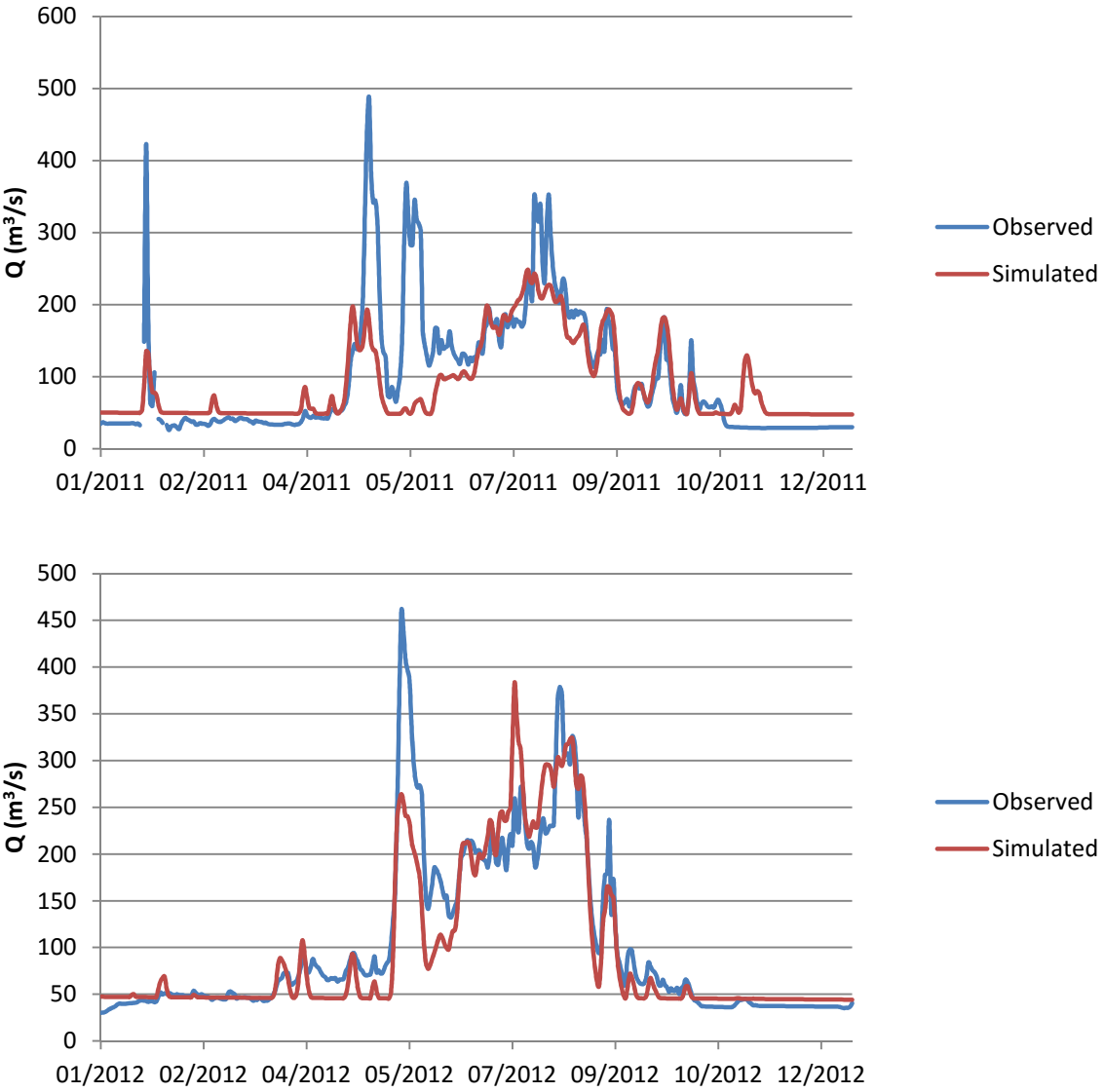

Figure A.0.8 Observed and simulated daily discharge for 2011 and 2012 (validation).

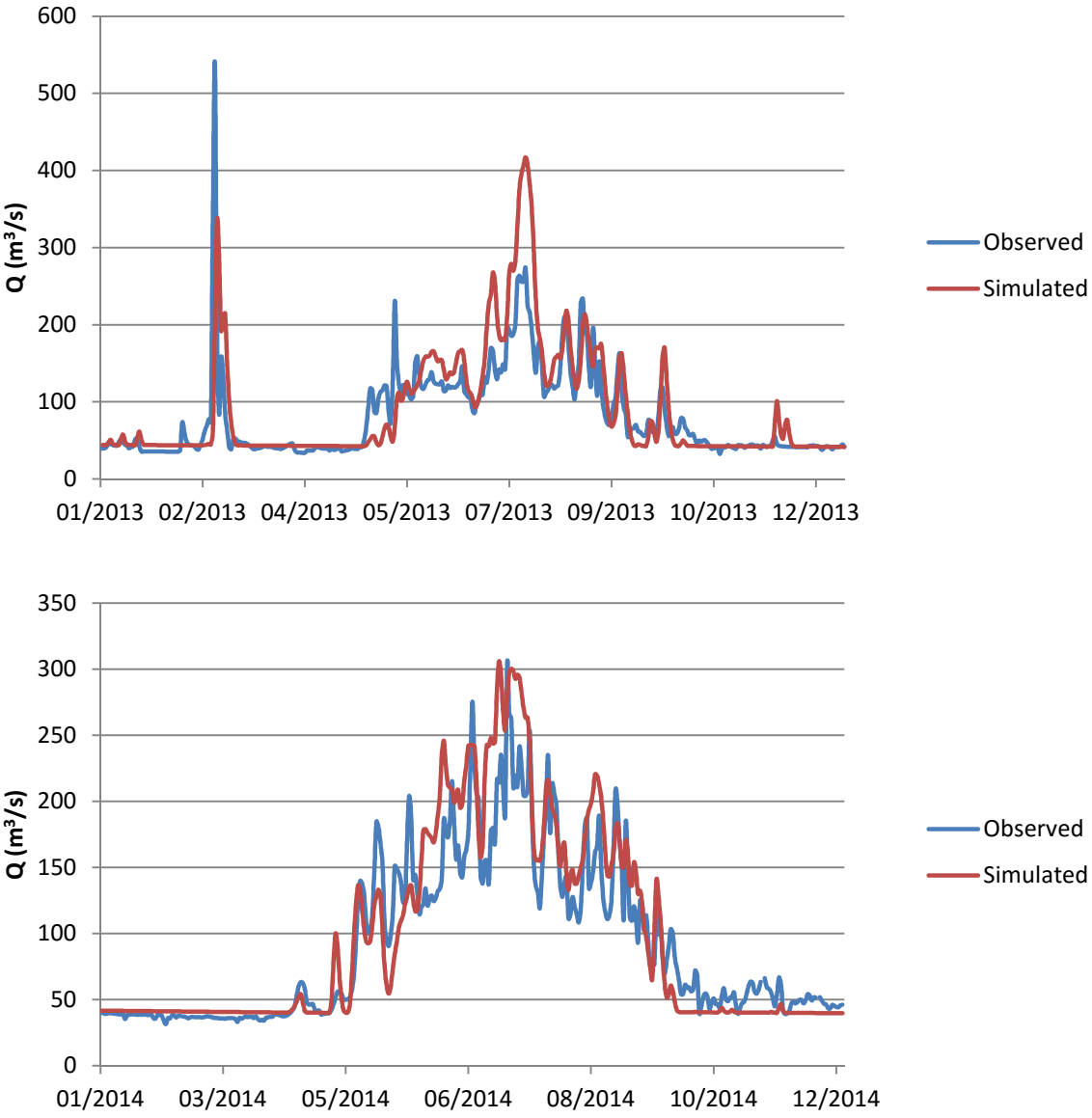

Figure A.0.9 Observed and simulated daily discharge for 2013 and 2014 (validation).

Appendix C

Table 0.1 Input parameters for the HBV model.

Symbol	Descrption	Unit
alfa	measure of non-linearity of the reservoir	-
athorn	conversion factor for computing potential evaporation with Thornweits method	-
β	ccontrols the contribution to the response function from rainfall or snow melt.	-
cflux	capillary flow from upper zone to soil moisture zone	mm/day
cfmax	melting factor	$mm^oC^{-1}\Delta t^{-1}$
cfr	refreezing factor	-
dt	deviation of temperature from normal	°C
etf	correction factor to adjust potential evaporation	-
gmelt	melting factor for the glacier	$mm^oC^{-1}\Delta t^{-1}$
fc	maximum soil moister storage	mm
icfi	interception storage capacity	mm
k4	recession coefficient for lower responce box	1/day
khq	recession coefficient for upper respnce box	1/day
lp	a soil moister value that tells when the actual evapotranspiration has reached potential value	-
maxbaz	transformation function	-
pcalt	precipitation lapse rate	-
perc	perculation from upper zone to lower	mm/day
rfcf	rainfall correction factor	-
sfcf	snowfall correction factor	-
stf	to describe seasonal variations in the relation between evaporation and temperature	-
tcalt	temperature laps rate	°C/100m
tt	threshold temperature.	°C
ttint	describes the transition when precipitation is assumed to be mix of rain and snow	°C
whc	water holding capacity	-